aerospace

MDPI

Review

Propulsion Technologies for CubeSats: Review

Suood Alnaqbi, Djamal Darfilal * and Sean Shan Min Swei

Khalifa University Space Technology and Innovation Center, Khalifa University of Science and Technology, Abu Dhabi 127788, United Arab Emirates; s.saood1997@gmail.com (S.A.); sean.swei@ku.ac.ae (S.S.M.S.)
* Correspondence: djamal.darfilal@ku.ac.ae

Abstract: This paper explores the wide-ranging topography of micro-propulsion systems that have been flown in different small satellite missions. CubeSats, known for their compact size and affordability, have gained popularity in the realm of space exploration. However, their limited propulsion capabilities have often been a constraint in achieving certain mission objectives. In response to this challenge, space propulsion experts have developed a wide spectrum of miniaturized propulsion systems tailored to CubeSats, each offering distinct advantages. This literature review provides a comprehensive analysis of these micro-propulsion systems, categorizing them into distinct families based on their primary energy sources. The review provides informative graphs illustrating propulsion performance metrics, serving as beneficial resources for mission planners and satellite designers when selecting the most suitable propulsion system for a particular mission requirement.

Keywords: propulsion; CubeSat; miniaturization; in space; review

Citation: Alnaqbi, S.; Darfilal, D.; Swei, S.S.M. Propulsion Technologies for CubeSats: Review. *Aerospace* **2024**, *11*, 502. https://doi.org/10.3390/aerospace11070502

Academic Editors: Martin Tajmar, Kyun Ho Lee and Chae Hoon Sohn

Received: 20 February 2024
Revised: 27 March 2024
Accepted: 27 March 2024
Published: 21 June 2024

1. Introduction

The last decade witnessed a significant increase in the number of small satellite launches, mainly due to the lower costs of development and of the launch of small satellites compared to those of larger satellites. Small satellites include CubeSats, which refer to cuboid-shaped satellites that consist of at least one $10 \times 10 \times 10$ cm^3 cube unit denoted by 1 U. CubeSats come in a variety of sizes depending on the number of cube units used to create the satellite platform. Along with relatively low launch and development costs, the standardized shape of CubeSats facilitates access to space, especially for educational institutions and startups. The standardized shape enables ease of integration with launch vehicles and enables the mass-scale production of CubeSats, supporting the development of various small satellite constellations for communication and Earth observation applications. The low cost and standardized form are both attractive features of CubeSats, which led to the rise of small satellite commercialization in the space sector. Small satellites are classified based on their mass as shown in Table 1.

Table 1. Small satellite classification based on mass [1].

Satellite Category	Mass (kg)
Femtosatellites	0.001–0.1
Picosatellites	0.1–1
Nanosatellites	1–10
Microsatellites	10–100
Minisatellites	100–180

According to the Nanosatellite Database, a total of 25 nanosatellites launched in 2012, whereas the total number of nanosatellites' launches increased tenfold to 334 in 2022 [2]. The miniaturization of satellite subsystems is necessary due to the mass and volume constraints of small satellites. The complexity and range of small satellite missions

have also increased, which led to a rise in demand for in-space micro-propulsion for small satellites. Micro-propulsion is used for attitude control, station-keeping, end-of-life deorbiting, and orbital maneuvers of small satellites. It enables an increase in mission range, capabilities, and lifetime. Micro-propulsion systems are utilized for a variety of applications in small satellite missions such as in-phasing maneuvers, constellation deployment, and interplanetary travel.

Propulsion systems have an extensive heritage in large spacecraft; therefore, the propulsion technologies are well understood. Propulsion systems are typically bulky and consist of propellant storage and management devices. The miniaturization of propulsion technologies is challenging due to the limited volume available and limited power budget for propulsion systems in small satellites.

The aim of this paper is to provide a review of micro-propulsion systems developed for satellites with a mass not exceeding 100 kg, as well as other potential propulsion systems that are suitable for small satellite constraints. A literature survey was conducted to review and highlight the development efforts undertaken for the miniaturization of propulsion systems for small satellites.

2. Propulsion Performance

The performance of the propulsion system is evaluated based on the efficiency of propellant consumption to provide the required thrust output. Specific impulse (I_{sp}) is a measure of the thrust delivered given the propellant mass flow rate. It is a propulsion system performance parameter that depends on the molecular mass of the propellant and its temperature. A propulsion system with a higher specific impulse consumes less propellant mass to produce the same thrust compared to that of a system with a lower specific impulse. Specific impulse is calculated as follows [3]:

$$I_{sp} = \frac{F}{\dot{m} g_0} \tag{1}$$

where F is the magnitude of the thrust force, $\dot{m}$ is the mass flow rate, and g_0 is the gravitational acceleration value at sea level, which are used to make the I_{sp} unit in seconds.

The satellite change in velocity (ΔV), which is delivered by the propulsion system, is another important mission design input that indicates the amount of propellant needed for a given specific impulse. The ΔV requirement is mission-dependent; therefore, it is usually given as an input. It can be calculated using Equation (2) [3]:

$$\Delta V = I_{sp} g_0 \ln\left(\frac{m_0}{m_f}\right) \tag{2}$$

where m_0 is the initial total wet mass (including the propellant) and m_f is the total dry mass (without the propellant). Other important factors for evaluating propulsion system design are the dry mass of the propulsion system elements, the complexity of the system, its compactness and volume, its power consumption, and its safety in terms of propellant toxicity and the level of propellant storage pressurization. Given the total propulsion system volume (V_p), the volumetric impulse measure is the ratio of how much total impulse (I_{tot}) is delivered per unit volume of the propulsion system [4].

$$I_{vol} = \frac{I_{tot}}{V_p} \tag{3}$$

3. Propulsion Technology Types

The propulsion technologies are classified based on the main source of energy that is converted to kinetic energy to generate thrust. The energy source can be obtained from pressurized gas kinetic energy, the bonds of reactants and products in chemical reactions, an electrical energy source, or an external source such as photonic pressure from solar

radiation or a laser beam. The main categories of miniaturized propulsion technology for small satellites are (1) kinetic, (2) chemical, (3) electric, and (4) non-propellant as shown in Figure 1. The first propulsion category is kinetic propulsion which produces thrust by expanding a compressed fluid in a typical converging-diverging nozzle. In this category, heating is usually applied to increase the mass flow rate of the expanding gas and thus enhance the performance of the system.

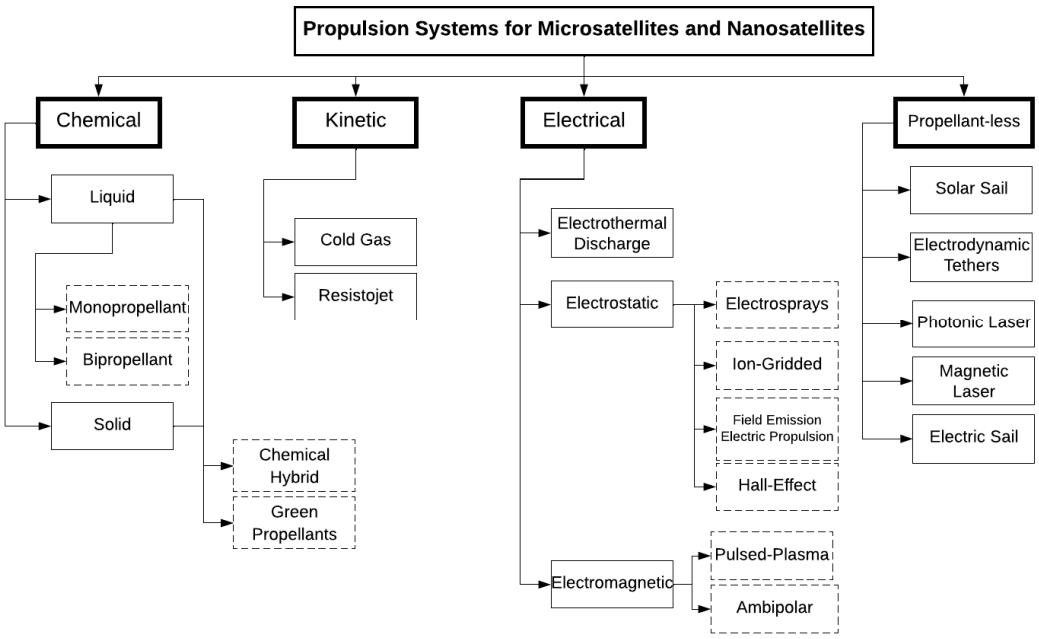

Figure 1. Overview of propulsion technologies.

Chemical propulsion technology utilizes the energy released from chemical reactions to generate thrust. Chemical propulsion technology has been used extensively to meet the propulsion requirements for previous space missions due to their relatability and high energy production capability. Chemical systems are classified as liquid, solid, and hybrid (solid and liquid) based on the types of fuel used. Green propulsion refers to chemical systems that use environmentally safe propellants with reduced toxicity. Nuclear propulsion generates thrust using nuclear fusion chemistry. All of these chemical propulsion systems will be introduced in more detail in their respective sections.

Electric propulsion systems use electrical power to accelerate the exhaust and are categorized based on the principles used to accelerate the exhaust. These categories are electrothermal, electrostatic, and electromagnetic principles.

Non-propellant systems include solar sail, electrodynamic tether, magnetic sail, electric sail, and photonic laser propulsion. These systems generate propelling force by interacting with external sources such as the sun, lasers, and a planetary magnetic field rather than using stored propellants. Such systems typically carry additional structural and/or electric elements to interact with the external sources.

3.1. Kinetic Propulsion

The primary source of energy in kinetic propulsion is the conversion of the internal energy of the pressurized propellant stored in a tank to kinetic energy. This conversion occurs by releasing compressed propellant to expand in a converging/diverging nozzle in order to generate thrust. Kinetic propulsion systems include cold gas, warm gas, and resistojet systems.

3.1.1. Cold Gas/Warm Gas

Cold gas propulsion generates a thrust by the expulsion of gas through a converging-diverging nozzle. The propellant is stored in a pressurized tank as a compressed gas or

saturated liquid. The expelled gas does not undergo any chemical reaction, and therefore cold gas thrust and specific impulse performance are significantly limited by tank pressurization. A cold gas propulsion system consists of the following main components: a propellant tank, a fill/drain valve, propellant feed lines, a flow control valve, and a nozzle as shown in Figure 2. The pressure regulator is not a primary element in pressurized gas systems; however, it can be used to change the pressure of the released gas before flowing through the rest of the thruster body.

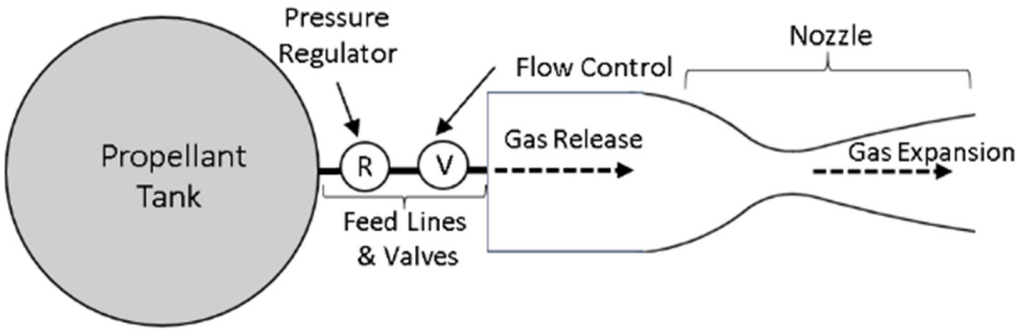

Figure 2. Cold gas propulsion schematic.

In the simplest cold gas system form, the propellant is stored as gas in a highly pressurized tank. The gaseous propellant is injected directly from the tank into the nozzle where it expands and accelerates the spacecraft. In the case of storing propellant in the liquid phase, the design consists of two tanks: a main tank that stores the liquid propellant and a second tank, referred to as the plenum, where the propellant is heated and vaporized to gas in preparation for firing. Heating can also be applied to the main propellant tank in the first case to vaporize all the propellant or increase the enthalpy of a gaseous propellant for enhanced propulsion performance, which is referred to as warm gas propulsion. In warm gas systems, the propellant tank is heated to increase its internal energy; therefore, the mass flow rate of the expanded gaseous propellant is increased due to higher propellant temperature, which in turn lead to higher propulsion efficiency by enhancing the I_{sp} of the system.

In an effort to mitigate the high pressures often linked with single-phase cold gas propulsion systems, two-phase propellant-based systems were developed. These systems utilize propellants characterized by low saturation pressures, allowing them to be stored within the propulsion tank as a saturated liquid. A saturated liquid is precisely defined as a state wherein both the liquid and gaseous phases of a substance coexist. Propellant selection is critical for cold gas systems because the thrust performance is dependent on the density and molecular weight of the propellant chosen. The propellant storage density is also critical for tank volume. Table 2 shows the most common cold gas propellants. The propellant storage density is a key factor in propellant selection for cold gas since, ideally, a large quantity of propellant will need to be stored in a small volume in order to provide the best propulsion performance. Some propellants, presented in Table 3, can be feasibly stored in the propellant tank as two-phase fluids where these propellants are in a phase change state between liquid and gas at the storage conditions. The use of two-phase propellants is advantageous due to their higher storage density, leading to a more volumetrically efficient propellant storage tank. In addition, these propellants do not require a pressurization system due to their self-pressurizing property at storage conditions.

Table 2. Characteristics of propellants [5,6].

Propellant	Density at 298.15 K, 101.325 kPa (g/cm^3) $\times$ 10^{-3}	Molecular Mass (g/mol)
H_2	0.0820	2.016
He	0.164	4.003
N_2	1.15	28.013
Xe	5.37	131.290
Ar	1.63	39.948
Kr	3.43	83.800
NH_3	0.696	17.031
N_2O	1.80	44.012
R-236fa	1360	152.038
R-134a	1210	102.031
Water	997	18.015
C_4H_{10}	573	58.122
SF_6	5.97	146.056

Table 3. Properties of self-pressurized propellants [5–9].

Propellant	Critical Pressure (MPa)	Critical Temperature (K)	Vapor Pressure at 21 °C (bar)	Liquid Density (kg/m^3)	Advantages ---------- Disadvantages
C_4H_{10}	3.80	425.12	2.6	556	- Ease of storage and handling due to low critical vapor pressure. - Vapor pressure is high enough to overcome internal inertial forces due to friction in the tubes and produce a thrust. ---------- - Flammability can be a safety concern. - Low liquid density.
R-134a	4.07	374.18	5.8	1150	- Moderate liquid storage density and high critical temperature. - Low saturation pressure that could be used without regulation, slightly resulting in higher than desired thrust. ---------- - Lower energy density compared to that of some other propellants. - Not available in some countries.
R-236fa	3.20	398.07	2.4	1320	- Ease of storage and handling due to low critical vapor pressure. - Moderate energy density compared to that of some alternatives. ---------- - Limited availability in some countries.
SF_6	3.77	318.69	21.7	1880	- Saturation pressure is less than half of that of comparable fuels. - Moderately low critical temperature. - The saturation pressure exceeds the suitable inlet pressure for a nozzle, necessitating the integration of a regulation system to have the ability for smaller impulse increments. This, in turn, leads to an augmentation in system complexity. ---------- - Presentation of a potential suffocation hazard because it will displace oxygen in the neighboring area. - Expensive and limited availability due to regulations.
N_2O	7.26	309.57	50.0	1220	- Moderate storage potential. ---------- - Moderate to high cost compared to that of some propellants. - Elevated vapor pressure within the tank would necessitate the implementation of supplementary safety protocols. - Low critical temperature.

Table 3. *Cont.*

Propellant	Critical Pressure (MPa)	Critical Temperature (K)	Vapor Pressure at 21 °C (bar)	Liquid Density (kg/m^3)	Advantages --- Disadvantages
NH_3	11.35	405.50	8.8	680	- Moderate liquid storage density and high critical temperatures - Low saturation pressures that could be used without regulation resulting slightly in higher than desired thrust --- - Increased development costs due to extra safety measures associated with potentially dangerous characteristics of NH3.
Xe	5.84	289.77	53.5	3060	- Xenon has the highest liquid density. --- - Because of its low critical temperature, it remains in a liquid state solely when subjected to high pressure, thereby presenting a safety risk to the ground crew, launch vehicle, and payload.

For small satellite propulsion systems, the initial cold gas system design is based on the following assumptions: (1) negligible losses in feed lines, valve, or regulator; (2) negligible pressure or mass flow losses in the nozzle; (3) an isentropic flow from the regulator to the nozzle exit; (4) an intermittent operation allowing the gas in the tank and the feed line to be isothermal at a specified temperature; (5) an ideal gas; and (6) one-dimensional, steady flow [3]. The thrust force equation is given by the equation as follows:

$$F = \lambda \left\{ \begin{array}{c} A_t P_c \gamma \left[\left(\frac{2}{\gamma-1} \right) \left(\frac{2}{\gamma+1} \right)^{\left(\frac{\gamma+1}{\gamma-1} \right)} \left\{ 1 - \left(\frac{p_e}{p_c} \right)^{\frac{\gamma-1}{\gamma}} \right\} \right]^{\frac{1}{2}} \\ +(p_e - p_a) A_e \end{array} \right\} \quad (4)$$

where λ is the nozzle efficiency, A_t is the throat area, A_e is the nozzle exit area, p_c is the chamber pressure, p_e is the exit pressure, p_a is the ambient pressure, and γ is the specific heat ratio. The characteristic exhaust velocity (c^*) can be calculated using Equation (5). It is a property that depends only on the propellant selection and operating temperature and not on the nozzle. It is a measure of the effective exhaust velocity of the propellant mass that is exhausted from the thruster system.

$$c^* = \frac{\sqrt{\gamma \frac{R}{MW} T_0}}{\gamma \left(\frac{2}{\gamma+1} \right)^{\frac{\gamma+1}{2\gamma-2}}} \quad (5)$$

where R represents the Universal Gas Constant, denoted as 8.314 joules per mole $-kelvin\left(\frac{J}{mol \cdot K}\right)$; MW is the molecular weight; and T_0 refers to the Propellant Operational Temperature.

The mass flow ($\dot{m}$) rate can be calculated as follows:

$$\dot{m} = \frac{A_t p_c}{c^*} \quad (6)$$

Surrey Satellite Technology Ltd. (SSTL) (Guildford, UK) started the effort to develop a cold gas propulsion system for small satellites. SSTL's UoSAT-12 mission, launched in 1999, demonstrated the use of a nitrogen cold gas propulsion system for orbit and attitude control [10]. UoSAT-12 is the first SSTL satellite with on-board propulsion. The UoSAT-12 satellite carried ten cold gas thrusters, providing thrust up to 150 mN with an I_{sp} of 60 s [11]. The thrusters were manufactured by both SSTL and Polyflex Aerospace Ltd. (Greenford, UK) The propulsion system was designed to deliver a ΔV of 14 m/s to the 325 kg spacecraft.

The propellant lifetime was 42,000 s using 27 L of nitrogen stored in three spherical tanks, each at 200 bar. The cold gas thrusters successfully executed a 120 s maneuver to change the semi-major axis of UoSAT-12 by 200 m [12]. Even though the mass of UoSAT-12 is 325 kg, its cold gas system is suitable for smaller satellites under consideration in this review and used as the basis for SSTL's first miniaturized cold gas system.

SSTL and the University of Surrey developed the first miniaturized cold gas propulsion system for its first nanosatellite SNAP-1 that was launched in 2000 [13]. The propulsion system carried 32.6 g of liquefied butane propellant that was used to raise the semi-major axis of SNAP-1 by 3 km. The thruster provides a nominal thrust of 65 mN at 2.1 bar (butane vapor pressure at 293.15 K) without needing a pressurization system for propellant storage. Butane was chosen due to its relatively high storage density of 0.54 g/cm^3, making it a more suitable choice for smaller satellites with size constraints. The total wet mass of the spacecraft was 6.5 kg, and the mass of the propulsion system was 450 g including the propellant [14]. The propellant was stored in a 1.1 m coiled titanium tubing (65 cm^3 storage volume), depicted in Figure 3, instead of a conventional tank in order to fit within a central triangular allocated space, have a more even mass distribution along the tube without needing a pressure vessel, and utilize low-cost standard tubing material. The valve was supplied by Polyflex Aerospace Ltd. The butane propulsion system provided a total mission ΔV of 2 m/s and achieved an I_{sp} of 43 s [14]. The achieved specific impulse was lower than the theorical value of 70 s due to liquid propellant being expelled at the start instead of gas, which reduced the efficiency of the system.

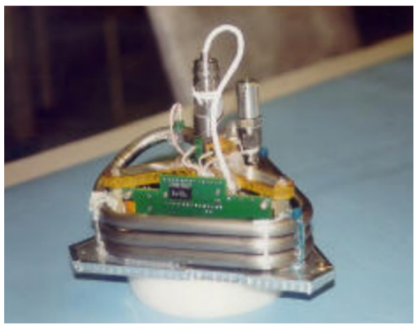

Figure 3. SNAP-1 propulsion module [14].

Moog Inc. developed miniature cold gas thruster heads for the Challenging Mini-Satellite Payload (CHAMP) and the Gravity Recovery and Climate Experiment (GRACE) missions. Even though the masses of CHAMP and GRACE are greater than 500 kg, Moog's efforts to develop miniature thruster heads are noted here for their potential suitability for use in smaller satellite missions. The CHAMP mission, launched in 2000, used Moog's 58E14316 thruster model that is capable of providing a 16 mN thrust using nitrogen at 1.5 bar [15]. The GRACE mission, launched in 2002, carried two Moog thruster models: two 40 mN thrusters for orbit control and twelve 10 mN thrusters to supplement the magnetic torque rods for attitude control [16].

VACCO Industries developed a cold gas micro-propulsion system for 1 U CubeSats to be used in the Aerospace Corporation Micro-Electromechanical Systems PicoSat Inspector (MEPSI) mission. VACCO used its Chemically Etched Micro System (ChEMS) technology to build the MEPSI propulsion unit. The propulsion unit has a total wet mass of 509 g and is capable of providing a thrust of 55 mN [17]. The propulsion system was designed to store 53 g of liquid butane in a 95 cm^3 tank. VACCO delivered this propulsion unit to Aerospace Corporation in 2004 meeting all the requirements to be integrated in the MEPSI picosatellite; however, Aerospace Corporation decided to build a low-cost alternative propulsion unit for the mission using the stereolithography apparatus (SLA) additive rapid manufacturing technique [18]. This method combines all necessary cold gas system components such as the tank, valves, and nozzles to be built in a single unit. Aerospace Corporation developed a cold gas propulsion unit for the MEPSI picosatellite that launched on STS-116 in 2006.

The United States Space Shuttle Discovery STS-116 mission ejected two picosatellites: the target with no propulsion and the inspector with propulsion. The propulsion unit weighed 188 g. The inspector picosatellite was designed to store R-236fa in a 20 cm^3 tank in order to provide the picosatellite with a ΔV up to 20 m/s. Since NASA required additional testing to ensure that the picosatellite would not hit the Orbiter, the Aerospace Corporation used xenon gas to provide a NASA-acceptable ΔV of 0.4 m/s without the need to perform additional safety testing.

VACCO developed a fully integrated propulsion system called the Palmoar Boeing micro-propulsion system [19]. It consists of eight 35 mN cold gas thrusters that are distributed to provide six degrees of freedom (DoF) in rotation and translation. The integrated system components are a main tank, a plenum, a pressure transducer, a temperature thermistor, a fill valve, an isolation valve, and eight thruster valves and thruster nozzles. The thruster testing performed over 200,000 firings in a simulated space environment. The propulsion system was designed to carry liquid isobutane. The total mass of the system is 1063 g. VACCO delivered this unit to Boeing Satellite Systems in 2006 [20].

Marotta Controls developed a cold gas micro-thruster that flew on the NASA ST-5 mission in 2006 [21]. The micro-thruster was integrated to be part of a welded propulsion system that consists of a propellant tank, pressure transducer, filter, fill and drain valve, braces, and tubing. The micro-thruster uses nitrogen as the propellant. It weighs 78 g and is capable of providing 2100 mN of thrust at 2000 psi and 100 mN at 100 psi. The ST-5 consisted of three 25 kg satellites. Each satellite incorporated a single cold gas micro-thruster into its propulsion system. Two of the micro-thrusters the flew were completely emptied and achieved 6000 in-orbit pulses with a tank pressure degrading to 30 psi at the end.

The Nanosatellite Propulsion System (NANOPS), developed by the University of Toronto's Space Flight Laboratory (SFL), flew on the CanX-2 mission in 2008 as a technology demonstration for the subsequent 2014 CanX-4 and CanX-5 formation flying mission [22]. The NANOPS is a cold gas propulsion system. It utilizes commercial-of-the-shelf (COTS) components for its design and uses non-toxic sulfur hexafluoride (SF_6) as the propellant. CANX-2 is a 3U CubeSat that has a mass of 3.5 kg. The NANOPS was designed to provide a total ΔV of 2 m/s, an I_{sp} of 40 s, and a thrust up to 50 mN. The NANOPS was a scaled down prototype of the Canadian Advanced Nanosatellite Propulsion System (CNAPS) that flew on the CanX-4&5 mission. Each CanX-4&5 spacecraft weighs approximately 6 kg [23]. The CNAPS consists of four cold gas thrusters that are capable of providing a thrust range of 12.5–50 mN with an I_{sp} of 45 s and a total ΔV of 18 m/s using 260 g of liquid SF_6. SF_6 was selected because it is a self-pressurizing propellant, is safe to handle, and has a high storage density. An interior view of the CNAPS is presented in Figure 4. Key features to note are the two contaminant removal filters to prevent solenoid valve damage and a pressure relief valve on the storage tank to prevent over-pressurization. The CNAPS accomplished the formation flying mission successfully and was used to bring the two satellites from a maximum range of 2300 km to the closest controlled range of 50 m.

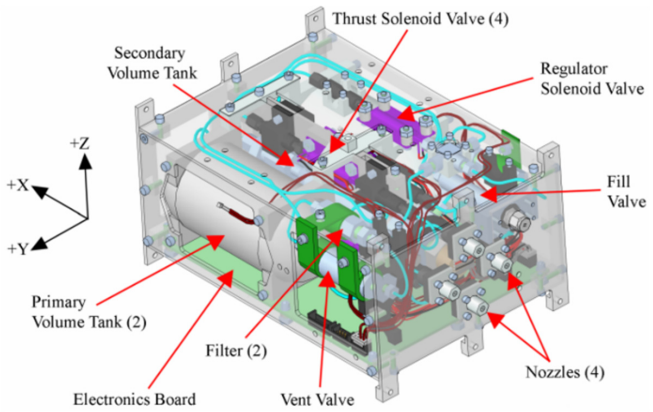

Figure 4. CNAPS propulsion system interior view [23].

The Prototype Research Instruments and Space Mission Technology Advancement (PRISMA) is a formation flying and rendezvous mission led by the Swedish Space Corporation [24]. The first NanoSpace miniaturized cold gas propulsion system, based entirely on Micro-Electromechanical Systems (MEMS) manufacturing technology (Robert Bosch GmbH (Gerlingen, Germany), Broadcom (Palo Alto, CA, USA), Qorvo, Inc (Greensboro, NC, USA) STMicroelectronics (Geneva, Switzerland)), flew on the PRISMA mission in 2010 as a flight experiment. The MEMS technology enables the miniaturization of propulsion system components and was chosen to reduce mass and volume, allowing for increased redundancy. The MEMS-based micro-propulsion consists of four thrusters that are designed to provide a thrust range from 0.01 to 1 mN using gaseous nitrogen. The thruster hardware and control electronics functioned successfully in orbit; however, transmitted data showed that there was no pressure in the tank which prevented the full demonstration of the thruster [25]. The mission team hypothesized that this was due to on-board leakage. Even though the PRISMA spacecraft mass is 145 kg, NanoSpace efforts to demonstrate MEMS micro-propulsion technology are noteworthy and relevant to the focus of this review. Leveraging its flight-demonstrated thruster hardware in PRISMA, NanoSpace developed a MEMS-based cold gas thruster called CubeProp that was launched in the TW-1/STU-2 CubeSat mission in 2015 [26]. CubeProp is a proportional closed-loop thrust control system for 3U CubeSats. CubeProp, also known as the 3U NanoProp, consists of four 1 mN thrusters with 5 µN thrust resolution [27]. The propulsion module can provide a ΔV up to 15 m/s for a 2.66 kg satellite using only 60 g of butane under 2–5 bar. The propulsion module contains a mass flow sensor to inform the proportional flow thrust controller and provide continuous thrust regulation ranging from 0 to 1 mN. NanoSpace, currently known as GomSpace, developed a scaled-up version of the 3U NanoProp for 6U CubeSat configurations [28]. The 6U propulsion system was flown on the GOMX-4B formation flying demonstration mission in 2018. A total of four 1 mN thrusters fired a series of burns for about 9 min and 40 s to bring the GOMX-4B into an orbit with a semi-major axis of 350 m above GOMX-4A [29]. GomSpace also signed a contract to supply the 3U NanoProp system for the Astrocast nanosatellite constellations [30]. Starting from the Astrocast 0.2 mission launched in 2019 until Astrocast 16 (launched in 2023), a total of 19 satellites were launched with the in-orbit propulsion capability provided by the 3U GomSpace propulsion system [2]. Both the 3U and 6U configurations of the GomSpace Butane Propulsion System are flight-proven MEMS-based micro-propulsion systems.

Delfi-n3Xt, launched in 2013, is the second Delfi 3U CubeSat of the Delft University of Technology (TU Delft) for education and technology demonstration [31]. The Delfi-n3Xt successfully demonstrated the T^3-μPS cold gas micro-propulsion technology that was developed by the TU Delft, TNO, University of Twente, and SystematIC Design BV. The micro-propulsion system uses Cool Gas Generators (CGGs) to ignite a solidified grain propellant and release nitrogen gas to be pressurized and stored in a tank for thrust operations. Therefore, this indicates that that system was only pressurized in space before the in-orbit thrust operation. The micro-propulsion system was capable of providing a thrust of 6 mN while consuming 10 W of power for the CGG's ignition for up to 10 s. Two ignitions were successfully performed in orbit; however, the ignition train malfunctioned. The technology demonstration mission concluded that incorporating a parallel design for the ignition train is recommended to avoid single-point failure and reduce the risk of ignition train failure.

A cold gas micro-propulsion system that consists of eight 1 mN micro-thrusters was developed by Microspace Rapid Pte Ltd. (Singapore) and flown on the POPSAT-HIP1 mission in 2014 [32]. The POPSAT-HIP1 is a 3U CubeSat with a mass of 3.3 kg. The system uses argon gas as the propellent. Six thrusters are located at the front of the satellite for yaw and pitch control, whereas two thrusters are located at the side of the satellite for roll control. The thrusters were placed in a such manner that they provide three-axis rotation control, as well as a net force for station keeping and formation flying missions. Each thruster provides a 1 mN nominal thrust using argon stored at 5 bar. Each nozzle is

operated using an electromagnetic microvalve with a short opening time of 1 milli-s. This system was successfully demonstrated in space. The mission-averaged specific impulse is 43 s, and the total mission ΔV was 3.05 m/s.

Glenn Lightsey team at the University of Texas Austin's Satellite Design Lab led the development of a 3D cold gas propulsion system for small satellites using the stereolithography process [33]. This method was chosen because it enables the manufacturing of complex volume and intricate features. This propulsion system uses a saturated R-236fa liquid propellant. It is made of Accura Bluestone plastic. The first flight prototype of this system was developed for the University of Texas at Austin's Bevo-2 satellite for technology demonstration in 2012. Bevo-2 is a 3 U CubeSat. The propulsion system weighs 400 g and has a size of 0.4 U. It has a rated thrust level in the range of 110–150 mN and a specific impulse range of 65 s to 89 s at 297.15–358.15 K. Bevo-2 was launched in 2016; however, its software did not function as planned after launch [34]. Leveraging the same manufacturing technique, the Texas Space Laboratory (TSL) and University of Texas Austin developed a modified version of the Bevo-2 thruster for the attitude control of the JPL's Interplanetary NanoSpacecraft Pathfinder In Relevant Environment (INSPIRE) spacecraft [35]. Two flight unit thrusters or INSPIRE spacecraft were developed and delivered to JPL in 2014. Each thruster has a total wet mass of 1090 g and a volume of 0.7 U. The thruster is capable of producing 60 mN of thrust at 20 °C, with a specific impulse of 65 s. The mission has not been launched yet.

VACCO Industries built a cold gas propulsion system in 2017 for the CubeSat Proximity Operations Demonstration (CPOD) mission [36]. The system uses R236fa to deliver a nominal thrust of 10 mN and a specific impulse of 40 s. It consists of a total of eight thrusters that performed +70,000 firings in vacuum at the US Air Force Research Lab. It has a total mass of 1.24 kg and a volume of 0.8 U. The system was demonstrated in the CPOD mission that was launched in 2022; however, challenges with the system-level guidance, navigation, and control systems led to fuel depletion earlier than expected [37]. The goal of the CPOD mission was to demonstrate rendezvous, proximity operations, and docking maneuvers of two 3U CubeSats. Although multiple rendezvous maneuvers brought one CubeSat from hundreds of miles to within a few hundred yards of the other CubeSat, the final docking objective of CPOD was not accomplished during this mission.

Aerospace Corporation developed a steam thruster for the AeroCube-7B/7C satellites launched in the NASA Ames Research Center's Optical Communications and Sensor Demonstration (OCSD) mission in 2017 [38]. The steam thruster is a warm gas micropropulsion system that works by heating a small tank of water in advance and releasing steam to generate thrust. It requires a water vaporization heat input of 2.9 W/mN in order to sustain continuous thrust operation [38]. Water was chosen because it is not toxic, not flammable, and does not require pressurization for propellant storage. A second generation of the steam thruster flew on the AeroCube-10B in 2020 [39]. The thruster is capable of providing a total ΔV of 6 m/s using 30 g of water. The thruster warms up water 20 min prior to the desired thrust operation. The total thrust capability of this steam thruster is 4 mN with a specific impulse of 70 s. Due to low thrust capability, this steam thruster is only used for proximity and station-keeping operations. In-orbit formation flying maneuvers used the steam thruster to reduce the separation of two satellites from over 1000 km to 0.1 km over the course of several weeks.

The Sapienza aerospace research center developed a nitrogen MEMS cold gas micropropulsion system that was launched on-board the Ursa Maior CubeSat mission in 2017 [2,40]. The thruster was designed to work as a pressure regulated system that provides a constant thrust performance despite fuel depletion [40]. The design utilized MEMS techniques to manufacture and integrate the valve–nozzle design. The in-orbit testing aims to apply a constant thrust for a specified duration for the attitude control of the Ursa Maior CubeSat.

The Mars Cube One (MarCO) technology demonstration was part of JPL's InSight mission, launched in 2018, and carried an integrated micro-propulsion system developed

by VACCO Industries [41]. MarCO is a 6U interplanetary CubeSat with a mass of 14 kg. The propulsion system uses R236fa as propellant and weighs 3.49 kg [42]. It is capable of a 25 mN thrust. The propulsion system consists of four thrusters for attitude control and another four for trajectory correction maneuvers (TCMs). Five TCMs were successfully performed during the interplanetary transit to Mars [41]. Although the thruster experienced leaks during the mission, the mission team managed to handle the issue and deliver MarCO to relay data for the InSight entry, descent, and landing operations.

ThrustMe developed the first prototype of the I_2T_5 iodine cold gas thruster and tested it on board the Xiaoxiang 1-08 satellite mission that launched in 2019 [43]. The I_2T_5 module is the first iodine propulsion system to be tested in space. The module uses the sublimation of solid iodine to build up a gas pressure in the storage tank. The prototype was designed to produce a 0.2 mN thrust. The I_2T_5 module is integrated in the Robusta-3A, the University of Montpellier 3U CubeSat mission, which is expected to launch in June 2024 [2,44].

Cornell University developed a 3D-printed cold gas propulsion system for the two 3U CubeSats in the Pathfinder for Autonomous Navigation (PAN) mission that was launched in 2022 [45,46]. The propulsion system uses 164 g of R236fa to produce a thrust of 25 mN with an I_{sp} of 33 s [45]. R236fa was chosen due to its flight heritage, low vapor pressure, and its relative safety compared to the those of the other possible propellant candidates. The system was manufactured using stereolithography and Accura Bluestone plastic.

A cold gas propulsion system was developed to maintain formation flying of three nanosatellites flown in the Adelis Space Autonomous Mission for Swarming and Geo-locating Nanosatellites (Adelis-SAMSON) mission in 2021 [47]. The mission was developed by the Asher Space Research Institute at Technion. The propulsion system consists of four 20 mN thrusters that use Krypton as the propellant [48]. The system has a rated specific impulse of 34 s. Krypton was found to be the most suitable propellant for the mission due to its density, meeting the mission volume constraint and ΔV requirement. The propulsion system weighs 2 kg and occupies a volume of 2U.

The Italian Space Agency developed and integrated a cold gas propulsion module for the Light Italian CubeSat for Imaging of Asteroid (LICIACube) mission that launched with the NASA Double Asteroid Redirection Test (DART) mission in 2021 [49,50]. The DART mission is the first mission to test the changing of the asteroid orbit as a result of kinetic impact. The LICIACube is a 6 U CubeSat with a total mass of 14 kg [50]. The propulsion system used in LICIACube has a ΔV capability of 56 m/s. It successfully fired a separation maneuver from the DART spacecraft in order to accomplish its mission goal and return images of the DART spacecraft impact with asteroids.

T4i developed cold gas propulsion systems that use R134a as the propellant [51]. PERSEUS has a volume of 2.5 U. It provides thrust in the range of 10–30 mN with an I_{sp} of 40 s. PERSEUS is designed for proximity operations, providing 3-axis attitude and thrust control. It was developed for the IPERDRONE.0 mission that is scheduled to launch in 2024. The IANUS module has a volume of 0.5U, and it provides thrust in the range of 6.8–26.2 mN with an I_{sp} of 40 s. It was developed for the Hera mission.

SSDL at Georgia Tech has developed a heritage of 3D-printed cold gas propulsion systems that are used in several small satellites missions [52]. The utilization of additive manufacturing offers customizability to the propulsion system volume and design for use in different space missions. SSDL cold gas heritage started with the development of propulsion modules based on the UT Austin 3D cold gas unit developed initially for the 2015 BEVO-2 mission. The baseline propulsion system design for all of SSDL's miniature cold gas heritage is a two-tank design where the main tank stores a saturated liquid/vapor mixture (R-236fa) and a smaller tank called the plenum that contains only vapor to be released into the nozzles. SSDL developed a cold gas thruster for the Air Force Research Lab's (AFRL) Ascent mission that launched in 2021 to test several small satellite technology demonstrations and the survivability of COTS in a Geostationary Earth Orbit (GEO) environment including the SSDL's cold gas thruster [53]. SSDL also developed a miniature 3D-printed cold gas system for the NASA BioSentitnel mission that launched in 2022 [2,54].

The propulsion system was designed to provide attitude control and momentum management for the interplanetary a 6U BioSentitnel CubeSat. The cold gas system, consisting of seven thrusters, is capable of providing nominal thrust in the range of 40–70 mN using the R-236fa propellant [54]. The propulsion systems developed for the formation flying of 6U CubeSats in the upcoming missions studying the sun: NASA's SunRISE mission, the VISORS mission, and the SWARM-EX mission are all based on the SSDL 3D cold gas heritage [52,55].

VACCO Industries developed the micro-propulsion system (MiPS) to provide the attitude control and orbital maneuvering for the following missions: CubeSat for Solar Particles (CuSP), Near-Earth Asteroid Scout (NEA Scout), and outstanding moon exploration technologies demonstrated by a NAno Semi-Hard Impactor (OMOTENASHI) that launched as secondary payloads of the Artemis 1 mission on the Space Launch System (SLS) in 2022 [2,19]. The MiPS system is a smart, self-contained cold gas system that is based on the flight proven VACCO's MarCO propulsion module developed for 6U CubeSats [19]. It uses a saturated R-236fa mixture as the propellant, and it consists of a varying number of 25 mN cold gas thrusters based on the specific mission requirements. The MiPS units come in a variety of sizes depending on the mission. The NEA Scout MiPS occupies a 2 U volume, while the CuSP MiPS occupies a 0.3 U volume [56,57].

Cold gas propulsion technology has demonstrated extensive flight heritage specifically for the attitude control of small satellites. Cold gas systems offer simple, compact, and low-cost solutions for small satellite propulsion; however, they provide relatively low thrust and specific impulse performance.

Cold gas systems can be further enhanced by adding heat to the working propellant before it enters the thruster body. The heat is applied without chemical reaction, raising the internal energy of the propellant. This leads to an increased mass flow rate and a slightly improved specific impulse performance. This enhanced cold gas system is referred to as warm gas propulsion.

3.1.2. Resistojet

Resistojet propulsion is similar in principle to cold gas propulsion, with the addition of heating the flowing gaseous propellant using electrical heating devices. The heating is applied to surfaces in the thruster body that the propellant flows through; therefore, heat is transferred to the flow in order to increase its temperature and thus its mass flow rate. The heated gas accelerates through the nozzle, propelling the spacecraft. The working principle is depicted in Figure 5.

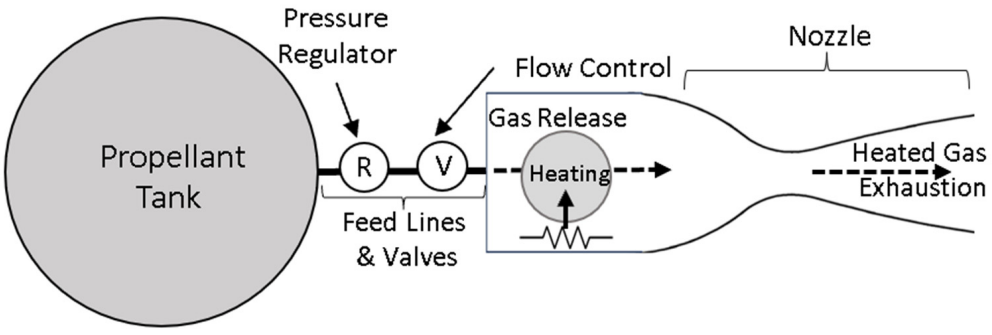

Figure 5. Resistojet system schematic.

In comparison to warm gas, the heating in resistojet systems is applied to the propellant flow as it enters the thruster chamber. Cold gas, warm gas. and resistojet propulsion share the same primary source of energy which is the internal energy of the stored pressurized fluid. In the case of resistojet, this energy is augmented by increasing the enthalpy of the flowing gas through electrical heating.

The heating element plays a critical role in the resistojet design system. The heating element uses electrical energy that is transformed into heat. The key theoretical thermodynamics equation is the heat rate as shown below:

$$\dot{q} = c_p \dot{m} \Delta T \tag{7}$$

where $\dot{q}$ represents the rate of change in heat. The term c_p signifies the specific heat at constant pressure. ΔT denotes the Temperature Change between the initial temperature and the temperature attained after heating.

In the University of Surrey, Tim Lawrance designed a 100 W resistojet system for a technology demonstration in the UoSat-12 mission that launched in 1999 [58]. The resistojet system was developed by Surrey Space Center for demonstrating resistojet propulsion orbit control for the UoSat-12 satellite. A short duration burn was conducted in 1999. The system was fired for 15 s at a power of 91 W, and it achieved a thrust of 95 mN and a specific impulse of 93 s. The system was qualified to use either nitrous oxide (N_2O) or water as the working propellant. N_2O is non-toxic, is low-cost, has relatively high storage density, and is self-pressurizing at 48 bar (vapor pressure); therefore, it does not require a pressurant system (less mass and volume required). The resistojet thruster body is made of stainless steel. It contains a 100 W cartridge heater to heat the propellant to 1073.15 K [59]. A silicon carbide (SiC) was used for the heat exchanger. The heater element is coiled onto a central bobbin to increase contact between the propellant flow and heater as shown in Figure 6.

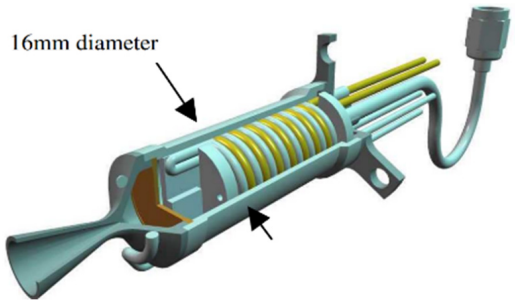

Figure 6. Sectional view of UoSat-12 100-W resistojet [59].

SSTL developed a low-power resistojet system for its earth observation constellation called the Disaster Monitoring Constellation (DMC) [60]. A low-power butane resistojet thruster, referred to as T15, was developed for the ALSAT-1 that launched in 2002. Butane was chosen due to its high storage density and its low vapor pressure at 2 bar. The thruster consists of a standard converging-diverging nozzle with a throat diameter of 0.42 mm and two cylindrical tanks aligned in an L-shaped orientation [59]. The T15 thruster is made of stainless steel. It contains two redundant 15 W heating elements inside its body in order to heat the vapor and increase the mass flow rate. Butane is stored in liquid phase. The resistojet thruster vaporizes the propellant to ensure none of the liquid phase propellent is expelled through the nozzle. This is accomplished through several design choices: keeping liquid away from tank exits via surface tension provided by aluminum mesh tank inserts, a line heater coiled around the tank outlet pipe and vent valve feed pipe to prevent condensation, and an integral heater to vaporize any residual liquid and enhance mass flow rate through the thruster body [60]. All heating elements have a warm-up time of around 10 min during each thrust operation. ALSAT-1's propulsion system performed a total of 273 firings with a cumulated firing time of more than 12 h 49 min. It achieved a total mission ΔV of 25.3 m/s, an average specific impulse of 99.9 s, and a mission average thrust of 48.8 mN. The same propulsion system technology was also flown in the NigeriaSat-1 (90 kg) and the UK-DMC-1 (90 kg).

A low-cost water micro-resistojet system experiment was developed and tested on-board the UK-DMC spacecraft in 2004 [61]. It is believed to be the first water propulsion system to be flown and tested in space. The thrust value achieved was 3.3 mN using 3 W of

power and 2.06 g of water propellant. The water micro-resistojet has a total mass of 188 g. The thruster needed to be pre-heated to around 473.15 K before each thrust operation. Even though the experiment encountered an early water depletion issue, the first firing was successfully performed and indicated the feasibility of water resistojet systems for small satellites in space.

Leveraging its butane resistojet flight heritage in the DMC as the basis, SSTL tested the same resistojet thruster system with xenon in 2003 [62]. The only difference was the thruster operating power. SSTL developed a xenon low-power resistojet system, referred to as T30, that was flown on several missions, including but not limited to the Beijing-1 in 2005, RapidEye in 2008, and Proba-2 in 2009. The T30 is capable of providing a specific impulse of 48 s using two redundant 30 W heaters with a typical operating temperature of 803.15 K.

The AFRL and University of Southern California designed and tested a free molecule micro-resistojet (FMMR), also known as a low-pressure micro-resistojet (LPM), concept for the on-orbit maneuvers of nanosatellites. The FMMR was first designed in the late 1990s [63]. In 2005, a design with the heater integrated in the expansion slot was proposed and tested [64]. The main parts of the FMMR system are the heater chip, the plenum, and the propellant feed system. The working principle is rarefied gas dynamics. The FMMR is characterized by low-pressure operation which is beneficial to nanosatellite mission since valve leak rates depend on operating pressure, and the FMMR is designed to maintain a propellant vapor pressure stored as either a liquid or solid at a nominal storage temperature. Propellant vapor molecules are fed to the plenum and flow through expansion slots as they are heated via a MEMS fabricated heater chip. The performance of the FMMR was assessed using a variety of propellants including helium, argon, nitrogen, and carbon dioxide. An FMMR technology demonstrator using water as the propellant was fabricated and tested in 2007 [65]. The experimental results indicate that the water FMMR is capable of providing a thrust of 0.129 mN and a specific impulse of 79.2 s with a heated wall temperature of 580 K. This experiment showed that the experimental data are similar to those of the predicted performance from kinetic theory.

Delfi-PQ, launched in 2022, includes a micro-propulsion technology demonstration of two of the TU Delft's water micro-resistojet concepts: the Vaporizing Liquid Micro-resistojet (VLM) and the LPM discussed above [2,66]. VLM is based on the vaporization, heating, and expansion of pressurized liquid water, whereas the LPM is based on the heating and acceleration of vapor molecules under free molecular flow conditions [66]. The technology demonstration includes one shared storage tank for the two micro-resistojet thrusters. The FMMR model, developed at the TU Delft, operates via ice sublimation at low pressure (600 Pa) [67]. As ice molecules sublimate in the tank, a heating element is used in the tank to maintain tank temperature and pressure conditions (600 Pa at 273.15 K). The FMMR was estimated to provide a thrust of 1.14 mN and a specific impulse of 88.1 s using 4.51 W. Advantages of this system are low power consumption, very low pressure, and using green propellant. The two Delfi-PQ thrusters are built on a silicon-based MEMS chip and include an integrated molybdenum (Mo) heater [66]. The VLM thruster releases water into a heating chamber in liquid state where it is slightly pressurized (1–5 bar), then vaporized using resistive heating, and finally accelerated in a conventional converging/diverging micro-nozzle. The LPM thruster releases water vapor molecules to the thruster plenum at very low pressure (1–5 milli-bar). It operates with rarefied gas flow conditions; therefore, a constant-area slot replaces the unnecessary nozzle configuration in this case. The propellant molecules are heated by collision with heated expansion slot walls and then expelled to generate thrust as depicted in Figure 7. The Delfi-PQ micro-propulsion demonstrator payload has a total mass of 66 g. The system is capable of producing a maximum thrust of 0.6 mN and a maximum heating power of 2 W with an initial pressure of stored water set to 1.1 bar.

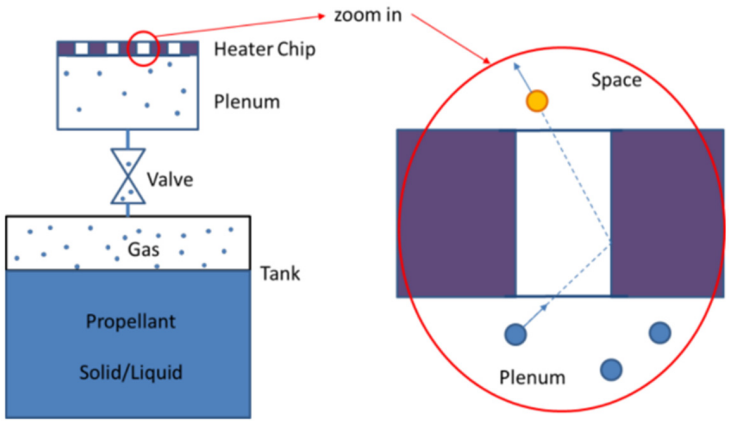

Figure 7. Conceptual working principle of the LPM system [66].

The University of Arkansas designed and manufactured a resistojet propulsion system for the 2U Rapid Prototyped MEMS Propulsion and Radiation Test (RAMPART) CubeSat in 2010 [68]. The propulsion system is based on 3D printing technologies and occupies a volume of 1 U. The propellant used is an R-134a refrigerant which is self-pressurizing at the operational temperature range, non-toxic, and non-flammable. The use of an MEMS heater that consists of bonded silicon layers raises the baseline vacuum specific impulse from 67 s to 90 s. The tank contains a MEMS membrane of porous channels that separates the propellent from the downstream components, as well as preventing liquid propellent from being injected into the thruster system. The MEMS phase separator utilizes surface tension at the walls of the channel to allow only gaseous propellants to pass through. The propulsion system was designed to generate 500 mN.

SSTL designed a butane resistojet system for the Autonomous Assembly of A Reconfigurable Space Telescope (AAReST) mission [69]. It consists of nine 1 W micro-thrusters providing a 6DOF motion and a total ΔV of 10 m/s. The system uses 80 g of liquified butane stored at 2 bar and expelled as gas at 0.5–1 bar using a pressure regulator. Butane was used due to its high density, extensive heritage at SSTL, and relative safety. The total wet mass of the propulsion system is 880 g. The system has a rated thrust range of 5–10 mN with a specific impulse of 80 s.

Alta S.p.A., merged into SITAEL, developed its first Xenon resistojet prototype in 2004 [70]. The prototype has a rated thrust of 50 mN, a rated power of 50 W, and an effective I_{sp} of 55 s for xenon and 75 s for argon. The first generation of SITAEL XR-50 resistojet thrusters were developed in 2006. The performance of XR-50 was improved due to reducing the diameter of a stainless-steel body from 40 mm in the first prototype to 16 mm. The XR-50 has a rated thrust of 100 mN at 50 W, as well as a specific impulse of 55 s using xenon. The XR-100, developed in 2008, has an enhanced thrust performance of 125 mN and an I_{sp} of 63 s for xenon (105 s for argon) using two redundant 50 W heaters. The XR-100 has a lifetime of 200 hrs. In 2017, two models of the SITAEL XR-150 were built and tested with xenon and krypton as propellants [71]. The testing results demonstrated that XR-150 series is capable of providing thrust in the range of 40–150 mN. At 100 W of power, the XR-150 has an I_{sp} of 56.5 s with xenon and 69.9 s with krypton. SITAEL XR-series resistojet thrusters (XR-50, -100, and -150) are low-power xenon-fed thrusters; however, they may be operated with any non-oxidizing gas or liquid droplets [72]. They were designed to be flexible to allow for mission-specific optimization. They can be operated in a cold gas mode with lower performance and lower thermal regimes or in a resistojet mode.

The CubeSat High Impulse Propulsion System (CHIPS) was developed by CU Aerospace and VACCO in 2015 [73]. The system includes a primary micro-resistojet thruster, as well as four 3-axis attitude control thrusters. The system is capable of operating in a resistojet mode or a cold gas mode. R236fa was chosen as the baseline propellant because it is self-pressurizing, non-toxic, and compatible with the International Space Station (ISS). The

system can also use R134a which provides slightly higher total performance, but it has higher tank pressure. The system occupies a volume of 1 U. The micro-resistojet uses a superheater cartridge (SHC) to heat the propellant flow by passing current through a thin-walled tube. In comparison to cold gas mode, the specific impulse is enhanced from 38 s to 60 s by heating the propellant [74]. In resistojet mode, the system is capable of producing a thrust of 23 mN and a specific impulse of 60 s using 25 W of power. It can deliver a ΔV of 123 m/s to a 4 kg CubeSat.

Comet-1000 is a water-based resistojet propulsion system developed by Bradford Space [75]. It has a thrust capability of 17 mN with a specific impulse range of 175–185 s. A continuous trust operation has a power consumption of 55 W, whereas a 1 min operation consumes 25 W of power. The system has a demonstrated flight heritage in the following small satellite missions: HawkEye 360, Capella Space, and BlackSky Global that launched in 2018. The HawkEye 360 pathfinder spacecraft has a mass of 13.4 kg and a total ΔV capability of 96 m/s using the Comet-1000 system [76].

CU Aerospace developed the monofilament vaporization propulsion (MVP) system in 2018 [77]. The system uses extrusion 3D printer technology to feed and melt solid polymer (Delrin fiber) in a temperature-controlled extruder; then, it uses CHIPS's micro-resistojet technology to resistively heat and evaporate the propellant with up to 1100 K heating. The working principle of the MVP system is depicted in Figure 8. Delrin fiber has a high storage density of 1.4 g/cm^3 and does not require pressurization. The system is currently rated at TRL 6 [78]. A flight unit was developed for the 6U DUPLEX CubeSat that is expected to launch in 2023. The MVP flight unit has a total wet mass of 1.055 kg. It can deliver a thrust of 4.5 mN and a specific impulse of 66 s. For a 4 kg CubeSat, the system can provide a ΔV of 75 m/s. This design does not require pressure vessel for the propellant and has a compact size of 1 U and an average specific thrust of 0.17 mN/W.

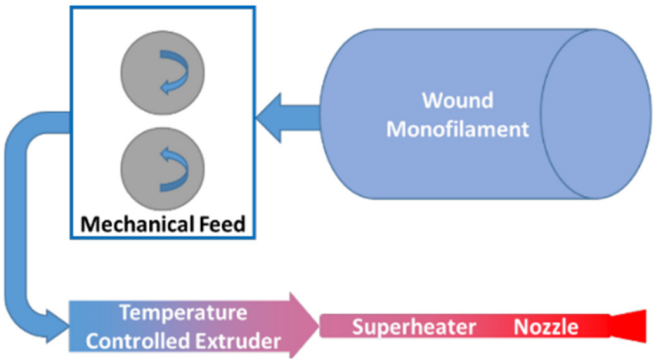

Figure 8. MVP system schematic [78].

The Algerian Space Agency developed a nitrogen resistojet that uses a 30 W coiled heater [79]. It is capable of providing 50 mN and an I_{sp} of 98 s using 2.04 kg of nitrogen propellant. This system was flown in 2019.

The University of Southampton developed a prototype of the Super-High Temperature Additive Resistojet (STAR) thruster in 2018 [80]. The system uses an innovative multifunctional monolithic heat exchanger, which was 3D-printed via Selective Laster Melting (SLM). The prototype is made of 316L stainless steel for proof-of-concept validation. The thrust was measured to be in the range from 9.7 mN to 29.8 mN using argon, and the maximum measured specific impulse was 80 s.

A water resistojet propulsion system called AQUARIUS (AQUA ResIstojet propUlsion System) was designed and developed by the University of Tokyo in 2016 [81]. It consists of a tank, a vaporization chamber, and a nozzle. A flight prototype was flown in the 3U CubeSat AQT-D (AQua Thruster-Demonstrator) that launched in 2019 [82]. In the AQT-D, the propulsion system includes a 4 mN Delta-V thruster that is characterized with an Isp of 70 s and power consumption of 18 W for orbital maneuver. In addition, it has four 1 mN reaction control thrusters with a power consumption of 4.5 W for reaction control.

The AQUARIUS system was integrated and flown in the 6U EQUULEUS interplanetary CubeSat in 2022 [2,81]. In the EQUULEUS mission, the system consists of two 4 mN Delta-V thrusters and four 2 mN reaction control thrusters [81]. The total power consumption is up to 20 W. The AQUARIUS system occupies 2U. Water is stored in a bladder inserted in the tank as depicted in Figure 9. It operates by supplying water to the vaporization chamber where water is heated and vaporized by means of electrical heaters and waste heat from communication components. Using waste heat is a design feature that reduces power consumption of the system. Water vapor is then supplied to the pre-heater. The pre-heater is made of aluminum and contains a helical flow pass to increase heating area. When the water vapor flows in the helical flow path, it is heated by heating the outside of aluminum. The heated water vapor is then accelerated at the nozzle to generate thrust.

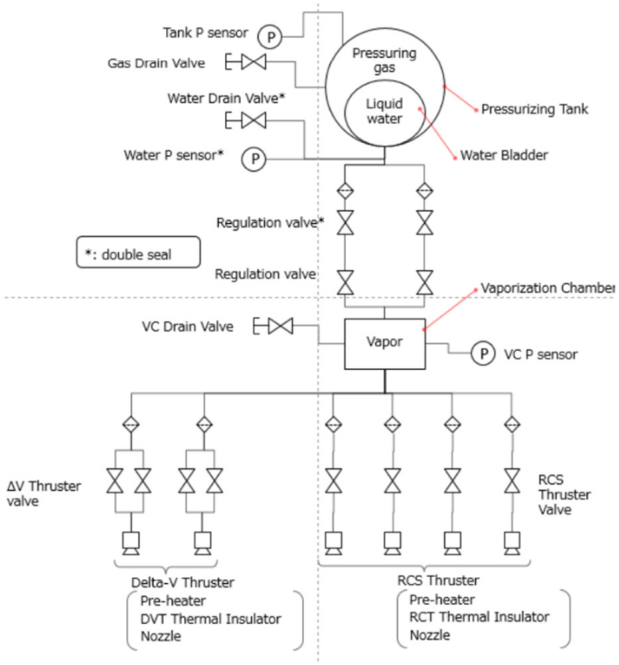

Figure 9. AQUARIUS propulsion system diagram [81].

Aurora Propulsion Technologies developed the Aurora Resistojet Module (ARM) family of water resistojet propulsion systems [83]. ARM-A is a full 3-axis attitude control system consisting of six resistojet thrusters. Each thruster is capable of providing a thrust up to 4 mN. The ARM-A system is available in different sizes for the 1–3 U sized CubeSat. A version of ARM-A was launched as a technology demonstration in the AurorSat mission in 2022 [84].

Steamjet Space Systems developed the Steam TunaCan Thruster for CubeSats [85]. This water-based resistojet system has a cylindrical shape (8 cm × 8 cm) and is designed to fit within the tuna-can volume in the CubeSat deployer. Therefore, the system is installed externally and does not occupy the internal limited volume in CubeSats. The system is characterized with a thrust of 6 mN, an I_{sp} of 172 s, a total impulse of 219 N-s, and a power consumption of 20 W. It uses a safe and green propellant to provide high I_{sp} performance for 1–6 U CubeSats. It has a wet mass of 540 g, and it is currently rated at TRL 7. Steam Jet also developed the Steam Thruster One system for larger CubeSats and small satellites. The baseline design of the Steam Thruster One contains a water tank with a 1 U volume; however, it can be scaled depending on the mission needs. The 1 U water tank delivers a total impulse of 1000 N-s. The thrust capability is 6 mN and can be increased if more than 20 W of power can be used.

Resistojet propulsion offers improved specific impulse performance at the cost of the increased power consumption required for heating. As presented in this section, many resistojet systems were designed and flown in small satellite missions since the power

consumption of resistojet systems is within an acceptable range that can be attained in small satellite missions.

3.2. Chemical Propulsion

The main source of energy in chemical propulsion is the chemical energy stored within the molecular bonds of the propellant. The energy in these bonds is released via an exothermic chemical reaction. The chemical reaction generates heat and products that accelerate to produce thrust. Chemical propulsion systems are categorized into liquid propulsion, including monopropellant and bipropellant, and solid propulsion. The combination of liquid and solid propulsion is referred to as hybrid.

3.2.1. Monopropellant

Monopropellant propulsion generates hot gaseous exhaust produced by thermal decomposition of a liquid propellant using catalyst. A monopropellant system consists of tank pressurization propellant storage, propellant feed system, flow control valve and injector feed, a catalyst bed, and a nozzle as depicted in Figure 10.

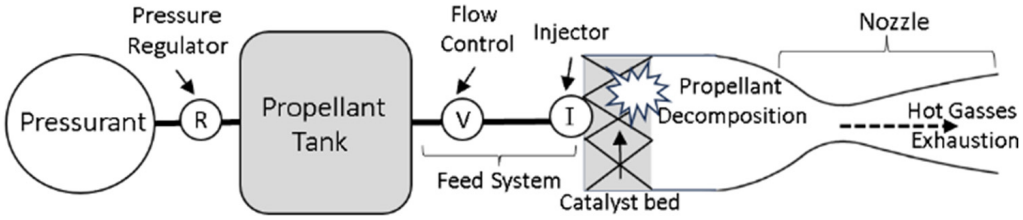

Figure 10. Schematic of monopropellant propulsion system.

The common conventional propellants for this system are hydrazine, (N_2H_4) which operated most monopropellant systems with flight heritage in the past. However, safer, high-performing, and non-toxic propellants such as hydrogen peroxide (H_2O_2), hydroxylammonium nitrate (HAN)-based propellants, and ammonium dinitramide (AND)-based propellants have been used as alternatives to hydrazine. Hydrazine is classified as a hazardous propellant and requires added measures to ensure safe handling and testing [86]. AF-M315E is a HAN-based propellant that was developed by the Air Force Research Laboratory (AFRL) in 1998 and was flight-demonstrated as a green chemical propellant in NASA's Green Propellant Infusion Mission (GPIM) in 2019. The full decomposition of AF-M315E produces an adiabatic flame temperature of around 2073.15 K, which is greater than that of hydrazine, leading to an approximately 13% increase in I_{sp} and a 63% increase in density I_{sp} performance [86–88]. Due to the much higher flame temperature, the decomposition of AF-M315E requires much higher catalyst pre-heating compared to that of hydrazine, therefore posing challenges in catalyst design [88]. LMP-103S is an ADN-based propellant that has flight heritage in the PRISMA spacecraft monopropellant thruster that was launched in 2010 [86,89]. The LMP-103S propellant has up to 30% higher density impulse performance compared to that of hydrazine [90]. Hydrogen peroxide offers slightly decreased specific impulse performance; however, it is widely available, less costly, and has less material restrictions due to its relatively lower flame temperature [91]. The use of AF-M315E and LMP-103S propellants poses additional challenges associated with thermal management, material selection, and catalyst bed design due to their relatively higher flame temperatures. The selection of propellants plays a critical role in the performance of monopropellant systems. The testing of green propellants shows comparable and slightly improved specific impulse performance as shown in Table 4 [92]. Thus, green monopropellants provide a more suitable option for small satellite in-space propulsion due to higher performance and better storage density compared to those of hydrazine-based systems.

Table 4. Monopropellant performance characteristics [92].

Propellant	Density (g/cm^3)	Theoretical I_{sp} (s)
N_2H_4	1.01	242
AF-M315E	1.47	266
H_2O_2	1.45	161
LMP-103S	1.24	252

Technology employing 1N class hydrazine monopropellants has extensive heritage for small-sized to medium-sized satellites with a mass typically larger than 100 kg. However, the 1N class series can potentially be usable in <100 kg satellites. ArianeGroup developed the 1N monopropellant hydrazine thruster for small satellites. It has a thrust range of 320–1000 mN and a nominal specific impulse of 220 s [93]. This thruster was successfully flight-demonstrated, with more than 500 units launched into space. ArianeGroup's 1N thruster was flown in Alsat-2A (117 kg) satellite in 2010. The thruster features a flow control valve, an internal redundant catalyst bed heater, and thermal insulation. Moog developed the MONARC-1 thruster [94]. The thruster uses hydrazine as the propellant. It has a rated thrust up to 1000 mN and a specific impulse of 227.5 s. MONARC-1 is the smallest thruster (and with the lowest thrust capability) in the Moog's space-proven MONARC series. Northrop Grumman's flight-demonstrated MRE-0.1 thruster is capable of providing a thrust of 400 mN at maximum operating pressure (420 psi) using hydrazine as the propellant [95]. It has a steady state specific impulse of 216 s at 250 psi.

Aerojet Rocketdyne developed the Modular Propulsion System (MPS) family for CubeSats. MPS-120 uses hydrazine and is scaled to fit in a 1 U or 2 U envelope [96]. The system uses a piston tank that includes a piston, a propellant tank, and a condensable pressurant tank. MPS-125 uses hydrazine that is stored in a pump tank system that includes a propellant management device (PMD). The MPS-125 system can be scaled to a variety of sizes: 4 U, 6 U, or 8 U. The MPS family utilizes Aerojet Rocketdyne's extensive heritage of monopropellant thrusters. Each MPS unit consists of an array of thrusters, typically four thrusters as the baseline. Each thruster is capable of providing a thrust ranging from 250 mN to 1000 mN.

Due to the hazards associated with hydrazine and its effects in mission safety measures, Aerojet Rocketdyne also developed alternative green monopropellant propulsion systems for CubeSats with AF-M315E as the propellant. The thrusters that use AF-M315E are referred to as the GR-1 thrusters which were flown in NASA's GPIM mission in 2019 [97]. The GPIM successfully demonstrated the first-generation Aerojet's green thrusters (GR-1s). The next-generation GR-1A thrusters utilized advances in catalyst manufacturing to enhance the performance and reduce cost. Following successful operation of GPIM, Aerojet Rocketdyne also developed the GR-M1 miniaturized 250–500 mN derivative of the GR-1 flown in the GPIM. Following the same modular approach for commercializing monopropellant propulsion for CubeSat, the MPS family also includes green systems such as the MPS-130 and the MPS-135 [96].

Busek's BGT-X5 uses AFM315E to provide up to 500 mN of thrust with a specific impulse range of 220–225 s at 400 psi feed pressure [98]. It features a fully welded titanium bellows tank, a post-launch pressurization system cell, a space-proven piezo microvalve, and a patented catalyst reactor that is robust to AFM315E's high temperature and oxidizing combustion. The system occupies a 1 U volume. It is capable of delivering a ΔV of 146 m/s to a 4 kg CubeSat.

Bradford ECAPS's High Performance Green Propulsion (HPGP) Thruster uses LMP-103S to provide attitude and orbit control for small satellites [99]. The 1N class HPGP was successfully flight-demonstrated aboard the PRISMA spacecraft that launched in 2010, as well as the SkySat constellation with first launch in 2016 [99,100]. The PRISMA's HPGP includes two 1 N thrusters that are capable of delivering a total ΔV of 60 m/s [99]. Each thruster consumes 7.3 W of average power to pre-heat the catalyst reactor up to 613.15–633.15 K. Since the HPGP thruster operates at a combustion temperature of 1873.15 K,

ECAPS developed a unique high-temperature resistant catalyst which provides a more efficient combustion compared to that of a hydrazine thruster. The HPGP system provides a 6% theoretical Isp increase compared to that of hydrazine, and for the first half of the PRISMA mission, the HPGP system provided an average I_{sp} increase of 8% over that of the hydrazine system. The 100 mN class HPGP thruster was developed based on scaling down space-proven thruster technology, especially to be more suited for small satellites and CubeSats [100].

The Georgia Tech Space Systems Design Laboratory, NASA Marshall Spaceflight Center, and Jet Propulsion Laboratory developed the Lunar Flashlight Propulsion System (LFPS) [101,102]. The LFPS consists of four 100 mN thrusters (PP3490-B), developed and commercialized by Plasma Processes LLC, that use AF-M135E and has a steady-state-specific impulse of 220 s [103,104]. The green propellant is stored in a titanium tank consisting of two halves that are electron-beam-welded together. LFPS is a pump-fed system with PMD [101]. The pump-fed system design was chosen over a cylindrical pressure-fed system due to the cubic geometry of a CubeSat, as well as the reduced system pressure level provided by the pump. The tank includes the liquid monopropellant and a nitrogen ullage gas to maintain tank pressure. Plasma Processes LLC developed a monolithic metal foam catalyst to be compatible with the green propellant since using the more traditional granular ceramic catalyst leads corrosion due to the high combustion temperature of the green propellant [102]. NASA's Lunar Flashlight launched in 2022; however, the LFPS was unable to generate enough thrust to put the spacecraft into lunar orbit [105]. The design team suspected that the additively manufactured fuel feed system likely developed debris that obstructed fuel lines.

VACCO Industries developed a Micro Propulsion System (MiPS) that consists of four 100 mN bradford ECAPS thrusters that deliver a total ΔV of 237 m/s for a 14 kg CubeSat [106]. The baseline propellant is LMP-103S; however, it can be easily configured to use AF-M315E. The green monopropellant MiPS was developed based on the Lunar Flashlight mission requirements. VACCO's Integrated Propulsion System (IPS) features four space-proven Bradford ECAPS 1N LMP-103S green thrusters that first launched in 2010 [107]. The total four thrusters can produce 3.97 N of thrust. Each individual thruster can be off-pulsed to achieve a desired thrust vector maneuver.

CU Aerospace developed a Monopropellant Propulsion Unit for CubeSats (MPUC) [91]. The propellant utilized is a diluted mixture of hydrogen peroxide (H_2O_2) and alcohol, known as CUA MonoPropellant #10 (CMP-X), which CU Aerospace developed in 2016. Standard stainless-steel manufacturing was used due to the relatively low operational flame temperature (<1273.15 K) of the CMP-X compared to that of the AF-M315E and LMP-103S thrusters that need more costly refractory metal. As a result, the H_2O_2/ethanol blend not only further reduces manufacturing expenses but also offers safer handling compared to that of hydrazine. The propellant is driven by gaseous helium pressurant. The MPUC contains a screen-retained granular iridium-loaded catalyst bed. Performance testing measured an I_{sp} of 180 s at 174 mN, and a higher thrust of 450 mN was measured at an I_{sp} of 154 s. MPUC features two units: a 1.5U MPUC and a 2U MPUC [108]. The 1.5U MPUC has a total wet mass of 2.5 kg and provides a ΔV of 159 m/s to a 12.5 kg CubeSat. The 2U MPUC has a total wet mass of 3.1 kg and delivers a total ΔV of 259 m/s to a 13.1 kg CubeSat.

NanoAvionics developed the Enabling Propulsion System for Small Satellites (EPSS) to provide high-performance and green propulsion system for CubeSats [109]. The EPSS uses an ADN-based monopropellant. It comes in a variety of sizes: 1.5U, 2U, and 3U. It is capable of providing a thrust range of 220–1000 mN with an I_{sp} of 214 s. The EPSS was flight-demonstrated onboard the 3U CubeSat LituanicaSAT-2 3U mission that launched in 2017, and it was also flown in the M6P (6U CubeSat) mission in 2019.

The TU Delft and the University of Pisa developed the Modular Impulsive Monopropellant Propulsion System (MIMPS-G) that uses green propellant technology, specifically designed for CubeSats at LEO and to the moon [86]. MIMPS g can be scaled to meet the

propulsion capabilities of small-sized spacecraft. The baseline design of MIMPS g has a volume of 1 U and a rated thrust of 500 mN. It delivers a total impulse of 850 to 1350 N.s per 1 U. The system was analyzed with different green monopropellants; however, the baseline design uses AF-M315E as the propellant. Unconventional and more complex feed and pressurization systems were analyzed for use in micro-propulsion systems for small satellites. MIMPS g features autogenous pressurization and a micro-electric pump feed cycle that are developed with COTS components. The micro e-pump-feed system is responsible for circulating the propellant for evaporation, using the evaporated (non-decomposed) propellant to maintain minimal required storage tank pressure, as well as delivering the propellant from very low-pressure storage to a high-pressure thrust chamber at a given mass flow rate. These unconventional pressurization and feed systems allow tank structures to be more lightweight due to requiring low storage pressure at the cost of increased system complexity [110]. The employed micro-electric-pump-fed cycle also provides non-degrading thrust performance for longer time compared to that of other conventional monopropellant systems.

Monopropellant systems offer a high-thrust propulsion capability that is suitable for small satellites requiring relatively large impulsive orbital maneuvers. Green propellants such as AF-M135E, LMP-103S, and H_2O_2, are safe to work with, have flight heritage, and can provide high thrust and storage density performance. Therefore, green monopropellant systems are more attractive to small satellite missions compared to hydrazine-based systems.

3.2.2. Bipropellant

Bipropellant propulsion consists of a liquid oxidizer-fuel system that generates thrust by exhausting hot gaseous products from combustion reaction through a converging-diverging nozzle as shown in Figure 11. In comparison to monopropellant propulsion, this system offers higher specific impulse performance at the expense of increased complexity in both propellant storage and propellant feed systems. Similar to other chemical propulsion systems, bipropellant systems offer high thrust capability; therefore, they are widely used for larger spacecraft that require high-thrust orbital maneuvers.

A bipropellant water electrolysis propulsion system called HYDROS-C was part of the NASA Pathfinder Technology Demonstration mission that was launched in 2021 [111]. HYDROS-C, developed by Tethers Unlimited, operates by burning gaseous oxygen and hydrogen produced by water electrolysis. The HYDROS thruster system consumes power to split the water propellant in orbit. It is capable of providing a thrust up to 600 mN [112]. The system occupies a volume of 2U [111]. On-orbit GPS data indicated that HYDROS provided a total impulse performance of 3.38 N-s. The on-orbit I_{sp} was measured to likely be between 223 and 241 s. I_{sp} values above 300 s are expected using higher plenum pressures.

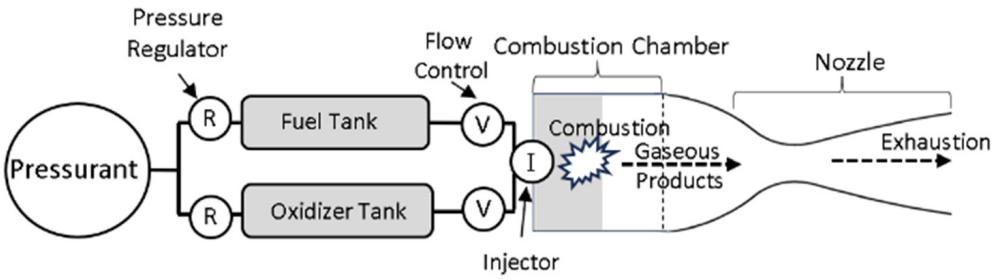

Figure 11. Bipropellant system schematic.

PM200 is a miniaturized 1 U Propene/N_2O bipropellant system developed by AAC Hyperion and Dawn Aerospace [113]. This propulsion module is designed to provide a nominal thrust of 500 mN and an I_{sp} of 285 s for 3–12 U CubeSats. It is capable of delivering a ΔV of 230 m/s to a 4 kg CubeSat. PM200 was integrated into the ION-SCV (In Orbit Now–Satellite Carrier Vehicle) that launched in 2020 [114].

The University of Miyazaki in Japan has proposed a prototype development of a 400 mN class premix-type thruster [115]. It is a N_2O/dimethyl ether (DME) bipropellant system with a thrust of 400 mN and a maximum theorical specific impulse of 290 s. Both N_2O and DME are liquified gases that have low toxicity and low reactivity features. This system stores N_2O and DME in liquid form and then feeds them as gaseous propellants in a coil-type pre-mixer prior to entering the combustion chamber as depicted in Figure 12. The pre-mixing does not necessitate mixing and evaporating times within the combustion chamber which reduces the size of the combustion chamber and leads to an overall more compact and environmentally safe thruster design for microsatellites.

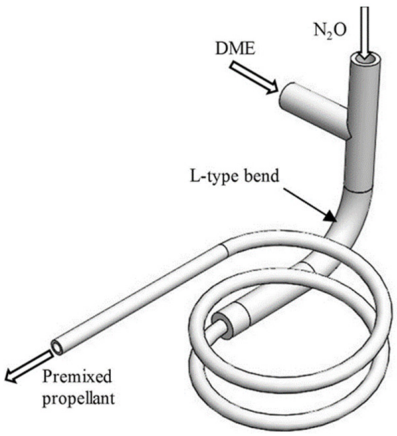

Figure 12. Coil-type pre-mixer [115].

Miniaturized bipropellant chemical systems have limited flight heritage for small satellites due to their relatively large mass and manufacturing limitations. However, its technology is well understood and widely used for general space propulsion; therefore, they can be further developed and utilized to extend the lifetime, range, and maneuvering capabilities of small satellite missions.

3.2.3. Solid

A solid chemical propulsion system works by the combustion of a solid propellant in the thrust chamber using an oxidizer and an ignition source. The gas produced from the burning of solid propellant is exhausted to generate thrust. A schematic of the working principle of solid propulsion is shown in Figure 13.

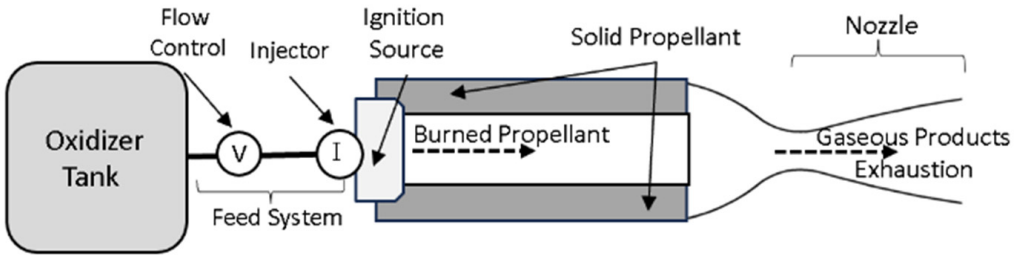

Figure 13. Solid chemical system schematic.

The mass flow rate of the gas produced depends on the solid propellant burn rate, as well as the propellant burn surface area. The burn rate is the rate at which the exposed propellant surface is consumed [3]. The mass flow rate and the burn rate can be calculated using the following equations:

$$r_b = a(P_c)^n \tag{8}$$

$$\dot{m}_{in} = \rho_p r_b A_b \tag{9}$$

where r_b is the propellant burning rate, a is the burn rate coefficient, n is the burn rate exponent, $\dot{m}_{in}$ is the mass flow into a control volume, r_p is the propellant density, and A_b is the propellant burn surface area.

Solid rocket motors have been widely used for deorbiting, orbit insertion, and as boosters for launch vehicles. The CubeSat Agile Propulsion System (CAPS) system, flown by SpinSat in 2014, was developed by Naval Research Laboratory and Digital Solid-State Propulsion (DSSP) LLC (Reno, NV, USA). SpinSat demonstrated in-orbit performance of electrically controlled solid propellant technology for small satellites applications [116–118]. The propellant employed in this system is known as HIPEP-501A [116]. The ignition process is initiated through a capacitor discharge mechanism that provides the necessary power [117]. Once ignited, the solid propellant continues to burn as long as a continuous supply of electrical power is maintained [118]. This electrically controlled solid propellant technology offers the unique capability of re-igniting the propellant, thereby enabling electrical control over the ignition process of solid chemical propulsion systems.

The Pico Satellite Solar Cell Testbed-2 (PSSCT-2), launched in 2011, included four small solid rocket motors developed by CU Aerospace [119]. The first solid motor operated successfully and raised the apogee of the PSSCT-2 spacecraft by 10 km. The thrust vector alignment through the satellite's center of gravity was off by several millimeters which led to an apogee change that was four times smaller than that which was originally planned. The remaining three solid motors were commanded to fire; however, the motor ignition did not occur, leading to orbit decay and reentry after 4.5 months. The mission team suspected that the cause of this issue could either be due to the prolonged exposure of the solid propellant in the vacuum or due to the effects of the first motor ignition.

The Tokyo Metropolitan College of Industrial Technology (Tokyo, Japan) developed a laser ignition micro-thruster unit [120]. It uses a CW diode laser to ignite small solid-propellant pellets. The gaseous products from a combustion reaction are exhausted to generate thrust. Boron potassium nitrate (B/KNO_3) was chosen as the propellant due to its ease of ignition in a vacuum, as well as its space-proven reliability. A schematic of the laser-ignited thruster is shown in Figure 14. Moreover, 1 W laser irradiation ensured 100% ignition probability of the B/KNO_3 pellets, leading to an impulse of 60 mN-s with a specific impulse of 100 s [120]. The system was developed due to its compact size and low weight since it does not require any valves or pipes. Each thruster unit consists of two laser ignition micro-thrusters to enable a change in rotational velocity maneuver (0.72 rad/s). Two units were integrated to the Kouku Kousen Satellite No. 1 (KKS1) microsatellite that launched in 2009. The mission encountered communication issues that prevented the in-orbit demonstration of this thruster.

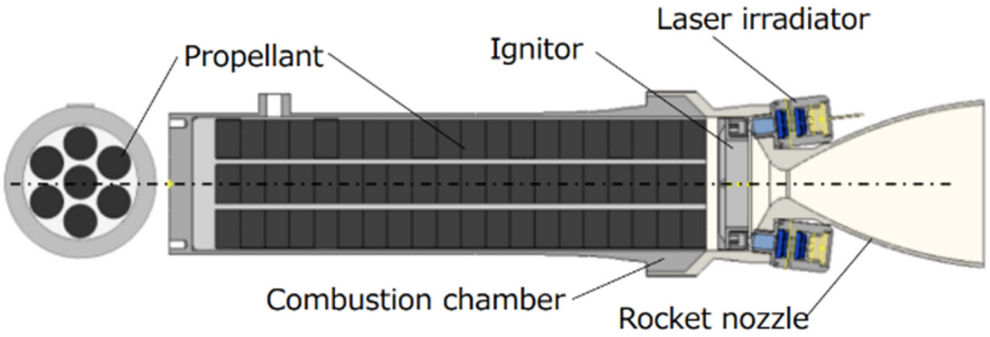

Figure 14. Laser-ignited solid chemical system schematic [121].

Pacific Scientific Energetics Material Company (PacSci EMC) (Chandler, Arizona) developed the Modular Architecture Propulsion System (MAPS) system that consists of an array of solid thrusters that are commanded by a low-power, flight-proven Smart Energetics Architecture (SEA) bus [122]. The MAPS has a minimum specific impulse of 210 s. It features three independent inhibitors against firing. Thrust can be produced within 5 milli-s of powering on the system. MAPS was successfully flight-demonstrated

onboard the PACSCISAT CubeSat that launched in 2017. PACSCISAT included SEA control electronics, four MAPS solid thrusters, and four independent initiation devices.

Chosun University developed the MEMS-based solid propellant thruster array for a technology demonstration in the STEP Cube Lab (Cube Laboratory for Space Technology Experimental Project) (Gwangju, Republic of Korea) mission that launched in 2018 [2,123]. The main purpose of the technology demonstration mission was to verify the MEMS fabrication process for space application rather than the capability and performance of the propulsion system [123]. The system consists of four layers of photosensitive glass, a micro-nozzle layer, an intermediary layer and a micro-igniter, a seal layer, and the solid propellant. The micro-igniter is installed under the glass membrane to ensure efficient ignition performance due to direct contact. It has a maximum rated thrust of 3620 mN and an I_{sp} of 62.3 s.

The University of Miyazaki developed a solid-propellant micro-thruster that can be throttled through laser heating [124]. Combustion can be controlled via semiconductor laser heating applied to the burning surface. The proposed thruster has a theoretical specific impulse of 204.5 s using a combustion-controllable hydroxyl-terminated poly butadiene/ammonium perchlorate-based solid propellant. The prototype uses propellant holders that expose the solid-propellant surface to the laser beam: the polymethyl methacrylate (PMMA) propellant holder. Performance testing indicated stable combustion with a thrust of 60 mN and a specific impulse of 144 s using PMMA propellant holder.

Solid chemical propulsion systems have a high thrust capability; however, their applications in CubeSats are limited due to the CubeSat Standards limitations on pyrotechnics [125]. Due to their high impulsive thrust capability, they provide substantial thrust force that requires having a more robust attitude control onboard.

3.2.4. Hybrid Chemical

A hybrid chemical propulsion system contains solid propellant and liquid or gas propellent in an oxidizer–fuel combustion system. Typical hybrid systems are composed of a liquid/gas oxidizer that is injected into the solid fuel grain stored in the thrust chamber. Hybrid systems are considered to be safer than solid systems since the oxidizer storage and transfer mechanisms are separate and the solid propellant is usually more stable with higher activation energy. Thus, this reduces the risk of pre-initiating ignition in the combustion system; however, it indicates that it is more difficult to initialize the combustion reaction. This leads to the need for additional means to ensure sufficient ignition. Conventional hybrid propulsion systems offer higher thrust levels than desired for small satellites; therefore, efforts on miniaturization development of chemical hybrid systems are limited. Hybrid chemical propulsion systems typically have two configurations for their design as shown in Figure 15. The difference is in how the energy is produced to initiate combustion of the solid propellant. In the first configuration, the propellant stored in the tank (liquid/gas) works as an oxidizer to burn the solid propellant via an ignitor and becomes exhausted along with generated combustion products in order to generate thrust. In the second configuration, the propellant is thermally decomposed to burn the propellant and becomes exhausted with the resulting products.

JPL developed and tested a green PMMA/gaseous oxygen (GOX) hybrid system for a 12 U CubeSat (EnduroSat, Sofia, Bulgaria) with an Isp greater than 300 s [126]. The hybrid system was tested using two different ignition systems—an augmented spark methane–oxygen ignition torch system and a laser igniter system. The hybrid motor conducted 24 ignitions successfully in a vacuum environment, bringing this technology to TRL 5. This compact, easily scalable system could deliver a ΔV of 800 m/s to a 25 kg spacecraft.

Utah State University (USU) and the Space Dynamics Lab (SDL) designed and tested a prototype of an end-burning miniaturized green hybrid chemical propulsion system [127]. The miniaturization of a conventional hybrid system, with thrust levels less than 5 N, leads to inefficient combustion due to a low oxidizer flow and thus reduced convective heat. This

hybrid system design relies on the flight-demonstrated arc-ignition technique and provides a thrust range of 500–1000 mN with a vacuum I_{sp} of greater than 150 s. During testing, they used acrylonitrile butadiene styrene (ABS), PVC, Nylon-12, and polymethyl methacrylate (PMMA) as fuel and GOX as the oxidizer.

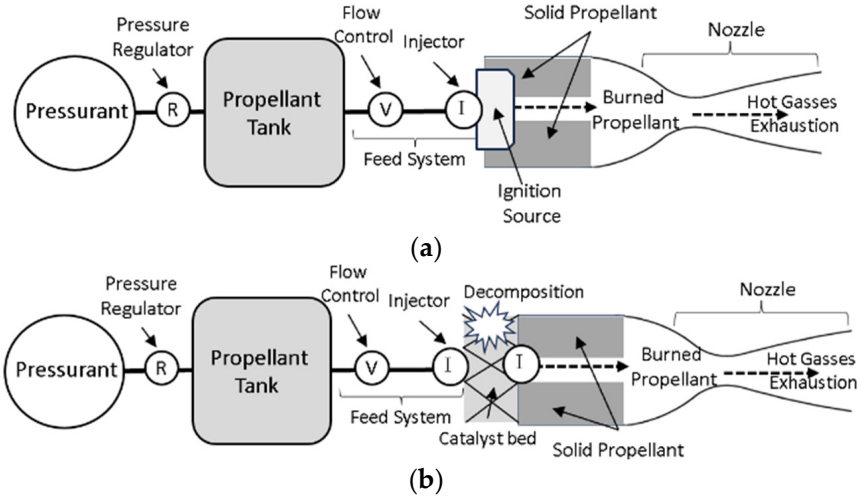

Figure 15. (**a**) Hybrid chemical configuration 1 and (**b**) hybrid system configuration 2.

Miniaturization efforts of hybrid chemical propulsion are presented above; however, they indicate that this technology is not yet suitable to be used within small satellite mission requirements, as well as small satellite volume and mass constraints.

3.3. Electric Propulsion

Electric propulsion systems consume electrical power to accelerate the exhaust using electrothermal, electrostatic, or electromagnetic principles. Electric energy is the main source of energy that is converted to produce thrust in all electric propulsion systems.

3.3.1. Electrothermal Discharge

Electrothermal discharge systems use discharge means to heat the propellant flow. In arcjet systems, an electrode configuration is used to induce an electric arc discharge that passes through the propellant flow in the nozzle. This electric discharge raises the temperature of the flowing gas. The heated gas flow is then exhausted to generate thrust. The working principle of arcjet discharge propulsion is depicted in Figure 16. Plasma discharge is another mechanism to heat the flowing propellant. Since the arcjet system lifetime is limited by the erosion of electrodes, electrodeless plasma discharge can also be used to heat a flowing propellant gas using a high-power excitation source such as a microwave or radio-frequency energy source input. This is called a Microwave Electrothermal Thruster (MET) system when using microwave energy, and it is called Radio-Frequency Electrothermal Thruster (RFET) when a radio-frequency power input is used. The discharge arc heating usually achieves higher working temperatures compared to resistojet systems; therefore, arcjet systems have higher specific impulse performance [128].

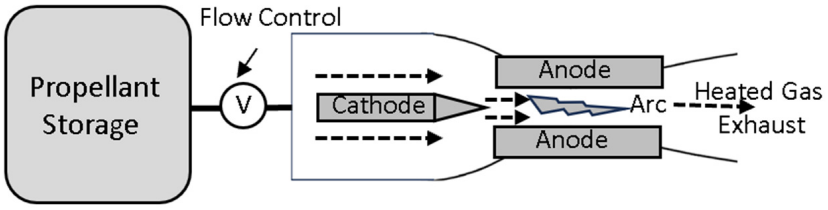

Figure 16. Arcjet electrothermal discharge system schematic.

The arcjet propulsion system consumes high power that is not currently attained by CubeSat missions that are power-limited. The NASA Lewis Research Center started the effort of arcjet miniaturization by developing a miniaturized arcjet thruster laboratory model with a supersonic arc attachment operating at 100–300 W [129]. Both simulated ammonia and simulated hydrazine were used in testing the model. Arc instabilities were observed during very low-power operation (100–300 W), which decreased the efficiency of the system. When operating at a very low arcjet power level, the performance was found to be dominated by the viscous effects in the propellant flow rate. Simulated ammonia resulted in improved performance with an I_{sp} of 410 s at 300 W compared to 370 s when using hydrazine [130]. The Institute of Space Systems (IRS) developed a very low-power arcjet (VELARC) with power levels ranging from 100 W to 300 W for small satellites (200 kg) [129]. The VELARC thruster model was tested with argon, hydrogen, and ammonia. At 100 W, stable operation was achieved only using argon, however, at the expanse of a much reduced I_{sp} (170 s). The thrust measured for a 100 W argon arcjet was 27.5 mN. The performance of the VELARC with ammonia was characterized by a thrust of 35 mN and an I_{sp} of 350 s at 240 W, whereas hydrogen achieved 14 mN of thrust and an I_{sp} of 820 s at 310 W. Despite arcjet miniaturization efforts, the current performance of miniaturized arcjet system and their power consumption range are more suitable for small satellites with a relatively large mass (100 kg or more) due to high power demand, as well as arc instabilities and reduced efficiency at a very low-power operation. Assuming a high-power source is available on small satellite missions, arcjet offers medium thrust and relatively high specific impulse performance that can be useful for extending the maneuvering capabilities of small satellite mission capabilities.

A micro-cavity discharge (MCD) thruster for nanosatellites was developed by CU Aerospace and the University of Illinois [131]. The MCD thruster consists of two or more aluminum (Al/Al_3O_2) electrodes powered by an AC power source, as well as a 100–200 µm diameter cavity in which micro-discharge plasma is created to heat the flowing propellant. The heating occurs over a very short distance due to the innovation of the way plasma discharge is created in a microcavity. The schematic of MCD thruster is shown in Figure 17. The MCD thruster is characterized by a high thrust-to-power ratio compared to that of other electric propulsion forms, a very short warm-up time in the sub-millisecond, and low wall heat loss due to a small wall area per cavity [131]. The MCD is capable of heating the gaseous propellant in the range of 1000–1500 K, thus achieving a specific impulse in the range of 80–400 s depending on the propellant. The propellants selected initially for the study were argon, neon, and nitrogen. Microcavity plasma devices were created using the MEMs microfabrication technique.

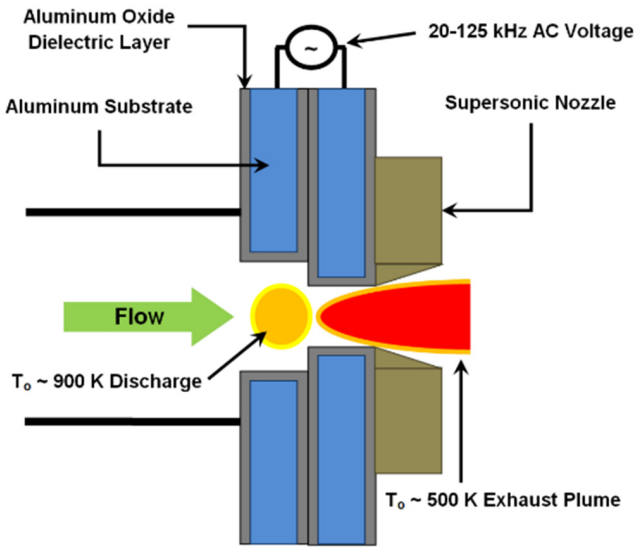

Figure 17. Micro-cavity thruster schematic [132].

The Propulsion Unit for CubeSats (PUC) system was designed, fabricated, tested, and delivered to the U.S. Air Force Research Laboratory by CU Aerospace, LLC (Champaign, IL, USA), and VACCO Industries (El Monte, CA, USA) in 2014 [133]. The PUC is a fully integrated unit with all-welded titanium casing. The system operates in two modes: (1) a cold gas mode and (2) an MCD warm gas mode. The MCD mode is based on the MCD technology developed by CU Aerospace and the University of Illinois [131,133,134]. The system uses sulfur dioxide SO_2 as the propellant due to its self-pressurizing property, high mass density, low vapor pressure, and its common use as a refrigerant prior to development of freons [133]. Testing results showed that the system was capable of providing a thrust of 4.5 mN and an I_{sp} of 46 s in a cold gas mode and a thrust of 5.4 mN and an Isp of 70 s in an MCD warm gas mode. For a 4 kg CubeSat, the system is capable of delivering a ΔV of 48 m/s in a warm gas mode and 32 m/s in a cold gas mode. The baseline design fits within a 0.25 U volume; however, the system can be scaled to a variety of sizes such as 0.25 U–1 U. MCD heating in the 0.25 U PUC consumes 15 W of power.

The Pennsylvania State University (PSU) developed an MET propulsion system for CubeSats in 2012 [135,136]. The MET operates by using a 17.8 GHz microwave energy antenna to generate plasma inside a resonant cavity that heats the flowing propellant at an input power of 10 W [135]. The schematic of MET system is depicted in Figure 18. The separation plate shown is used to lower resonant frequency within the cavity, as well as to prevent plasma formation near the antenna [136]. The cavity acts as a pressure chamber where the injected propellant is heated by plasma ignition, and the propellant vortex flow contributes to sustaining the formed plasma and also provides a cooling effect on the cavity walls. MET research at the PSU began in the 1980s [135]. The recent MET development focused on the miniaturization of this technology to provide a feasible propulsion capability for CubeSats using less than 50 W of power. The developed MET models used and tested a variety of propellants: helium, ammonia, hydrazine decomposition products, and water [136]. In 2016, MET plasma ignition was achieved using helium and an input microware power of 1.2 W up to 28 W, whereas ammonia achieved plasma ignition with 8.3 W–34 W [137].

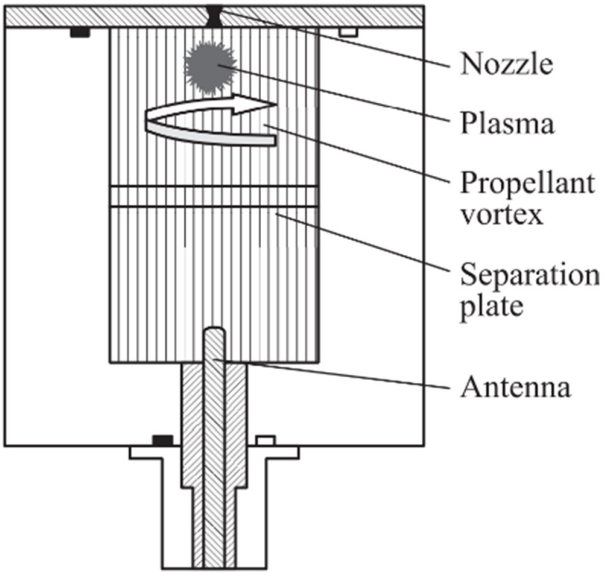

Figure 18. Microwave Electrothermal Thruster schematic [138].

The California Polytechnic and State University developed a 1 U+ CubeSat propulsion module that incorporates an RFET called a Pocket Rocket [139]. A schematic of an RF electrothermal thruster is shown Figure 19. The system operates using radio-frequency (RF) power to create and sustain plasma in the thruster body that transfers heat to the propellant flow. RF power is used to ionize a fraction of the propellant to plasma that is used to heat the remaining neutral propellant through charge exchange collisions. The heated propellant

is accelerated through the nozzle to generate thrust. Pocket Rocket development work started at the Space Plasma, Power, and Propulsion Laboratory at the Australian National University in 2011 [139,140]. The system uses either argon or xenon gas as the working propellant. The thruster generated a thrust of 2.4 mN with an I_{sp} of 100 s at 10 W DC power using argon.

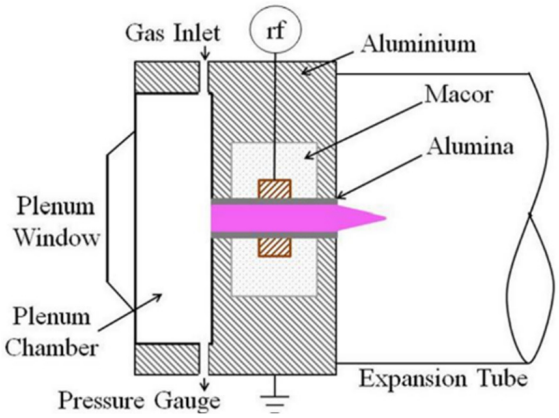

Figure 19. RF electrothermal thruster schematic [141].

Electrothermal plasma micro-discharge heating systems offer a feasible propulsion capability for CubeSats missions due to their power levels that are within the CubeSat power capability, as well as their relatively improved specific impulse performance due to heating the flow. Arcjet systems are not yet practical for CubeSat missions due to high power consumption.

3.3.2. Electrospray

Electrosprays operate by using electrostatic principles to extract and accelerate ions or droplets from ionic liquid propellants. The propellant is sprayed to an emitter where an electric field is applied to distort the propellant and form a Taylor cone at the emitter tip due to surface tension. The ions or droplets are then accelerated through an applied static electric field. Electrospray thrusters commonly use 1-ethyl-3-methylimidazolium tetrafluoroborate (EMI-BF4) and bis(trifluoromethylsulfonyl)imide (EMI-Im) as propellants. The source of energy in electrospray propulsion is from the electric field that is created by the voltage difference between two electrodes: the emitter and extractor grid. The working principle of electrospray propulsion is depicted in Figure 20. The energy balance equation is given by [142]:

$$qV = \frac{1}{2}mc_f^2 \tag{10}$$

where q is the charge of ion or droplet, V is the voltage difference, m is the mass of the droplet or ion, and c_f is the final velocity of the charged particles. The Child–Langmuir law can be used to calculate the current limit between two electrodes in space [142,143]:

$$J = \frac{4\varepsilon_0}{9}\sqrt{\frac{2q}{m}}\frac{V^{\frac{3}{2}}}{d^2} \tag{11}$$

where J is the current density, d is the separation between the two electrodes, and ε_0 is the permittivity of free space. The mass flow rate and a relationship between the applied voltage and maximum thrust (F_{max}) can be found using the following equation:

$$\dot{m} = JA\frac{m}{q} \tag{12}$$

$$F_{max} = \left(\frac{8\varepsilon_0}{9}\right)\frac{A}{L^2}V^2 \tag{13}$$

where $\dot{m}$ is the mass flow rate and A is the total surface area of the emitter array.

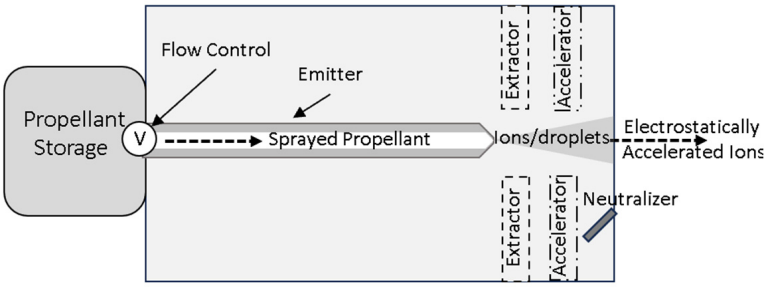

Figure 20. Schematic of electrospray and FEEP systems (electrostatic propulsion).

The above equations show that the performance of electrospray propulsion is dependent on the mass-to-charge ratio of the charged particles and the applied voltage which is limited by the current density limit.

Busek Co., Inc. (Natick, MA, USA) and JPL developed the Colloid Micro-Thruster (CMT) system for the LISA Pathfinder mission that launched in 2015 [144,145]. Busek started developing this thruster in 2002 and delivered it to JPL in 2008 for integration [145]. The thruster uses EMI-Im as the propellant. The thruster includes an integrated heater, a PPU, a piezo-actuated microvalve to control the propellant flow, as well as bellows to store the propellant. It operates by the emission and electrostatic acceleration of charged droplets. The CMT system has a rated thrust range of 0.005–0.03 mN. Two CMT systems were flown and each CMT system contained four independent colloid thrusters. The CMT demonstrated over 20,000 h of cumulative flight operation using eight colloid thrusters. Even though the mass of the spacecraft is more than 100 kg, the CMT is the first successful spaceflight demonstration of electrospray propulsion system [146].

Busek developed a miniaturized, passively fed electrospray thruster called the BET-300-P for the precision reaction control of small satellites [147]. This passive electrospray thruster operates and feeds the propellant using electrostatic fields, without moving parts. The thruster has a continuous thrust capability in the range of 0.001–0.15 mN. The thrust range had a thrust resolution within the sub-μN level. Busek reported that the thruster was operated for 461 h at a nominal thrust of 0.055 mN in 2020, where the average I_{sp} was 850 s and the average thrust-to-power ratio was 65 μN/W. The multi-axis BET-MAX system is an integrated 1.25 U propulsion module that consists of four BET-300-P thrusters, a centralized PPU electronic unit, as well as a carbon nanotube field emission cathode for charge neutralization [148].

The MIT's Space Propulsion Lab (SPL) developed a MEMS-based Scalable Ion Electrospray Propulsion System (S-iEPS) [149]. The S-iEPS is an integrated system consisting of eight thrusters firing along a single axis. The system consists of an array of 480 emitter tips for each thruster. The emitters are manufactured by a laser ablation out of a single piece of porous glass [150]. The system uses a non-reactive ionic salt propellant. Each thruster sprays the low vapor pressure propellant to porous emitter arrays using capillary forces without needing pressurization or an active pumping system. Thus, the system size and mass are reduced to be well suited for CubeSat design restrictions. The system was designed to fit within 0.2U [149]. It is capable of delivering a thrust of 0.074 mN with an I_{sp} up to 1150 s and power consumption less than 1.5 W. The S-iEPS was flight-demonstrated in the AeroCube-8A&B (1.5U) mission in 2015 [2,151].

Accion Systems Inc. commercialized the MIT's S-iEPS system and developed the Tiled Ionic Liquid Electrospray (TILE) thruster system using MEMS techniques [152]. The TILE system contains a porous emitter, extraction electrode, and a supportive structural frame as shown in Figure 21. The emitter and structural frame are fabricated from silicon and glass wafers. It uses EMI-BF4 as the propellant. The TILE-2 system consists of a total of four thrusters [153]. It has a total mass of less than 500 g and a total volume of 0.5 U. It is capable of producing a thrust of 0.05 mN and an I_{sp} of 1800 s. The electrospray system

was flown as a technology demonstration in the 3 U MIT's BeaverCube mission in 2022 [2]. The BeaverCube mission demonstrated a 3.5 h maneuver to result in an attitude change of 280.5 m [153]. A burn over 8 days at 0.05 mN of thrust delivers a ΔV of 8.8 m/s to the 4 kg CubeSat. A scaled-up thruster version, referred to as TILE-3, was flown in the D2AltaCom in 2021 [2,154].

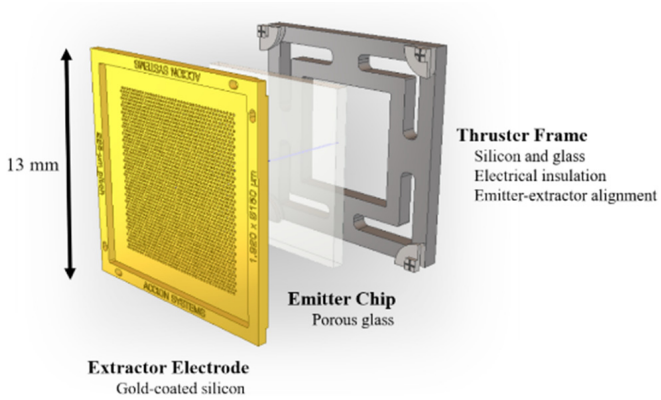

Figure 21. Components of Tiled Ionic Liquid Electrospray system [152].

The Northwestern Polytechnical University developed the Modular Ionic Liquid Electrospray Thruster (MILET) [155]. The MILET achieves an average thrust-to-power ratio of 65.2 μN/W with an I_{sp} of 1263 s. The applied voltage ranged from 1550 V to 2000 V, which is relatively low and within CubeSat capabilities.

Electrospray propulsion is particularly useful for nanosatellite missions with precision maneuvering capabilities that are characterized by high specific impulse performance. The use of this technology is well suited for CubeSat missions because the ionic liquids employed do not need an ionization chamber, utilize passive capillary forces for feeding propellant, and have extremely low vapor pressure, thereby eliminating the necessity for pressurized storage systems [156].

3.3.3. FEEP

FEEP in principle is similar to the way electrospray systems, depicted in Figure 20, accelerate the charged particles; however, they differ in terms of how the charged particles are produced. FEEP uses liquified metal such as indium and cesium as propellants [157]. The propellant is typically stored as a solid; however, it is liquified using heaters prior to thrust operations. Localized electric field and surface tension at the emitter tip forms a Taylor cone that increases the strength of the electric field and ionizes the propellants [158]. The emitted ions are accelerated electrostatically through the nozzle. The thrust and specific impulse can be approximated using the following equations [159]:

$$F = I\sqrt{2V_e\frac{q}{m}}f \tag{14}$$

$$I_{sp} = \frac{\eta}{g_0}\sqrt{2V_e\frac{q}{m}}f \tag{15}$$

where I is the net emitted current, V_e is the emitter voltage, f is a factor account for the beam spreading, and η is the mass efficiency of the emitter (depending on emission current and emitter properties).

Centrospazio developed Cesium FEEP thrusters with a slit emitter design, referred to as FEEP-5 and FEEP-50 thrusters [160,161]. FEEP-5 produces a thrust of 0.04 mN and an I_{sp} of 9000 s at 2.7 W, whereas FEEP-50 produces 1.4 mN at 93 W [161]. The FT-150, developed by Alta SpA (currently known as SITAEL) was also a cesium FEEP with a slit-shaped emitter [162]. It was designed to meet the requirements for the LISA Pathfinder mission; however, the system was not flown for that mission. It produces a thrust in the range of

0.0001–0.15 mN. It consumes a nominal power of 6 W for a 0.1 mN nominal thrust operation. Despite the low melting point, low ionization potential, and high molecular weight of cesium, it is very reactive and corrosive [163]. Alta Spa also developed the Ionic Liquid FEEP thruster (IL-FEEP) system that uses ionic liquids instead of cesium due to difficult handling of cesium, at the cost of a reduced I_{sp} (1600–1800 s) [164]. SITAEL commercialized Alta SpA's FEEP technology heritage for CubeSats. The CubeSat One–Module FEEP Ion Thruster (COMFIT) was developed by SITAEL [165]. It occupies a volume of 0.9 U. It can provide a thrust up to 0.25 mN and an I_{sp} range of 3500–5000 s. It has a maximum power consumption of less than 20 W.

The Austrian Research Centers (ARCs), currently known as AIT Austrian Institute of Technology GmbH, started developing miniaturized Liquid Metal Ion Sources (LMISs) in the late 1990s [166]. The LMIS emits an indium ion beam to create thrust. An indium propellant was chosen due to its wetting properties, safe handling, and low ionization potential. However, the LMIS was successfully demonstrated for the first time in orbit in 1991 for spacecraft potential control and not for propulsion. The ARC started developing the LMIS as a miniaturized FEEP thruster for small satellites in 2004–2005. In-FEEP development targeted meeting LISA Pathfinder mission requirements [167]. It was developed to provide a thrust up to 0.1 mN and an I_{sp} of more than 4000 s using a cluster of nine LMIS-based emitters in one FEEP thruster unit. This indium FEEP development effort was leveraged to develop and commercialize a miniature FEEP thruster, referred to as the ENPULSION NANO Thruster.

The ENPULSION NANO Thruster (ENPULSION, Wiener Neustadt, Austria), formerly referred to as IFM NANO Thruster, was developed by FOTEC and commercialized by ENPULSION [168,169]. The ENPULSION NANO system consists of a passively fed porous ion emitter. Following the development and qualification of the emitter technology for FEEP propulsion by the ARC until 2010 [170], FOTEC continued to work on the same technical concept [170]. The thruster uses an indium propellant stored as a solid and liquified using heaters [171]. In comparison to cesium, indium is non-reactive and safe; however, it has a higher melting point [163]. The system consists of propellant reservoir, two redundant neutralizers, an ion emitter, and a power processing unit [171]. The thruster contains 28 porous tungsten needles wetted with liquid indium [159]. The neutralizer is used to eliminate spacecraft charging. The thrust can be controlled by varying the electrode voltage potential. The first flight demonstration of this system was performed successfully in 2018 [169]. The ENPULSION NANO is the first FEEP system to be flown in space. The propulsion system occupies an approximately 0.8U volume [172]. It can be operated in the power range of 10–40 W. It can deliver a thrust up to 0.35 mN and an I_{sp} range of 2000–6000 s, adapting to mission needs and power availability. The success of the first flight demonstration led to the development of next-generation ENPULSION R^3 systems in 2018, featuring increased environmental resilience and scalability to larger satellites, as well as increased reliability [169]. The ENPULSION NANO AR^3 features an added thrust vector steering capability. This capability provides the steering of the emitter ion beam by spatially distributed differential throttling without moving parts. This capability has been tested and verified. Another scaled-up version, called the MICRO R^3, was developed for small–medium-sized spacecraft and was successfully flight-demonstrated in 2021. ENPULSION has delivered hundreds of commercialized, flight-ready FEEP systems to various customers.

The Dresden University of Technology (TU Dresden) and Morpheus Space developed the NanoFEEP system [173]. The system was first flight-demonstrated in the 1 U UWE-4 (University Würzburg Experimental satellite-4) CubeSat that launched in 2018. The system consists of four thruster heads, two neutralizers, and two PPUs for voltage supply. A heater is also integrated into the thruster head to liquefy the propellant. The NanoFEEP system uses an electric voltage up to 12 kV between the needle and extractor cathode to ionize and accelerate ions using electrostatic forces. NanoFEEP consists of a porous tungsten needle to supply liquefied propellant to the needle tip via capillary effects. Each thruster head has a volume of less than 3 cm^3 [174]. One thruster head is capable of generating a

continuous thrust up to 0.008 mN with short-term peaks of up to 0.022 mN using very low power of 50 and 150 mW. NanoFEEP uses gallium propellant because of a low melting point approximately at 303.15 K. The maximum possible ΔV is about 15 m/s for the 1.1 kg CubeSat at thrust levels up to 0.02 mN.

FEEP systems have very high specific impulse performance compared to that of other propulsion technologies [158]. They also provide a wide range of low thrust levels that are attractive in missions requiring precise maneuvering.

3.3.4. Gridded Ion

A gridded-ion system creates plasma discharge that ionizes a propellant and then uses electrostatic grids to accelerate the ions. It includes a neutralizer to maintain the neutrality of the ejected ion beam. Plasma discharge is created by electrodes using collision with emitted electrons or a high-frequency generator that provides RF or microwave excitation as depicted in Figure 22. The system can use a metallic propellant or noble gases such as xenon or iodine which are used in recent gridded-ion thrusters. High-voltage power supply is required for this technology due to discharge ionization, electrostatic acceleration, and ion beam neutralization. The mass flow rate of ions is given by the following:

$$\dot{m} = I\frac{m}{q} \tag{16}$$

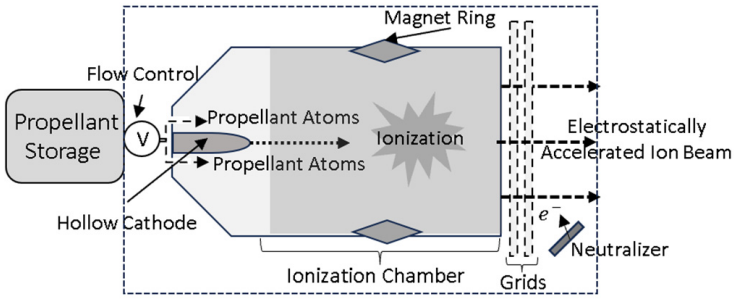

(**a**)

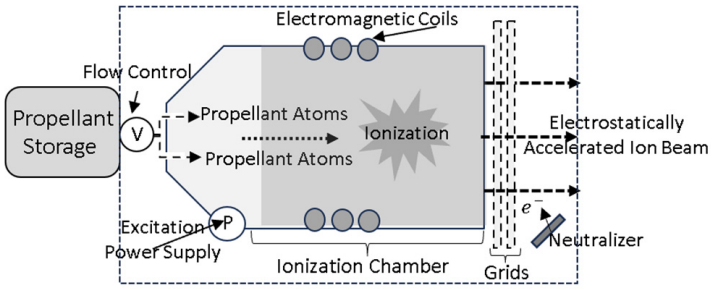

(**b**)

Figure 22. (**a**) Gridded-ion system using cathode and (**b**) using high-power excitation source.

Busek Inc. (Natick, MA, USA) developed the iodine-fueled BIT-3 ion propulsion system [175]. Two flight systems of BIT-3 were flown on two 6U CubeSats that launched in 2022: Lunar IceCube and LunaH-Map [2,175]. The first prototype, developed in 2015, demonstrated iodine propellant compatibility with the ion-gridded technology [175]. The performance of the system was verified with xenon and iodine propellants; however, iodine was chosen as the baseline for the system due to its high storage density at solid and low vapor pressures compared to that of xenon, which reduces system volume and eliminates the need for a high-pressure tank. The BIT-3 PPU includes a radiation-tolerant RF power supply for a deep-space environment. The plasma discharge ionization chamber is made of corrosion-resistant ceramic material due to the high corrosivity of iodine. BIT-3 also includes

the first BRFC-1 RF cathode neutralizer to be demonstrated with an iodine propellant in electric propulsion. It uses an inductively coupled plasma discharge to eliminate the need for lifetime-limited internal discharge electrodes [176]. BIT-3 occupies a volume of 1.6U. It is capable of providing a thrust range of 0.66–1.24 mN, an I_{sp} range of 1400–2640 s, and a ΔV up to 2.39 km/s for a 14 kg 6U CubeSat [175]. The power consumption is 56–80 W.

Earlier efforts in the miniaturization of laboratory gridded-ion models tested cesium and mercury propellants, with the earliest cesium miniature ion thruster reported in 1967 [177]. However, the modern miniaturization development of ion thrusters used a noble gas propellant for a more desirable performance. JPL and California Institute of Technology developed the Miniature Xenon Ion (MiXI) thruster in 2001 [178,179]. It is the first successful noble gas miniature ion thruster that was reported [179]. It features a 3 cm diameter discharge chamber and uses a permanent magnet DC electron bombardment discharge mechanism to ionize gaseous xenon propellant [180]. It was designed to use a ring-cusp magnetic field. It has a rated thrust level of 0.4–1.5 mN and an I_{sp} range of 1764–3184 s using 14–43 W power.

The University of Tokyo and JAXA developed a miniature gridded-ion thruster, called a 1μ ion thruster, designed for 50 kg small spacecraft [181]. It uses an electron cyclotron resonance plasma excited by a 4.2-GHz microwave in the discharge chamber. It uses xenon as the working propellant. Xenon is an inter propellant that is characterized by a high specific impulse and high thrust efficiency. It includes a miniature neutralizer that was evaluated in two different operations in 2011: unipolar operation and bipolar operation. The unipolar operation includes a two-grid ion beam source made of molybdenum and a neutralizer, whereas the bipolar operation includes a special grid system consisting of a combination of the plasma sources for ion beam extraction and electron emission neutralization. The evaluation concluded that the unipolar operation achieved higher performance, whereas the bipolar operation offered a simpler lightweight design. The unipolar miniature ion thruster's typical performance was calculated to be 0.297 mN for thrust and 1100 s for specific impulse using 15.1 W total power. The development of a miniature ion propulsion system (MIPS) for the 50 kg class HODOYOSHI-4 spacecraft started based on the University of Tokyo's μ1 ion thruster [182]. The MIPS consists of an ion thruster unit, a PPU, gas management unit, and a control unit. The ion thruster unit contains the microwave discharge chamber in the μ1 model. Xenon is stored in a pressurized tank made of carbon-fiber-reinforced polymer. The MIPS flight model has a wet mass of 8.1 kg and a volume of 34 cm $\times$ 26 cm $\times$ 16 cm [183]. It is capable of providing thrust of 0.21 mN and an I_{sp} of 740 s using 27 W of power. It is capable of delivering a ΔV of 140 m/s for 50 kg spacecraft. MIPS was successfully flight-demonstrated in the HODOYOSHI-4 in 2014.

The performance of the microwave-discharge miniature ion thruster using water as a propellant was tested and characterized at the University of Tokyo [184]. It is based on the University of Tokyo's 1μ thruster and has a similar structure to that of the xenon miniature ion thruster that launched in HODOYOSHI-4. Water was chosen due to its safety handling and availability. Both the ion source and the neutralizer were operated using water vapor propellant. Pale Blue Inc., a University of Tokyo spinoff company, commercialized the water miniature ion thruster, referred to as PBI-40. It has a rated thrust level of 0.15–0.3 mN and a rated I_{sp} of 1300–2600 s at 30–60 W [185]. It has a total wet mass of under 2 kg and occupies a volume of 1 U. The miniature water ion thruster was added along with four resistojet thrusters in one unified propulsion system for the JAXA's Satellite Innovation Technology Demonstration 3 program [186]. The Kakushin-3 water ion thruster and resistojet thruster (KIR) system includes one 0.15 mN ion thruster with a rated I_{sp} of 500 s. This unified propulsion system will be discussed further in the Multi-Mode and Hybrid Systems Section. The KIR system was launched onboard the RAISE-3 satellite; however, the payload did not reach orbit [187,188]. The water ion thruster was also integrated with a water resistojet system and successfully operated in the 6U EYE 1 (Star Sphere 1) CubeSat that launched in 2023 [189].

ArianeGroup developed a scalable family of ion-gridded thrusters that utilizes their space-proven Radio-Frequency Ion Technology (RIT) [190]. ArianeGroup's RIT technology was successfully demonstrated first in the European Retrievable Carrier (EURECA) launched in 1992. The RIT-µX is the smallest thruster in the RIT family. It offers a thrust level that ranges from 0.005 mN to 0.5 mN [190,191]. RIT-µX can be used to compensate for atmospheric drag or provide high-precision formation for small satellites. RIT features electrodeless ionization of xenon by RF ionization [190]. It uses an RF coil surrounding the ionization/discharge chamber to form plasma that ionizes xenon gas. The heavy positive ions are accelerated by electrostatic acceleration grid configuration and then ejected to cause thrust, while the light electrons are added to the plasma neutralizer to prevent spacecraft charging. Another RIT scaling-down effort started in 2004 at Giessen University [192]. A scaled-down version of RIT called the µNRIT-2.5 was developed by Giessen University for highly precise micro-propulsion. The performance of µNRIT-2.5 indicated a thrust capability of 0.575 mN with an I_{sp} of 2861 s using 34.4 W.

The Pennsylvania State University developed the miniature radio-frequency ion thruster (MRIT) and the miniature microwave-frequency ion thruster (MMIT). The MRIT is an inductively coupled RF ion thruster [193]. The performance testing used argon as the working propellant instead of xenon due to its lower cost. The testing indicated that the MRIT can produce a maximum thrust of 0.059 mN with an I_{sp} of 5489 s using 15 W of power. The MMIT was developed based on the MRIT [194]. It uses a coaxial antenna to deliver microwave-frequency ionization at 4.2 GHz. It can use either argon or xenon. After propellant ionization, a two-grid system applies a voltage potential of 2000 V at a total of 6 W to electrostatically accelerate the ions. The MMIT is predicted to provide a thrust of 0.25 mN with a theoretical I_{sp} of 5500 s.

The Miniaturized Differential Gridded Ion Thruster (MiDGIT) was designed by the University of Southampton to provide both coarse and fine thrust control [195]. It uses RF-inductive plasma discharge for propellant ionization. It has a differential ion beam control capability to provide stable discharge operation for very low thrust levels that are required for formation flying missions. For the coarse thrust control, the MiDGIT prototype demonstrated thrust levels between 0.2 and 0.5 mN and a specific impulse range of 400–1100 s using 95V/950V accelerator grid voltages. The coarse thrust control has a specific power of 55 W/mN. For the fine thrust control, thrust levels of 0.004–0.025 mN with an I_{sp} range of 5–220 s were achieved using an applied voltage that ranges between −75 V and −325 V. However, varying the grid potentials for fine thrust control could not achieve the full targeted thrust range of 0.0001–0.15 mN. MiDGIT development and testing confirmed that two stable ion beams can be extracted simultaneously from a common indictive plasma discharge, and the extracted ion beams can be controlled to produce a net offset in thrust [196].

NPT30-I2, developed by ThrustMe (Verrières-le-Buisson, France), is a fully integrated iodine-fueled propulsion system [197,198]. Iodine was used to avoid sloshing and provide flexibility in the geometrical design [199]. Heaters are used to sublimate iodine and an RF-inductive antenna is used to ionize the gaseous propellant [198]. The gridded extraction system is powered with an RF voltage supply instead of a conventional DC voltage [197]. Accelerator grids powered by RF are used to provide a continuous ion beam neutralized by electrons exiting the thruster in short instants during the RF cycle, therefore eliminating the need for an electron neutralizer in the system. This innovative ThrustMe technology tested both iodine and xenon. NPT30-I2 is capable of providing a thrust of 0.3–1.1 mN and a maximum I_{sp} of 2400 s using 35–65 W power [199]. It occupies a volume of 1 U and has a total wet mass of 1.2 kg. It was successfully demonstrated in the 12 U Beihangkongshi-1 satellite that launched in 2020 [198,200]. It performed two 90 min burns to change the satellite's altitude by 700 m [198]. Another unit was also launched in the NorSat Technology Demonstrator (NorSat-TD) in 2023 [201].

The Lanzhou Institute of Physics developed the Lanzhou Radio-Frequency-Induced Thruster (LRIT) [202,203]. LRIT-30 RF ion thruster consists of a ceramic discharge chamber,

RF coil, accelerator grid, gas distributor, and gas circuit insulator [203]. It can achieve a thrust of 0.5–2.3 mN and an I_{sp} range of 869–2653 s at 2 MHz and the RF power of 40–65 W.

3.3.5. Hall Effect

The Hall thruster mainly consists of a cathode–anode system, discharge chamber, and magnetic field generator. The thruster applies an axial electric field ($\boldsymbol{E}$) that is perpendicular to a radial magnetic field ($\boldsymbol{B}$). The magnetic field is generated by magnetic coils. The force generated by the cross-field interaction of the $\boldsymbol{E} \times \boldsymbol{B}$ fields results in an azimuthal electron current and the Hall thruster's current that spirals around the thruster axis [143]. The electrons in this current collide and ionize the neutral propellant flow as depicted in Figure 23. The generated ions are electrostatically accelerated and ejected to generate thrust. Even though the magnetic field plays a critical role in the operation of Hall thrusters, Hall thrusters are considered to be electrostatic since the ion exhaust is electrostatically accelerated. A fraction of the electrons emitted by the cathode exit the thruster with the ions to neutralize the charge. The velocity of the electrons (v_e) resulting from the cross-field interaction can be calculated using the following equation:

$$v_e = \frac{\boldsymbol{E} \times \boldsymbol{B}}{B^2} \tag{17}$$

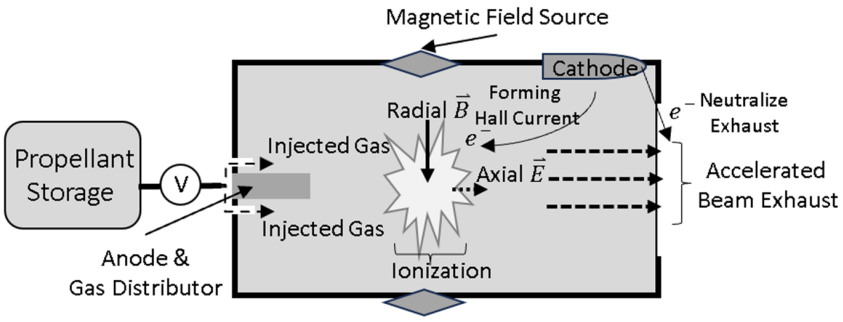

Figure 23. Schematic of Hall propulsion.

The Hall current density ($\boldsymbol{J_{Hall}}$) and thus the force on the ions ($\boldsymbol{F_{ion}}$) are given as follows:

$$\boldsymbol{J_{Hall}} = -qn_e\boldsymbol{v_e} \tag{18}$$

$$\boldsymbol{F_{ion}} = \boldsymbol{J_{Hall}} \times \boldsymbol{B} \tag{19}$$

where n_e is the electron density.

The ExoMG-nano propulsion system, also referred to as spaceware-nano, was developed and commercialized by Exotrail. The flight demonstration was conducted in the NanoAvionics R2 6U CubeSat launched in 2020 [2,204,205]. The EcoMG-nano is a fully integrated propulsion system that consists of 50 W miniature Hall thruster head, xenon propellant management system, PPU, and control unit [206]. Experimental performance testing indicated that the thruster was capable of producing a thrust of 2 mN and an I_{sp} of 800 s at 53 W of power. The thruster was successfully used to change R2 CubeSat's semi-major axis by 700 m [205]. The first five firings achieved a realized thrust range of 2.25–3.12 mN [204]. The thrust values realized from the firings were slightly higher than expected. The R2 mission is the first successful demonstration of a miniature Hall thruster system flown on a less than 100 kg satellite.

BHT-100, developed by Busek, is a 100 W Hall thruster that was designed to use both iodine and xenon propellants [207,208]. It was designed to have a lifetime of over 10,000 h [207]. Leveraging its space-proven Hall effect technology in BHT-200, BHT-100 has a power operation range of 75–125 W which is more suitable for smaller spacecraft. Magnetic shielding is used in BHT-100 to increase its lifetime and reduce the channel erosion that limited the lifetime of BHT-200. It has a rated nominal thrust of 7 mN with

an I_{sp} of 1000 s. It has a diameter of 8 cm and a length of 5.5 cm. The total thruster mass (including the cathode) is 1.16 kg.

SITAEL developed the HT100 thruster unit, depicted in Figure 24, which is qualified to launch in the μ-HETSat mission [209]. HT100 was tested with both xenon and krypton with operating power levels as low as 100 W. HT 100 contains two HC1 cathodes that were internally developed by SITAEL. At 125 W, HT 100 is capable of providing a thrust of 6 mN and an I_{sp} of 850 s. It is capable of producing a thrust of 9 mN and a specific impulse of 1300 s using 175 W power.

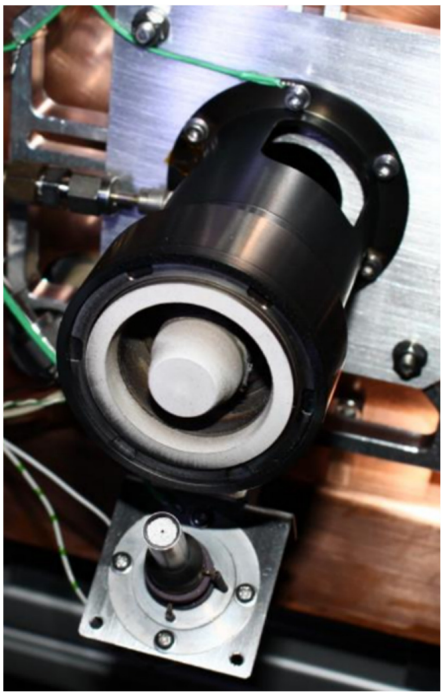

Figure 24. Schematic of HT-100 system [210].

The Space Electric Thruster Systems (SETSs) developed the SPS-25 propulsion system that consists of the ST-25 Hall thruster, xenon storage and feed system, and a PPU [211]. It has a rated input power of 100–200 W. It provides a thrust range of 5–11 mN with an I_{sp} of up to 1200 s. The total dry mass of the SPS-25 is 6 kg [212]. It was designed for small satellites with a mass of up to 500 kg. A permanent magnet was used to create the radial magnetic field at a relatively reduced power input [211].

The MUlti-Stage Ignition Compact (MUSIC) thruster was developed by Aliena Pte. Ltd. [213]. The MUSIC thruster system operates in three modes. The self-ignition mode was designed for nanosatellites and provides a thrust up to 0.25 mN with an I_{sp} of 200 s using an input power of no more than 20 W [214]. It has a volume of 1.5 U and a total wet mass of 2 kg. The first prototype with self-ignition mode was launched on the 3 U CubeSat NuX-1 mission in 2022 [213]. The first prototype used permanent magnets, xenon as the propellant, and a design that eliminated the need for an external neutralizer. The hot mode operation provides a thrust up to 5 mN with an I_{sp} of 1000 s using no more than 100 W [214]. The hot mode system was designed for microsatellites, has a wet mass of 5 kg, and occupies a volume of 4U. It includes a heated hollow cathode [215]. The dual mode operation combines both the self-ignition technology and the heated hollow cathode technology, providing a wider thrust range and a fault-tolerant system [214].

ExoTerra developed the compact Halo thruster for small satellites [216]. It has a volume of 0.375 U. It provides a thrust range of 4–30 mN with an I_{sp} of 700–1500 s using 100–450 W and xenon as the propellant. The flexibility of Halo's design allows for the use of a less expensive krypton propellant, at the cost of slightly decreased performance (thrust

range of 4–16 mN and I_{sp} range of 600–1000 s). Halo was successfully flight-demonstrated aboard the DARPA's Blackjack Aces satellites that launched in June 2023 [217].

Orbion Space Technology, Inc. (Houghton, MI, USA) developed the Aurora fully integrated propulsion system for small satellites with a mass as small as 70 kg [218]. It uses xenon as the propellant due to its reliability, high performance, and extensive heritage in Hall thrusters. It is a magnetically shielded Hall thruster [219]. It uses a barium oxide cathode. It has a thrust capability of 5.7 mN–19 mN with an I_{sp} ranging from 950 s to 1370 s at a 100–300 W operating power.

The Cylindrical Hall Thruster (CHT) was developed by the University of Toronto's SFL [220]. The CHT uses xenon as the baseline propellant. Miniaturization of conventional annular Hall thrusters leads to a high channel surface area to channel volume due to their annular geometry. This causes increased plasma interaction with the channel walls resulting in increased heating and erosion of thruster inner parts. The CHT has a cylindrical chamber instead of the traditional annular chamber, shown in Figure 25, in order to mitigate erosion of the thruster and thus increase lifetime at the expense of slightly decreased thruster performance. Two iterations of the CHT were conducted [221]. Electromagnets were used in the first iteration to create the magnetic field; however, the lifetime of the thruster was limited to 100 h. In the second iteration, permanent magnets were used which reduced the size and mass of the system and also slightly increased the lifetime to 400 h. The chamber insulation is made of Boron Nitride ceramic [220]. The CHT produced a thrust of 6.2 mN with an I_{sp} of 1139 s at 200 W using electromagnets. A schematic of CHT is depicted in Figure 26.

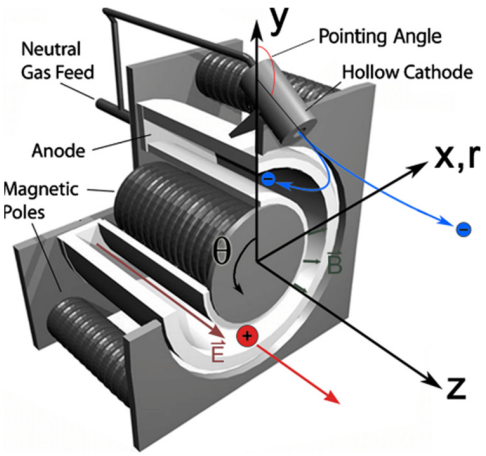

Figure 25. Schematic of Hall thruster with annular chamber [222].

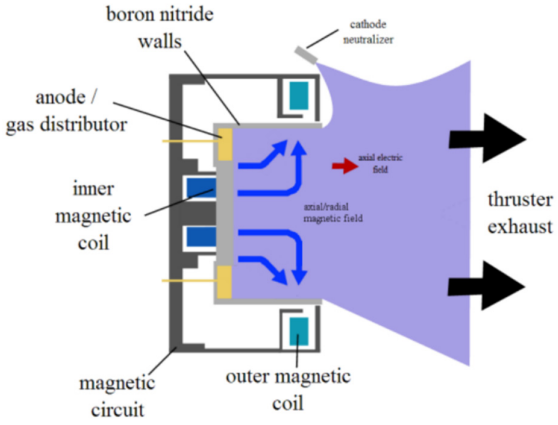

Figure 26. Schematic of Cylindrical Hall Thruster [220].

3.3.6. Pulsed Plasma and Vacuum Arc

The Pulsed Plasma Thruster (PPT) operates by inducing a discharge to ablate and ionize the propellant, which is typically solid [143]. The ablated material forms a current flow that generates a magnetic field. The ablated material is then accelerated by electromagnetic means through the $\boldsymbol{F_{Lorentz}}$. The pulsed operation includes a current pulse that is driven by the discharge capacitor [223]. The PPT system consists of two electrodes, a discharge capacitor, an ignitor, and a propellant feed system. The schematic of electromagnetic PPT propulsion is shown in Figure 27. In Vacuum Arc Thrusters (VATs), the propellant is the cathode which is used as the propellant and the electrode for discharge. Lorentz force is given by the following equation [143]:

$$\boldsymbol{F}_{Lorenzt} = q(\boldsymbol{E} + \boldsymbol{v} \times \boldsymbol{B}) \tag{20}$$

where $\boldsymbol{E}$ is the electric field, $\boldsymbol{v}$ is the charged particle velocity, and $\boldsymbol{B}$ is the magnetic field.

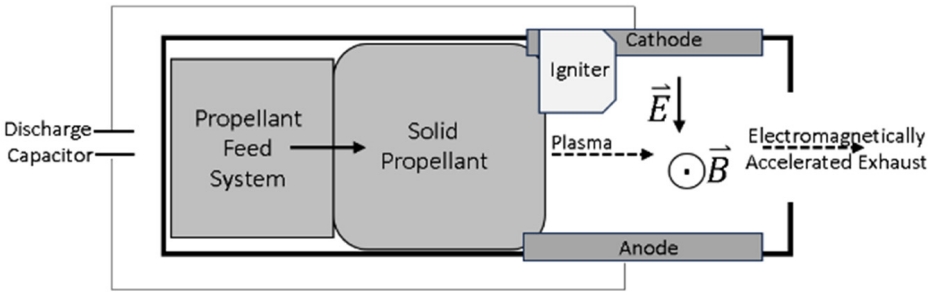

Figure 27. Schematic of pulsed plasma electromagnetic propulsion.

The Pulsed Plasma Thruster for CubeSat Propulsion (PPTCUP) was developed by Mars Space Ltd. (Southampton, UK), Clyde Space Ltd. (Glasgow, Scotland), and the University of Southampton in 2013 [224]. The propellant is Polytetrafluoroethylene (PTFE) [225]. A full flight qualification program for the PPTCUP was completed. The PPTCUP produces a thrust of 0.04 mN with a specific impulse of 600 s at 2 W of nominal power [224,226]. The NanoPPT is a modular thruster system designed for nanosatellites that can provide a 0.09 mN of thrust with an I_{sp} of 640 s at 5 W [224].

CU Aerospace developed the Fiber-fed Pulsed Plasma Thruster (FPPT) system [227,228]. It features a unique gimbal-less thruster vectoring capability that enables reaction wheel desaturation and attitude control outside Earth's magnetic field [227]. It uses Teflon as the propellant because it is non-toxic, non-corrosive, and provides on-demand thrust performance. The FPPT is depicted in Figure 28. It has a rated thrust level of 0.085–0.5 mN at 16–96 W. The maximum I_{sp} is 3200 s. It occupies a 1.7 U volume and has a total mass of 3.03 kg. An FPPT flight unit is planned to be launched in the DUPLEX mission.

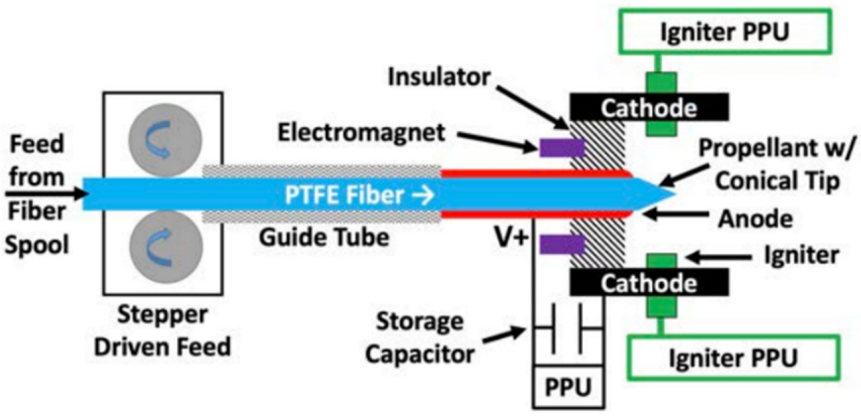

Figure 28. Schematic of Fiber-fed PPT Thruster [228].

The George Washington University (GW) developed the Micro-Cathode Arc Thruster (μCAT) [229]. Thrust is produced by using the cathode to create an arc discharge, forming charged particles that are accelerated by Lorentz force. The thruster was successfully demonstrated in orbit for the first time in the BRICSat-P mission in 2015 [230]. Using titanium cathode, the μCAT is capable of providing a thrust of 0.001–0.05 mN with an I_{sp} range of 2500–3000 s at 2–14 W. The material-dependent erosion rates and molecular weight are two important factors in cathode material selection. Titanium has a lower molecular mass that results in higher specific impulse performance, whereas nickel offers a higher thrust production. The thruster has also flown on BRICSat-2 in 2019 [2].

Alameda Applied Sciences Corporation (AASC) developed a metal plasma thruster (MPT) for nano- and microsatellites [231]. It does not require standby power and does not use neutralizer. It can use refractory metal cathodes such as the molybdenum cathode or niobium cathode as the solid propellant. The molybdenum MPT has a volume of 0.93U [232]. It is capable of providing a 0.482 mN thrust with an I_{sp} of 1774 s at 40 W.

The University of the Federal Armed Forces in Munich and Wuerzburg University developed the μVAT propulsion system which was one of the propulsion system candidates for the UWE-4 picosatellite [233,234]. The system operates by applying a voltage between the anode and cathode, which leads to the erosion of the cathode material. The eroded cathode material forms plasma that is ejected in space to generate the thruster. It was designed to provide a thrust range of 0.002–0.01 mN and an I_{sp} range of 900–1100 s using 0.5–2 W of power [233]. The UWE-4 mission, launched in 2018, ended up using the NanoFEPP system instead of the μVAT one [173].

Busek Co. Inc. developed the BmP-220 PPT thruster that uses Teflon as the propellant [235]. It operates with a power less than 3 W. It was designed to provide up to 175 N-s of impulse to CubeSats and micro-satellites. It is based on a miniature pulsed plasma thruster (μ-PPT) technology, also referred to as Micro-Propulsion Attitude Control System (MPACS), that was originally developed by the AFRL for a technology demonstration in the FalconSAT-3 [236]. MPACS consists of eight thrusters that are capable of producing a thrust of 0.01 mN. MPACS successfully operated onboard FalconSAT-3.

Comat developed a VAT system, known as Plasma Jet Pack (PJP30), for nanosatellites and microsatellites [237]. It does not require preheating. It has a lifespan of at least five years. The thrust generated is a function of the pulse frequency determined by the High-Voltage Trigger System frequency. Using a copper cathode, it can provide a thrust up to 0.27 mN with an I_{sp} of 2400 s at 30 W. The VAT system is depicted in Figure 29 below.

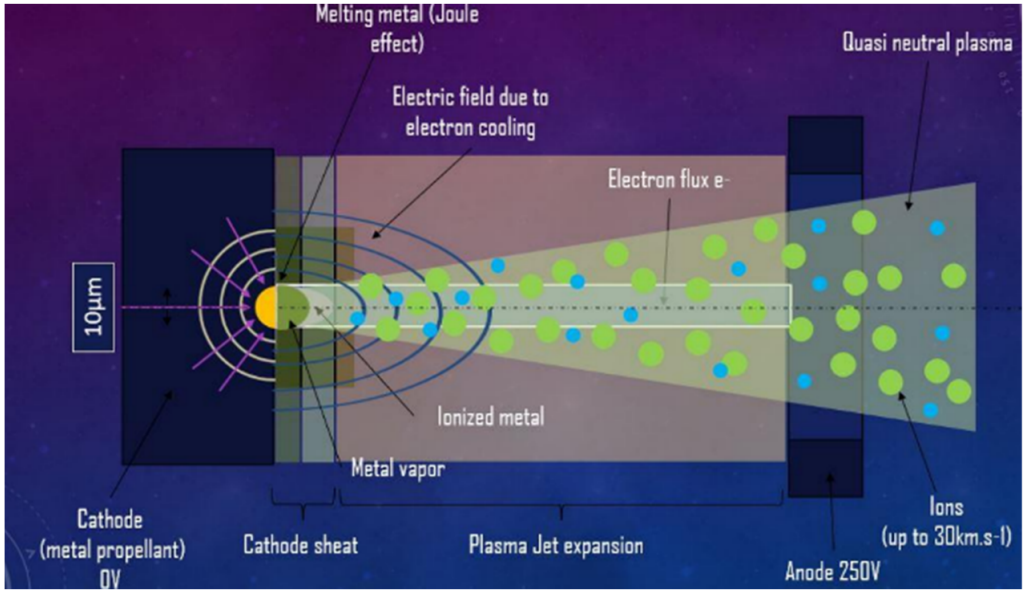

Figure 29. Schematic of Comat Vacuum Arc Thruster [237].

The University of Illinois developed a miniaturized VAT propulsion system for the Illinois Observing Nanosatellite (ION) [238]. The ION's propulsion system consists of one PPU and four VAT thruster heads. The system is characterized by a thrust-to-power ratio of 0.01 mN/W.

SSTL developed a pulsed plasma propulsion system for the STRaND-1 mission that launched in 2013 [239]. The propulsion system is made from three PC104 boards: one board is the PPU and the other two boards have four thrusters each. The system consists of two parallel CR09 ceramic chip capacitors per thruster. The thrust operation is initiated by a spring-loaded contact trigger mechanism using a piezo-electric motor which forms a current that causes the electrodes of each capacitor to become eroded. The eroded material forms plasma that is accelerated due to the Lorentz force. Vacuum tests conducted at the University of Stuttgart indicated that the propulsion system has an I_{sp} of 1340 s, a thrust of 0.0009 mN, and a power consumption of 1.5 W.

Nanyang Technological University (NTU) developed a dual-axis PPT system for the AOBA VELOX-III that was launched in 2016 [2,240]. The PPT increased the lifetime of the AOBA VELOX-III mission from three months to six months due to drag compensation at low Earth orbit (LEO) [240]. AOBA VELOX-IV, launched in 2019, contained a four-head PPT that is based on NTU's flight-demonstrated PPT unit [2,241]. The four-head PPT consists of a PPU and four thruster heads. Each head carries 5.72 g of Teflon. It occupies a volume of 0.5 U. It produces an impulse bit of 25.2 μNs and an I_{sp} of 676 s by consuming 2.25 W.

The University of Washington developed a PPT system for the 3 U CubeSat HuskySat-1 that launched in 2019 [242]. In comparison to Teflon PPT, the system used a serrated coaxial cathode with solid sulfur propellant to provide a twofold increase in specific thrust performance. The thruster performance is characterized by an I_{sp} of 1200 s and a specific thrust of 0.045 mN/W using sulfur. No information was found on the in-orbit performance of the flown system.

The Fachhochschule Wiener Neustadt and FOTEC developed a PPT propulsion system for the 2U PEGASUS that launched in 2017 [243]. The PPT system provides 2-axis attitude control. It generates 400 V at 1mA for ignition. It consists of four independent ignition circuits and four thruster heads. Each thruster head can produce a thrust of 0.0022 mN at an I_{sp} of 600 s. The lifetime of the PPT is at least 700,000 discharges which produce a total ΔV of 6 m/s for the 2U PEGASUS.

3.3.7. Ambipolar

Ambipolar thrusters use RF antennas to ionize the propellant within a discharge cavity and heat electrons, thus creating a charge imbalance that accelerates ions out of the cavity via ambipolar diffusion. This thruster provides the thruster plume with neutral charge; thus, no neutralizer is necessary. This technology does not use electrodes; therefore, it eliminates concerns with electrode material compatibility and erosion.

The Technology for Propulsion and Innovation (T4i) developed the REGULUS propulsion system based on the magnetically enhanced RF plasma propulsion technology [244]. The system consists of a dielectric cylindrical ionization chamber, an RF antenna, a gas injection system, and a magnetic system for plasma confinement. Iodine was chosen as the baseline propellant due to its high storage density, lower cost compared to that of xenon, and requiring no pressurization. The first flight demonstration of this system was launched in the UniSat-7 in 2021. The flight unit has a total wet mass of 2.5 kg, and it occupies a volume of 1.5U. It is capable of providing a thrust of 0.6 mN with an I_{sp} of 600 s at 50 W.

CubeSat Ambipolar Thruster (CAT) technology was developed by the University of Michigan [245]. It operates by using helicon electromagnetic waves to ionize the propellant. An RF PPU supplies RF energy that is provided via helical half-twit helicon antenna. The thruster includes permanent magnets to accelerate the plasma through a magnetic nozzle, generating thrust. The antenna wraps the plasma liner where the gaseous propellant is fed and ionized. The 3D-printed Faraday shield, made of titanium, is used to encase the

thruster and provide a structural support for the magnets [246]. CAT was tested with xenon and argon. Using xenon as the baseline propellant, the CAT has a thrust range of 0.5–4 mN with an I_{sp} range of 400–800 s at 10–50 W for 3 U CubeSats [245]. This ambipolar technology is commercialized by Phase Four LLC. The Phase Four Radio-Frequency Thruster (RFT) technology was tested in two thruster units: a low-power CubeSat-optimized unit (35 W to 100 W RF power) and a higher power small satellite unit (100 W to 500 W RF power) [247]. The two units can generate a thrust range of 0.3–9 mN with an I_{sp} range of 61–1500 s. This technology was flight demonstrated in the Phase Four Maxwell thruster unit flown in two satellites as part of the Transporter 1 mission in 2021 [248]. The schematic of the ambipolar thruster technology is shown in Figure 30.

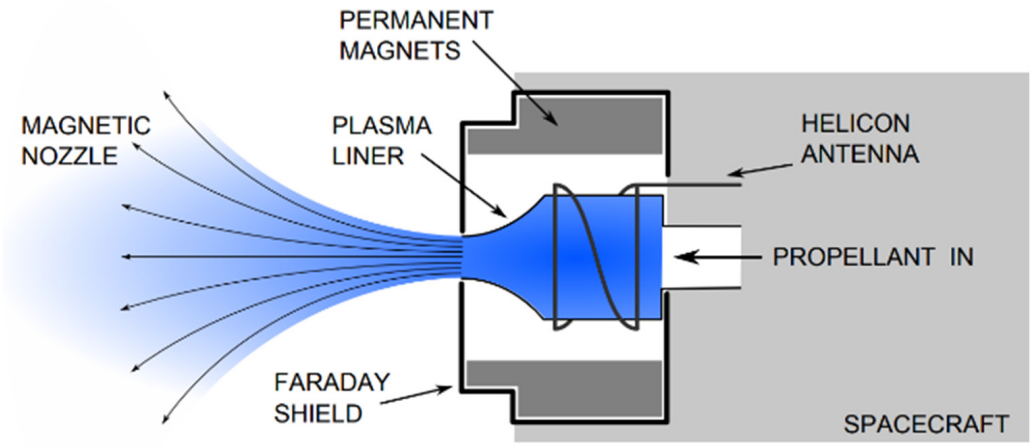

Figure 30. Schematic of CubeSat Ambipolar Thruster [245].

3.4. Propellant-Less

Propellant-less systems interact with external sources such as the sun, planetary atmosphere, planetary magnetic field, or external laser sources in order to provide a thrusting force. A solar sail uses solar radiation pressure as the propelling force, whereas electrodynamic conductive tethers utilize planetary the magnetic field and plasma to generate a Lorentz force that propels the spacecraft. Instead of carrying propellant onboard, the propellant-less system employs additional deployable structures such as tethers, wires, and reflective sheets that interact with the external sources and produce a realized thrusting force on the spacecraft.

3.4.1. Solar Sail

Solar sail propulsion utilizes solar radiation pressure force while in orbit to produce thrust. Solar sail missions typically carry deployable lightweight structures surfaces to increase the area that receives solar radiation pressure in order to propel the spacecraft. These deployable structures can also be used for deorbiting application by increasing atmospheric drag force on the spacecraft. Solar flux (S) and the resulting incident radiation force magnitude (F_i) exerted by solar radiation pressure can be calculated using the following equations [3]:

$$S = S_0 \left(\frac{D_0}{D} \right)^2 \tag{21}$$

$$F_i = \frac{SAsin(\theta)}{c} \tag{22}$$

where S_0 is solar flux at 1 Astronomical Unit (AU) (1.36 kW/m^2), D_0 is the distance from Earth to the sun (1 AU = 150 $\times$ 10^9 m), D is the distance from the sun, A is the flat solar sail area, θ is the tilt angle of the solar sail with respect to the sun–sail line, and c is the speed of light.

JAXA demonstrated the first successfully interplanetary solar power sail technology in the IKAROS mission in 2010 [249]. The IKAROS mission demonstrated the deployment of solar sail technology in space, the generation of solar power via a solar sail, solar pressure acceleration by the sail, as well as guidance and navigation by solar sailing. The solar sail membrane is made of 7.5 μm polyimide. It consists of four trapezoidal petals, with a Flexible Solar Array (FSA) cell for power generation up to 300 W. The deployed sail structure has a span of 20 m. The IKAROS spacecraft successfully used solar sail technology to perform a Venus flyby. Although the IKAROS mass is larger than 100 kg, it is noted here since the mission provided a significant demonstration of the solar sail technology.

NASA developed the NanoSail-D2 mission to demonstrate solar sail technology in space for deorbiting. The sail is made of a reflective polymer called CP-1 [250]. It uses four booms to support the sail membrane structure once deployed. The sail area is 10 m^2 oriented towards incoming solar radiation that will ultimately reflect the solar photons as depicted in Figure 31. The angle, shown for demonstration purposes, is the sunlight reflection angle, also known as the incident light angle, which affects the resulting effective incident force. A 1600 m^2 sail in Earth orbit will provide about 0.03 N of thrusting force due to solar radiation pressure [251]. The NanoSail-D2 mission was launched aboard the Fast Affordable Science and Technology SATellite (FASTSAT), and the solar sail was ultimately deployed in 2011. Commands to eject the NanoSail-D2 from the FASTSAT were unsuccessful [252]. After more than one month, the NanoSail-D2 freed itself in 2011 and the sail deployment was demonstrated. NASA's Near-Earth Asteroid (NEA) Scout uses a solar sail as the main propulsion for the 6U CubeSat. The solar sail subsystem consists of a 2.5 μm thick CP1 aluminized sail and uses a deployer system that is based on the NanoSail-D design [253]. NEA Scout mission was launched in 2022; however, communication with the spacecraft was not established.

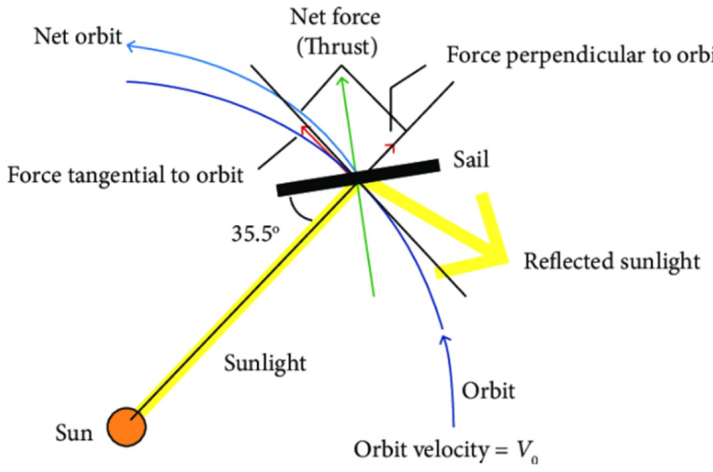

Figure 31. Schematic of solar sail propulsion technology [251].

The Planetary Society developed the LightSail program that consists of two missions: the LightSail 1 mission that validated the solar sail deployment sequence in 2015 and the LightSail 2 mission that successfully demonstrated controlled solar sailing in Earth's orbit in 2019 [254]. The 3U LightSail 2 contained a single-axis momentum wheel and magnetic torque rods to control the attitude and the orientation of the solar sail relative to the sun. The solar sail system has four sail sections that are made of 4.6 μm aluminized Mylar. The total deployed area is 32 m^2. The sail segments are deployed and supported by 4 m booms made of elgiloy alloy. The LightSail 2 was deployed into a near-circular orbit with an altitude of 720 km. The solar sailing technology was used to provide thrust into the orbital velocity direction, thus increasing orbital energy and opposing atmospheric drag perturbations at some time intervals. Received data suggest that the orbit apogee steadily increased following controlled sail deployment, and the perigee decreased, thus making

the orbit more eccentric. However, atmospheric drag eventually dominated the solar sail acceleration and the LightSail reentered in 2022 [255]. The orbital decay rate was notably slower in the solar sailing mode, declaring success of the demonstration mission [254].

The University of Surrey developed the Deorbitsail technology demonstration mission [256]. The goal of Deorbitsail was to demonstrate rapid deorbiting due to atmospheric drag using solar sails. The sail system consists of four deployable, rectangular quadrants. It has an area of 25 m^2 and is made of 12.5 μm semi-translucent Kapton HN membrane. The mission launched in 2015; however, the solar sail system did not deploy [257]. The CNUSAIL-1 mission, developed by Chungnam National University, was designed to demonstrate the deployment of a 4 m^2 sail and use of the sail for deorbiting [258]. The sail is made of a 0.25 μm Kapton sheet.

CU Aerospace and The University of Illinois developed the CubeSail mission to demonstrate solar sail deployment in space [259]. The mission was designed to separate the 3 U CubeSail into two 1.5 U CubeSails with a solar ribbon deployed between them. The solar ribbon is 250 m long and 8 cm wide. The orientation of the solar ribbon sail can be controlled at either end by controlling each 1.5 U CubeSat. The mission launched in 2018; however, the technology was not demonstrated because communication with CubeSail was not established [260].

3.4.2. Electrodynamic Tethers

Electrodynamic tether propulsion utilizes the current flowing in a conductive tether to interact with the Earth's magnetic field. This interaction results in a Lorentz force that either provides a thrust force that increases the orbital energy or a drag force that decreases the orbital energy. The orientation of the current in the tether determines whether this force is along the orbital velocity vector or against it. The current can also be generated by the collection of charged particles from the ionospheric plasma at different ends of the tether.

Tethers Unlimited Inc. developed the NanoSat Terminator Tape (NSTT) electrodynamic tether unit for passive deorbiting [261]. The NSTT contains a deployable conductive tape that is 0.15 m wide and 70 m long. The purpose of this system is to increase the orbital decay rate of spacecraft using electrodynamic drag and aerodynamic drag. For the electrodynamic force, the conductive tape, deployed in Earth's orbit, interacts with Earth's magnetic field leading to a voltage bias that charges the ends of the deployed tape relative to the ionospheric plasma. This voltage bias attracts the ionospheric ions and electrons, forming a current flow along the tape as shown in Figure 32. This current flow interacts with Earth's magnetic field and induces a Lorentze force that is oriented to act as a friction force that reduces orbital energy. Since the tape increases the effective area that the atmospheric drag acts on, the drag force is increased. The NSTT unit was successfully demonstrated in the Prox-1 mission in 2019. The U.S. military space Surveillance Network observed that the Prox-1 satellite deorbited more than 24 times faster than before deploying the tape [262]. The NSTT unit was also used in NPSat-1 and Alchemy in 2020 [261].

The Naval Research Laboratory developed the Tether Electrodynamics Propulsion CubeSat Experiment (TEPCE) to test electrodynamic tether propulsion technology [263]. The TEPCE is a 3 U CubeSat that separates in orbit into two 1.5 U CubeSats connected by a conductive tether. TEPCE was launched in 2019. The actual post-tether deployment orbital lifetime was 78 days, which is more than that of the analysis prediction (30–60 days). The difference was due to the partial deployment of the tether; therefore, a smaller area-to-mass ratio led to an increase in orbital lifetime. The objective is to demonstrate deorbiting using propellant-less technology. The electrodynamic tether reduced the orbital lifetime of TEPCE by 6 years.

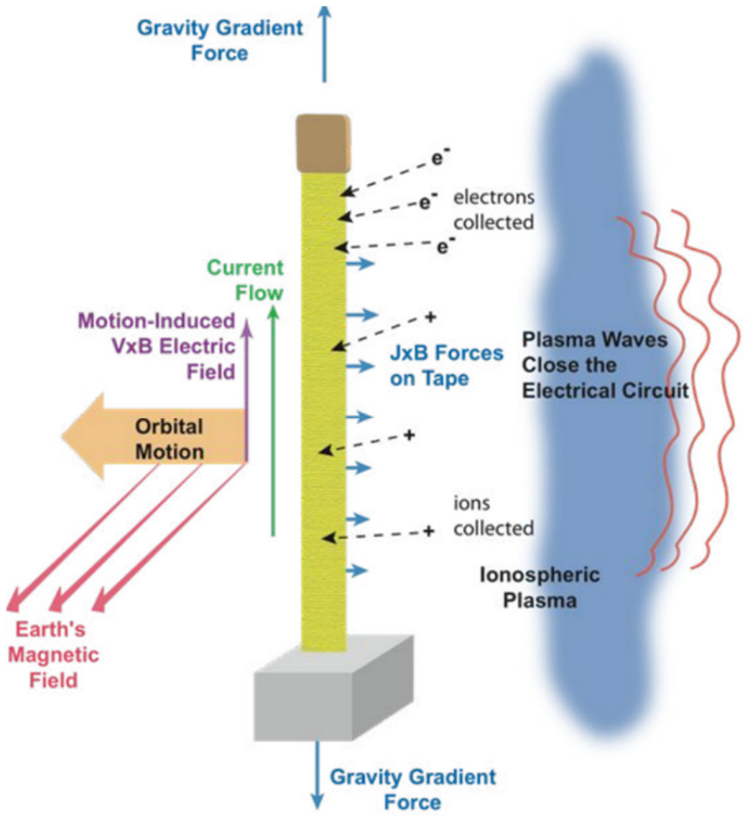

Figure 32. Schematic of electrodynamic tether technology [261].

The Miniature Tether Electrodynamics Experiment (MiTEE) was developed by the University of Michigan [264]. MiTEE is a 3 U CubeSat with a picosatellite mounted at the end of a 1 m deployable boom. MiTEE-1 was launched in 2021 with the purpose of characterizing the electron current collection of the picosatellite and the 3 U CubeSat in order to support electrodynamic tether propulsion system for future missions. The 1 m boom used was short and, therefore, the objective was not to realize any thrust effects on MiTEE-1. The University of Michigan is planning to develop a subsequent mission, MiTEE-2, that will utilize the data and lessons learned from MiTEE-1 in order to demonstrate electrodynamic tether propulsion. The boom will be replaced by a tether that has a length in the range of 10 to 30 m.

Kagawa University launched the Space Tethered Autonomous Robotic Satellite (STARS) mission in 2009 [265]. It consists of a mother–daughter satellite connected by a 5 m deployable tether. The mother satellite deploys a tether connected to the tethered space robot (daughter satellite). The primary goal of the mission was to demonstrate the tethered space robot technology in space. The two satellites separated successfully; however, the tether only deployed up to several centimeters instead of several meters due to a malfunction in the compression mechanism used in the deployment springs. The STARS-II mission was launched in 2014 to demonstrate electrodynamic tether technology; however, data about the tether deployment demonstration and its details were not obtained due to a computer malfunction [266]. It was inferred that the tether was deployed due to a shorter orbital lifetime (52 days) compared to that of a satellite of the same mass but without a tether. The Shizuoka University's STARS-C mission, launched in 2016, included a mother–daughter system connected by a 100 m long Kevlar tether. The communication system experienced an issue that prevented telemetry data transmission. The tether deployment was evaluated and inferred using the orbital lifetime and it was inferred that the tether did not fully extend. STARS-Me, launched in 2018, was developed to demonstrate a miniature elevator climber system on a 3 m tethered CubeSat.

3.4.3. Other Propellent-Less Concepts

Photonic laser propulsion refers to the emission of photons to exert photonic pressure that transfers momentum to the spacecraft in order to generate thrust, which is slightly similar to the concept of reflecting solar photons. However, photons are emitted by either an external high-power source or a laser source carried onboard the spacecraft. This principle requires significantly high-power sources, as well as large space platforms in order to provide sufficient propelling force. Y.K. Bae Corporation developed the Photonic Laser Thruster (PLT) that uses a photonic amplification process through trapping and bouncing photons between two high-reflectance (HR) mirrors, forming an optical cavity that recycles photonic energy [267,268]. The schematic of the amplified photonic laser system is shown in Figure 33. Laboratory demonstration of this technology was conducted and demonstrated that the maximum achieved thrust was 3.36 ± 0.18 mN with a specific thrust-to-power ratio of 7.1 ± 0.6 mN/kW [269]. This is due to using the amplification process that translates the provided laser power into an intracavity laser beam that is much more powerful.

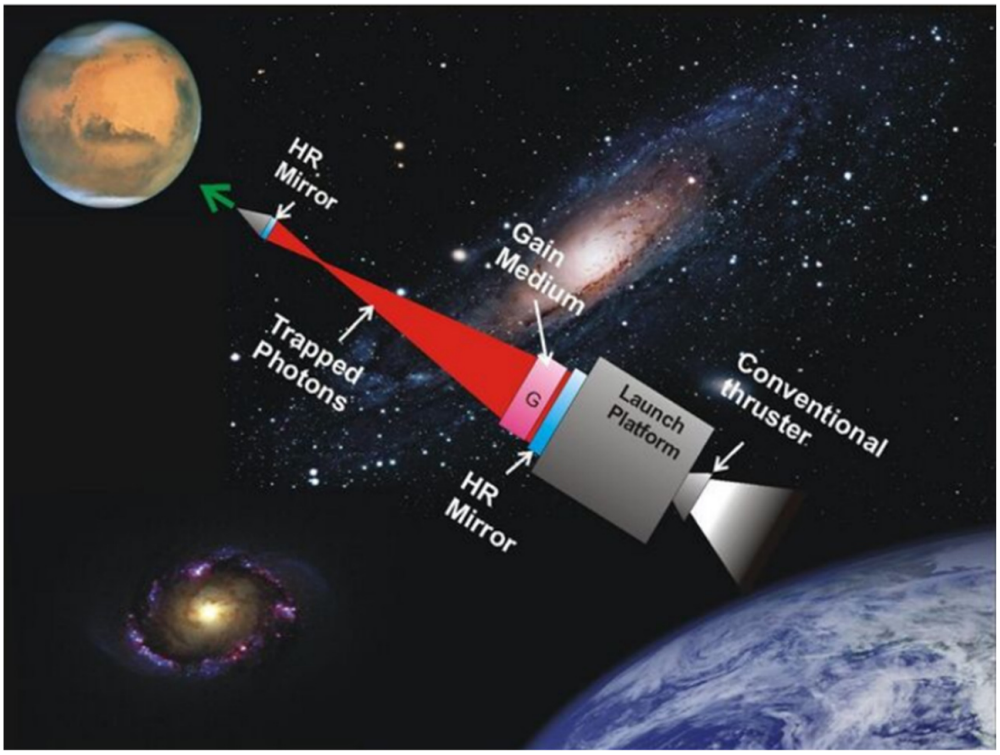

Figure 33. Schematic of amplified Photonic Laser Thruster (Y.K. BAE CORP, Tustin, CA, USA) [270].

The magnetic sail concept includes a loop of a superconducting cable or coil to generate an artificial magnetic field that interacts and deflects charged particles in solar wind or interplanetary plasma wind, causing the transfer of momentum that propels the magnetic sail spacecraft. In 1991, the magnetic sail concept was studied and modeled for interplanetary travel application [271]. The diameter of the cable loop is in the order of tens of kilometers. A recent numerical simulation analysis showed that a 25 km loop radius provides a minimum flight time of less than one year in the Earth–Venus's transfer case, whereas a 30 km loop radius provides a minimum flight time of less than two years in Earth–Mars transfers [272]. The magnetic sail propulsion technology is illustrated in Figure 34.

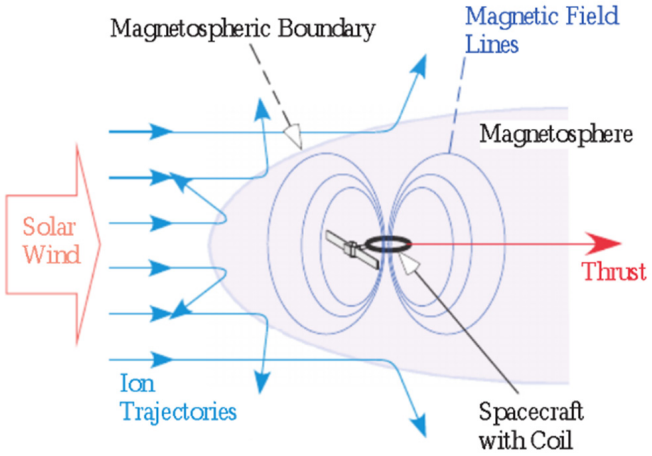

Figure 34. Schematic of magnetic sail [273].

The electric sail concept, depicted in Figure 35, uses charged tethers with a highly positive voltage to produce an electric field that electrostatically repels positively charged ions in the incoming solar wind [274]. This repulsion creates a momentum exchange that propels the electric sail spacecraft The electric sail system uses an array of multi-kilometer-length charged tethers to create an electric field that grows in an effective area as the spacecraft moves away from the sun. This is due to an increase in electron Debye length as the electric sail system moves away from the sun, leading to a growth in the size of the positive electric field and the apparent size of the sail. Therefore, this was calculated to result in a decrease in thrust levels at a rate of $1/r^{7/6}$ (r is the distance from the sun). In comparison to solar sail thrust declining at a rate of $1/r^2$, the electric sail system provides acceleration up to a 20 AU distance, whereas the solar sail is only effective up to 5 AU.

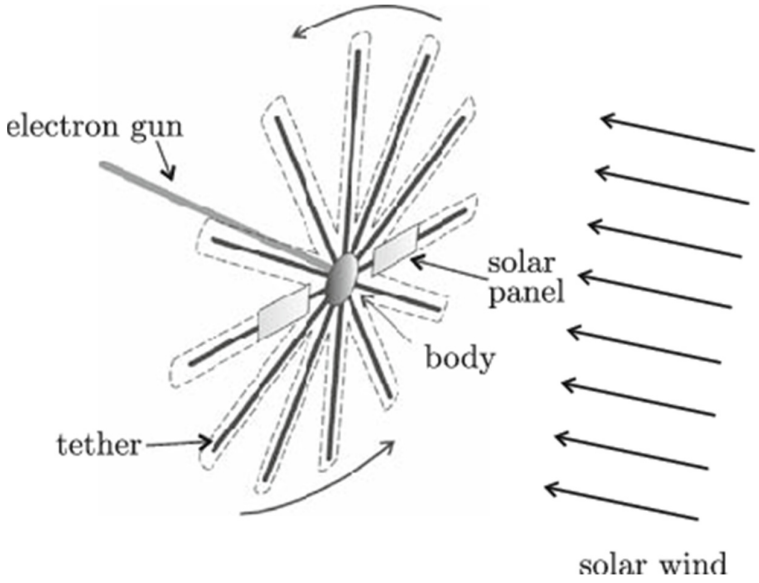

Figure 35. Schematic of electric sail propulsion. Thrust is generated from charged wires that extend to several kilometers [274].

Propellent-less propulsion technology eliminates the need to carry propellants, thus no pressurization, valves, and propellant management are needed. It also utilizes an external source of energy that is abundant and available for a very long time. Additional structures, typically large and lightweight, are used in propellent-less technologies instead of a propellant system. Even though external energy is abundant, very large systems are typically needed to utilize such energy and provide feasible and beneficial thrust levels.

3.5. Multimode and Hybrid Systems

Multimode propulsion refers to adding two or more independent propulsion technologies in a single spacecraft propulsion system, in which they share some components, mainly that of using a shared propellant tank to feed all onboard propulsion modes. The University of Tokyo developed the Ion Thruster and Cold Gas Thruster Unified Propulsion System (I-COUPS) multimode micro-propulsion system for the PROCYON spacecraft that launched in 2014 [275]. The propulsion system, depicted in Figure 36, consists of a cold gas thruster unit, an ion thrust unit, a PPU, a gas-management unit, and a control unit. Both types of thrusters share the same xenon gas system. The total wet mass of the system is 9.96 kg (including 2.57 xenon), and the total mass of the spacecraft is 70 kg. The power consumption of a two cold gas thruster operation is 11.5 W, whereas the ion thruster operation consumes 40 W. The ion thruster achieved a total operational time of 223 h during interplanetary travel with 0.345 mN nominal thrust value that was evaluated using Doppler shift data. The cold gas thruster has a rated thrust level of 21.3 mN with an I_{sp} of 24.5 s. The cold gas thruster unit was successfully operated (over 103 operations) as a reaction control system by unloading the wheel momentum. In multimode propulsion, the operation of one thruster system is not dependent on the functionality of the other system.

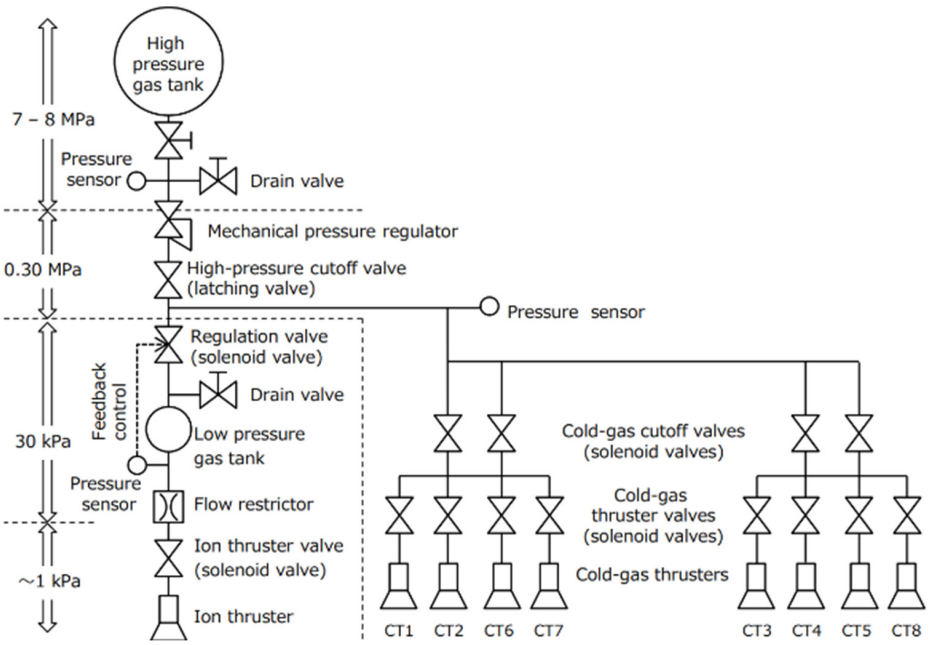

Figure 36. Schematic of I-COUPS multimode system [275].

The Glenn Lightsey Research group in the Georgia Institute of Technology's SSDL developed a dual-mode green propulsion system, referred to as Spectre [276]. Spectre consists of one 1000 mN monopropellant thruster and four arrays of 0.02 mN electrospray thrusters. Spectre uses AFM315E as the working propellant to feed the two firing modes. The chemical monopropellant mode is characterized by delivering a ΔV of 619 with an I_{sp} of 250 s using 4.464 kg of propellant, whereas the electrical mode consists of a total of 16 electrospray thrusters that provide a ΔV of 477 m/s with an Isp of 1500 s using 0.496 kg propellant. The chemical mode provides high thrust and requires relatively high temperature and pressure, whereas the electric mode provides higher specific impulse operation and only needs to be supplied with a propellant after every 150 h of firing.

Pale Blue Inc. (Kashiwa, Japan) and the University of Tokyo developed a dual-mode propulsion system operating in a resistojet mode or in an ion mode [186]. The system shares the water propellant tank for operating each propulsion mode. The resistojet system works by evaporating water and exhausting vapor to produce thrust. It consists of four thrusters. It has a relatively low I_{sp} of 48 s and provides a thrust of 0.46 mN using four

thrusters. On the other hand, the ion thruster uses electron resonance heating to generate and exhaust water plasma. It consists of one 0.15 mN thruster with an I_{sp} of 500 s.

On the other hand, hybrid propulsion, which is different from the chemical hybrid one, refers to merging propulsion technologies into one system. In hybrid propulsion, the operation of one propulsion technology is dependent on the functionality of some key elements in the other technology onboard. VACCO Industries developed an integrated hybrid micro-propulsion system for the 6 U ArgoMoon mission that was launched in 2022 [2,277]. The hybrid system consists of a green monopropellant propulsion unit and a cold gas propulsion unit in one single system as shown in Figure 37. The cold gas system contains four 25 mN thrusters that use R-134a as the working propellant, which is also used as a pressurant for the monopropellant system [277]. The monopropellant system consists of one 100 mN thruster that uses LMP-103S as the propellant. The monopropellant system can deliver a ΔV of 56 m/s for a 14 kg CubeSat. The operation of monopropellant propulsion relies on having the R-134a regulated gas pressurant which also directly feeds the cold gas system.

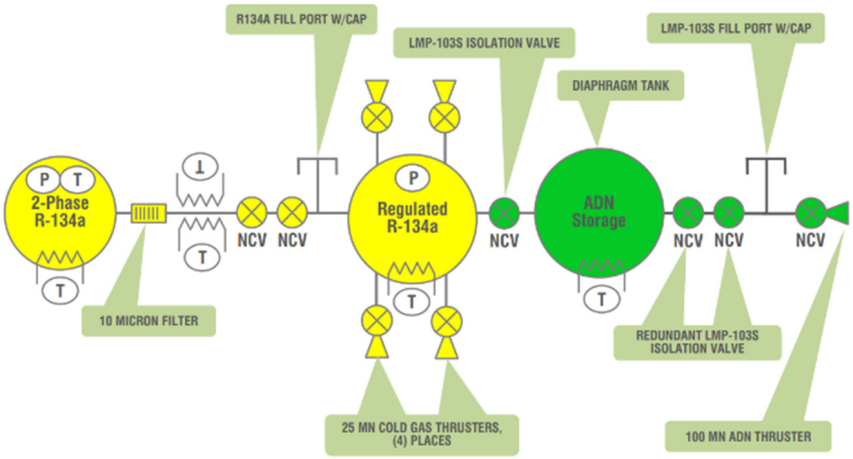

Figure 37. Schematic of ArgoMoon hybrid propulsion system [277].

Both multimode and hybrid systems can potentially be advantageous because they extend the in-space propulsion capabilities for small satellites. Such systems usually combine relatively high thrust, low specific impulse technologies such as kinetic and chemical propulsion with low thrust, and high specific impulse technology such as electric propulsion. Therefore, one single propulsion system (hybrid or multimode) can leverage the benefits of different propulsion technologies, however, at the expense of increased cost, mass, volume, and power.

4. Performance of Propulsion Technologies

Propulsion performance data of developed miniaturized propulsion systems were collected from commercial companies and experimental research papers. These data were plotted, as shown in Figure 38, in order to compare the performance of various propulsion technologies. Kinetic propulsion systems are characterized by a low I_{sp} and low to medium thrust levels.

Cold gas systems provide the lowest I_{sp} performance, whereas resistojet systems show improvement in I_{sp} performance due to augmenting heat to the propellant flow in the thruster body. Kinetic propulsion technology is relatively simple and lightweight in terms of design and operation, and it has been extensively used in small satellites in order provide attitude control and small orbital maneuvers (up to few tens of m/s).

Chemical propulsion systems, mainly green monopropellant systems, offer medium I_{sp} performance and high thrust levels that are suitable for performing large impulsive maneuvers for small satellites. However, chemical propulsion systems tend to be more massive due to larger components in the propellant storage and feed system.

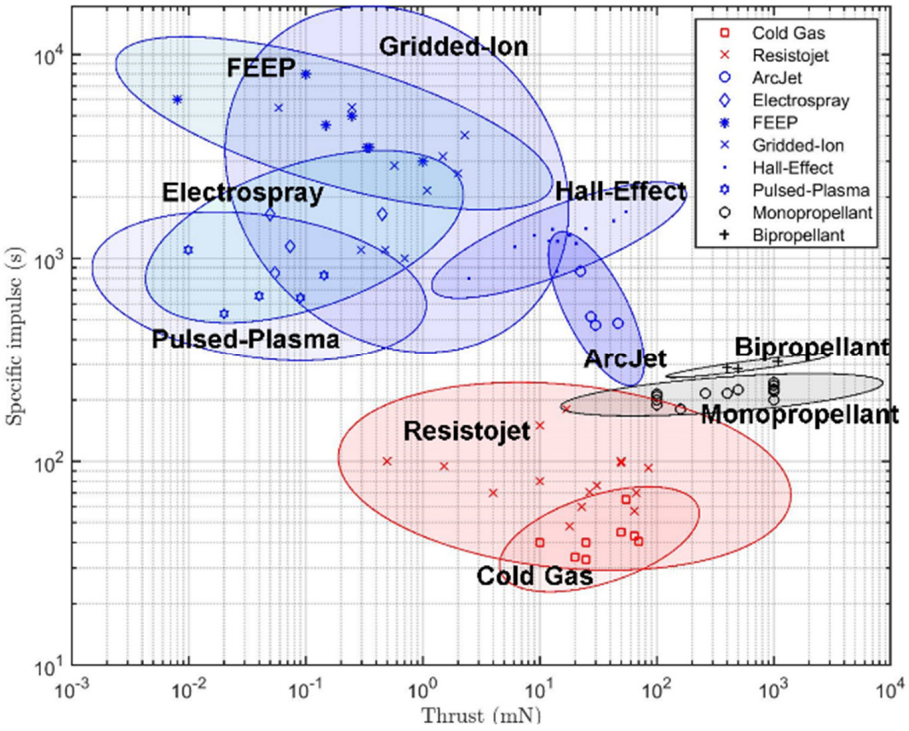

Figure 38. Propulsion performance of different propulsion technologies for small satellites.

Electric propulsion systems are characterized by a significantly higher I_{sp} performance that is accompanied by low thrust levels. In addition, electric systems consume the most power compared to other surveyed propulsion technologies due to using electrical power as the main source of energy for their thrust operation. Therefore, electric systems have the lowest level of thrust-to-power ratio performance when measured as indicated in Figure 39.

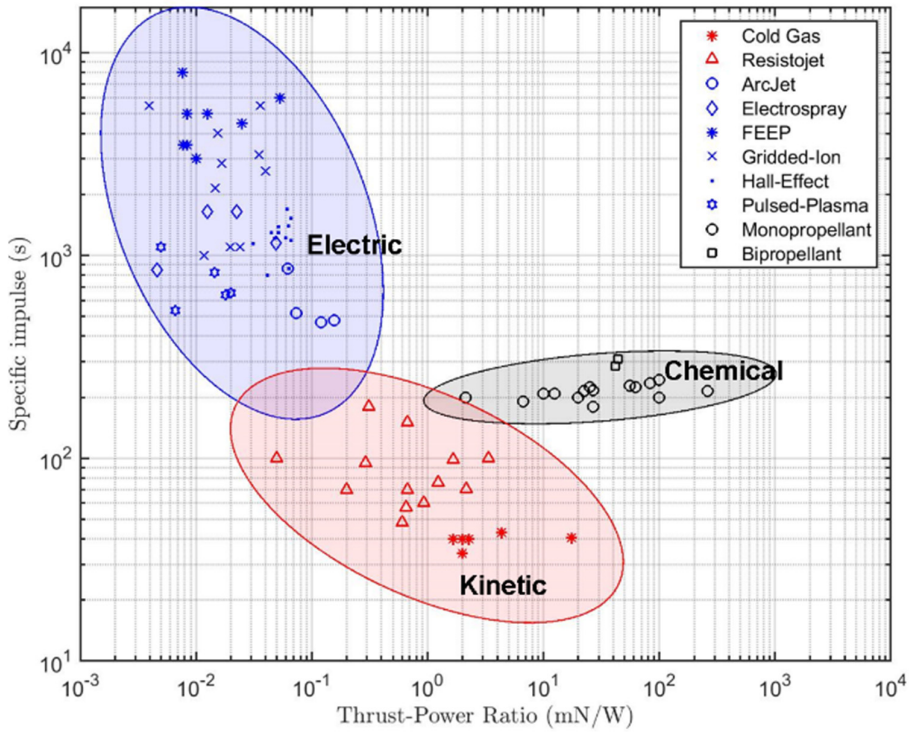

Figure 39. Thrust-to-power ratio performance of different propulsion technologies.

The choice of the propulsion system is dependent on the range, needs, and objectives of the specific mission. Small satellite missions have defined ΔV requirements, as well as constraints on mass, volume, and power. These mission inputs are used to inform the analysis of selecting the ideal propulsion system.

5. Future of Small Satellite Propulsion

The range and maneuvering capabilities of small satellite missions are limited by the amount of fuel carried onboard mainly due to volume and mass constraints. Enabling an in-orbit refueling capability will extend the utility and lifetime of small satellites in space. The U.S. Space Force announced its interest in in-orbit satellite refueling and awarded the Orion Space Solution, a contract to develop the geosynchronous hydrazine refueling technology demonstration mission, to the Tetra-5 experiment, which is expected to be launched in 2025 [278]. Orbit Fab's refueling port will be used in the Tetra-5 mission, with Orbit Fab having developed the Rapidly Attachable Fluid Transfer Interface (RAFTI) which was launched for a technology demonstration in the Tanker-001 Tenzing mission in 2021 [279]. Orbit Fab developed the RAFTI based on successful demonstration of fluid transfer within Project Furphy in the International Space Station (ISS) in 2019. The RAFTI consists of a service valve that functions as a passive fill/drain valve to enable in-orbit attachment and fuel transfer. Two RAFTI service valves were integrated in the 35 kg Tenzing spacecraft. The Tenzing spacecraft, the first propellant tanker, also carried a storable high-test peroxide (HTP) propellant to demonstrate propellant storage. NASA is currently developing the On-orbit Servicing, Assembly, and Manufacturing 1 (OSAM-1) mission that includes a robotic spacecraft servicer that will be used to refuel a satellite in orbit [280]. The OSAM-1 is expected to launch no earlier than 2025. As CubeSats launches continue to rise, the complexity and range of their missions are also increasing. Therefore, CubeSats will need to have increased maneuvering capability to meet the demand of using them in complex, extended space missions. The development of in-orbit refueling capability may offer a promising solution to extend CubeSat maneuverability without being limited by mass, volume, and power budgets.

Researchers at MIT's Space Propulsion Laboratory have researched an electric propulsion staging concept aimed at enhancing the capabilities of CubeSats for interplanetary missions [156,281]. They leveraged advances in micromachining processes for miniaturization to develop MEMS-based electrospray thrusters for CubeSats. The inherently small size factor and compactness of electrospray propulsion make it well suited for a staging-based electric propulsion system that consists of a series of electrospray thruster arrays. In a staging operation, thruster modules that deplete their fuel and reach their lifetime limit are ejected, resulting in a reduction in spacecraft mass. The staging concept results in an increased total ΔV capability during the mission due to the decreasing spacecraft mass. As an example, in the case of a 3U CubeSat transferring from GEO to the Moon, the research analysis revealed a 12.7% reduction in propellant mass consumption and time of flight when using a staged-based system compared to a fixed structural spacecraft [281]. The high specific impulse performance of miniature electric propulsion systems makes them attractive for powering small satellite deep space exploration, especially when combined with a staging concept that further reduces propellant consumption and mission duration. These factors are critical considerations in the development of a micro-propulsion system for small satellites.

Solar Thermal Propulsion (STP) operates by converting solar energy, collected via a concentrator, to thermal energy that is used to heat the propellant as depicted in Figure 40. The concept of STP was first conceived in 1956 by Krafft Ehricke [282]. Development of STP technology provides a moderate thrust level and a relatively high specific impulse which fills the gap in propulsion performance between chemical and electrical propulsion. STP can be a suitable, low-power propulsion solution to small satellites since it increases specific impulse performance by heating the propellant to high temperatures without requiring electrical energy. A micro-scale solar thermal engine was studied and developed at SSC

under a research program, initiated in 2001, that aimed at developing STP suitable for use aboard satellites of less than 100 kg [283]. The application of SSC's small satellite SPT was found to be beneficial for GEO insertion, near-earth escape, and lunar orbit insertion since STP is characterized with an I_{sp} of 400 s and a moderate thrust magnitude of several Newtons. During their micro-scale STP engine analysis in 2003, Kennedy and Palmer found that performing moderate thrust firings of approximately 5 N using STP engine will provide transfer times range from as little as 30–40 days for GEO transfer to 275 days for near-earth bodies. Propellants considered for STP engine were hydrazine, ammonia, and water. In 2019, Zhumaev and Shcheglov developed a mathematical model to numerically simulate the operational dynamics of STP for a CubeSat nanosatellite [284]. They found that a 1 U STP unit can provide a ΔV of more than 35 m/s for a 6U CubeSat in less than 24 h. With this ΔV, two satellites can be phased out to opposite points of a 600 km circular orbit in less than 5 days.

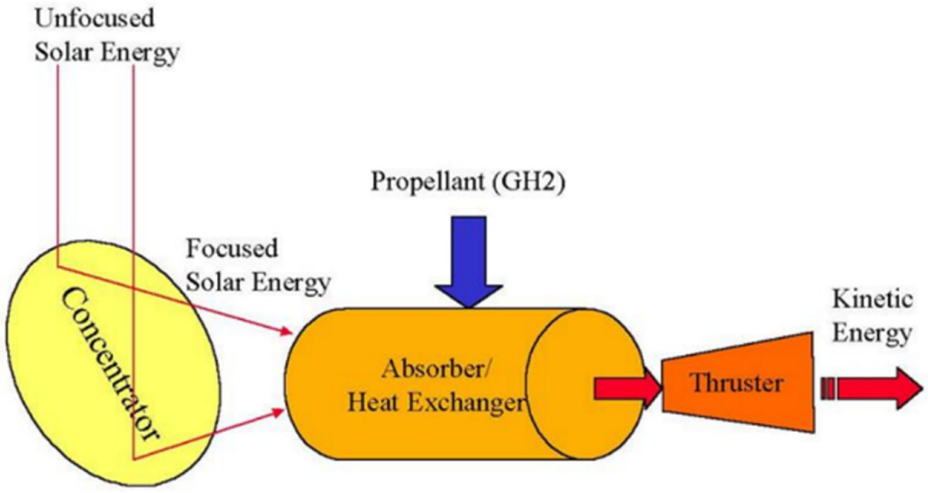

Figure 40. Schematic of Solar Thermal Propulsion [282].

In 2022, the National University of Defense Technology developed a design of an STP system with liquid ammonia propellant for microsatellites [285]. The results of their work show that the STP system can heat the propellant to more than 2050 K with a platelet heat exchanger, generating an intermittent thrust of about 26 N and delivering a ΔV of 1470 m/s to a 100 kg satellite within 19 days using only 42 kg of propellant. The advantage of this STP system is the possibility of full propellant utilization in order to provide a high specific impulse and thrust performance with relatively small mass and without requiring energy supply devices. On the other hand, the limitations of the design include complex control dynamics to receive solar radiation and inconstant propulsion performance due to variations in orbit and propellant mass, as well as reduced payload proportional mass due to the added mass of solar concentrators and heat exchangers used in the system. Solar radiation heat storage is one way to address the inconstant thrust performance of STP caused by variations in sun illumination in orbit. The Nanjing University of Aeronautics and Astronautics, China Aerodynamics Research and Development Center, and China Ministry of Industry and Information Technology investigated the feasibility of a regenerative STP system that incorporates a thermal energy storage mechanism in order to overcome STP failure to generate thrust in shadow areas, as well as issues related to synchronizing STP operation with sun illumination time in orbit [286]. Their numerical simulation used hydrogen as the regenerative STP system propellant, which is capable of providing 2 N of thrust with an I_{sp} of 690 s. The results of their work indicate that the maximum time needed to complete heat storage (4000 s) is within the illumination time in LEO and that that the regenerative STP system can provide a continuous 100 s operation at maximum thrust in the shadow area. STP offers a promising propulsion technology solution, especially for CubeSat missions beyond LEO.

6. Conclusions

In summary, this literature review highlights the critical importance of propulsion systems in the context of small satellite missions. CubeSats, with their miniature size, have revolutionized space exploration, making it more accessible to universities and startups while also increasing cost efficiency. Nevertheless, their inherent limitations in terms of volume and mass have been a constraint on their capabilities in orbit. This is where propulsion systems step in as transformative assets, enabling orbital maneuverability, increased mission capabilities, and extended mission lifetime. The presented information on miniaturized propulsion systems indicates that micro-propulsion is not a mere technological add-on but rather a strategic subsystem for the future of CubeSats. Micro-propulsion empowers CubeSats to execute complex missions that were traditionally limited to larger satellites. Furthermore, the illustrated graphs that depict the performance attributes of these systems serve as decision support tools for mission designers, offering clear insights into the trade-offs among key propulsion parameters and mission requirements. Fundamentally, micro-propulsion systems for small satellites represent the gateway to a new era of deep space exploration.

Funding: This research was funded by Khalifa University KUX project number 8434000368.

Acknowledgments: The authors would like to thank Khalifa University, UAE Space Agency, and Yahsat for supporting this work by funding the university research lab.

Conflicts of Interest: The authors declare no conflict of interest.

References

1. NASA. *What are SmallSats and CubeSats?* NASA: Washington, DC, USA, 2015.
2. Kulu, E. Nanosats Database | Constellations, Companies, Technologies and More. Available online: https://www.nanosats.eu/ (accessed on 4 September 2023).
3. Humble, R.W.; Gary, H.N.; Larson, W.J. *Space Propulsion Analysis and Design*; McGraw Hill: New York, NY, USA, 1995; pp. 10–11.
4. Legge, R.S.; Clements, E.B.; Shabshelowitz, A. Enabling microsatellite maneuverability: A survey of microsatellite propulsion technologies. In Proceedings of the 2017 IEEE MTT-S International Microwave Symposium (IMS), Honolulu, HI, USA, 4–9 June 2017; pp. 229–232.
5. Lide, D.R. *CRC Handbook of Chemistry and Physics*, 85th ed.; CRC Press: Boca Raton, FL, USA, 2004.
6. R-236fa. Climalife. 2013. Available online: https://climalife.dehon.com/uploads/media/3/241/241_1746_r236fa-fd-en-13.pdf (accessed on 4 September 2023).
7. Seubert, C.; Pernicka, H.; Norgren, C. Refrigerant-based propulsion system for small spacecraft. In Proceedings of the 43rd AIAA/ASME/SAE/ASEE Joint Propulsion Conference & Exhibit, Cincinnati, OH, USA, 8–11 July 2007; p. 5131.
8. Pahl, R.A. Integration and test of a refrigerant-based cold-gas propulsion system for small satellites. In Proceedings of the 24th Annual AIAA/USU Conference on Small Satellites, Logan, UT, USA, 9–12 August 2010.
9. Thermodynamic Properties of HFC-236fa (1,1,1,3,3,3-hexafluoropropane). DuPont Fluorochemicals. Available online: http://www.allchemi.com/download/tables/HFC-236fa-SI.PDF (accessed on 6 October 2023).
10. Steyn, W.H.; Hashida, Y. In-orbit attitude and orbit control commissioning of UoSAT-12. *Spacecr. Guid. Navig. Control Syst.* **2000**, *425*, 95.
11. El-Bordany, R. *In Orbit Calibration of Satellite Inertia Matrix and Thruster Coefficients*; University of Surrey: Guildford, UK, 2001.
12. Ward, J.; Sweeting, M. First in-orbit results from the UoSAT-12 minisatellite. In Proceedings of the Small Satellite Conference, Logan, UT, USA, 10–13 August 2009.
13. Gibbon, D.; Underwood, C. Low Cost Butane Propulsion Systems for Small Spacecraft, 15th AIAA. In Proceedings of the USU Conference on Small Satellites, Logan, UT, USA, 13–16 August 2001.
14. Gibbon, D.A.; Ward, J.A.; Kay, N. The design, development and testing of a propulsion system for the SNAP-1 nanosatellite. In Proceedings of the Small Satellite Conference, Logan, UT, USA, 16–18 October 2000.
15. Bzibziak, R. Update of cold gas propulsion at Moog. In Proceedings of the 36th AIAA/ASME/SAE/ASEE Joint Propulsion Conference and Exhibit, Las Vegas, NV, USA, 24–28 July 2000; p. 3718.
16. Schelkle, M. The GRACE cold gas attitude and orbit control system. *Spacecr. Propuls.* **2000**, *465*, 769.
17. Cardin, J.; Coste, K.; Williamson, D.; Gloyer, P. A cold gas micro-propulsion system for cubesats. In Proceedings of the Small Satellite Conference, Logan, UT, USA, 30 June 2003.
18. Hinkley, D. A novel cold gas propulsion system for nanosatellites and picosatellites. In Proceedings of the Small Satellite Conference, Logan, UT, USA, 22 May 2008.

19. VACCO Industries Micro Propulsion Systems. Available online: https://www.vacco.com/images/uploads/pdfs/MicroPropulsionSystems.pdf (accessed on 4 September 2023).
20. VACCO Industries VACCO ChEMSTM. Available online: http://mstl.atl.calpoly.edu/~workshop/archive/2015/Spring/Day%203/0920-Day-Micro%20Propulsion%20Systems.pdf (accessed on 4 September 2023).
21. Carlisle, C.; Webb, E.H. Space Technology 5-A Successful Micro-Satellite Constellation Mission. In Proceedings of the 21st Annual AIAA/USU Conference on Small Satellites, Logan, UT, USA, 13–16 August 2007. no. SSC07-VII-6.
22. Sarda, K.; Grant, C.; Eagleson, S.; Kekez, D.; Zee, R. Canadian advanced nanospace experiment 2: On-orbit experiences with a three-kilogram satellite. In Proceedings of the Small Satellite Conference, Logan, UT, USA, 22 May 2008.
23. Bonin, G.; Roth, N.; Armitage, S.; Newman, J.; Risi, B.; Zee, R.E. CanX–4 and CanX–5 precision formation flight: Mission accomplished! In Proceedings of the Small Satellite Conference, Logan, UT, USA, 10 August 2015.
24. Grönland, T.-A.; Rangsten, P.; Nese, M.; Lang, M. Miniaturization of components and systems for space using MEMS-technology. *Acta Astronaut.* **2007**, *61*, 228–233. [CrossRef]
25. Persson, S.; D'Amico, S.; Harr, J. Flight results from prisma formation flying and rendezvous demonstration mission. In Proceedings of the Small Satellite Conference, Logan, UT, USA, 19 May 2010.
26. Wu, S.; Chen, W.; Chao, C. The STU-2 CubeSat mission and in-orbit test results. In Proceedings of the Small Satellite Conference 2016, Logan, UT, USA, 11 October 2016.
27. Kvell, U.; Puusepp, M.; Kaminski, F.; Past, J.-E.; Palmer, K.; Grönland, T.-A.; Noorma, M. Nanosatellite orbit control using MEMS cold gas thrusters. *Proc. Est. Acad. Sci.* **2014**, *63*, 279. [CrossRef]
28. Palmer, K.; Li, Z.; Wu, S. In-Orbit Demonstration of a MEMS-based Micropropulsion system for Cubesats. In Proceedings of the Small Satellite Conference 2016, Logan, UT, USA, 11 October 2016.
29. Pérez, L.L.; Koch, P.; Smith, D.; Walker, R. GOMX-4 the most advance nanosatellite mission for IOD purposes. *Proc. 4S Symp.* **2018**, *125*, 12–30.
30. GomSpace. Astrocast Signs Contract with GomSpace Sweden to Deliver Propulsion Systems. 2018. Available online: https://gomspace.com/news/astrocast-signs-contract-with-gomspace-sweden.aspx (accessed on 25 September 2023).
31. Guo, J.; Bouwmeester, J.; Gill, E. In-orbit results of Delfi-n3Xt: Lessons learned and move forward. *Acta Astronaut.* **2016**, *121*, 39–50. [CrossRef]
32. Manzoni, G.; Brama, Y.L. Cubesat micropropulsion characterization in low earth orbit. In Proceedings of the Small Satellite Conference, Logan, UT, USA, 10 August 2015.
33. Arestie, S.; Lightsey, E.G.; Hudson, B. Development of a modular, cold gas propulsion system for small satellite applications. *J. Small Satell.* **2012**, *1*, 63–74.
34. Past Missions. University of Texas at Austin. Available online: https://sites.utexas.edu/tsl/past-missions/ (accessed on 25 September 2023).
35. Imken, T.K.; Stevenson, T.H.; Lightsey, E.G. Design and testing of a cold gas thruster for an interplanetary CubeSat mission. *J. Small Satell.* **2015**, *4*, 371–386.
36. NASA C-POD Micro CubeSat Propulsion System. VACCO Industries. Available online: https://cubesat-propulsion.com/reaction-control-propulsion-module/ (accessed on 25 September 2023).
37. NASA. CubeSat Proximity Operations Demonstration (CPOD). NASA. Available online: https://www.nasa.gov/directorates/spacetech/small_spacecraft/cpod_project.html (accessed on 25 September 2023).
38. Rowen, D.; Hardy, B.; Coffman, C.; Hinkley, D.; Welle, R.; Janson, S. The NASA optical communications and sensor demonstration program: Proximity operations. In Proceedings of the Small Satellite Conference, Logan, UT, USA, 4 August 2018.
39. Gangestad, J.W.; Venturini, C.C.; Hinkley, D.A.; Kinum, G. A sat-to-sat inspection demonstration with the AeroCube-10 1.5 U CubeSats. In Proceedings of the 35th Annual Small Satellite Conference, Virtual, 7–12 August 2021.
40. Piergentili, F.; Balucani, M.; Crescenzi, R.; Piattoni, J.; Santoni, F.; Betti, B.; Onofri, M. MEMS cold gas microthruster on Ursa Maior CubeSat. In Proceedings of the 64th International Astronautical Congress, Beijing, China, 23–27 September 2013.
41. Klesh, A.T.; Baker, J.; Krajewski, J. MarCO: Flight review and lessons learned. In Proceedings of the Small Satellite Conference, Logan, UT, USA, 9 August 2019.
42. JPL MarCO Micro CubeSat Propulsion System. VACCO Industries. Available online: https://cubesat-propulsion.com/jpl-marco-micro-propulsion-system/ (accessed on 25 September 2023).
43. Martínez, J.M.; Rafalskyi, D.; Rossi, E.Z.; Aanesland, A. *Development, Qualification and First Flight Data of the Iodine Based Cold Gas Thruster for Cubesats*; IAA: Rome, Italy, 2019.
44. Martínez, J.M.; Rafalskyi, D.; Aanesland, A.; Laurand, X.; Martinez, S.V.; Quinsac, G. An off-axis iodine propulsion system for the robusta-3A mission. In Proceedings of the Small Satellite Conference, Logan, UT, USA, 10 March 2020.
45. Aslan, S.; Fares, J.; DiStefano, M.; Peck, M.A. An adaptable, modular cold-gas propulsion system for small satellite applications. In Proceedings of the AIAA Scitech 2020 Forum, Orlando, FL, USA, 6–10 January 2020; p. 1666. [CrossRef]
46. Clark, S. Virgin Orbit Celebrates Third Successful Launch in a Row. Spaceflight Now. 13 January 2022. Available online: https://spaceflightnow.com/2022/01/13/virgin-orbit-celebrates-third-successful-launch-in-a-row/ (accessed on 25 September 2023).
47. Adelis-SAMSON. Asher Space Research Institute. Available online: https://asri.institute/space-missions/adelis-samson/ (accessed on 25 September 2023).

48. Zaberchik, M.; Lev, D.R.; Edlerman, E.; Kaidar, A. Fabrication and testing of the cold gas propulsion system flight unit for the adelis-SAMSON nano-satellites. *Aerospace* **2019**, *6*, 91. [CrossRef]
49. Simonetti, S.; Di Tana, V.; Miglioretti, F.; Cotugno, B.; Pirrotta, S.; Amoroso, M.; Pizzurro, S.; Impresario, G. LICIACube on DART mission: An asteroid impact captured by Italian small satellite technology. In Proceedings of the Small Satellite Conference, Logan, UT, USA, 10 March 2020.
50. Williams, D.R. LICIACube. NASA. Available online: https://nssdc.gsfc.nasa.gov/nmc/spacecraft/display.action?id=2021-110C (accessed on 25 September 2023).
51. IANUS & PERSEUS Cold Gas. T4i. Available online: https://www.t4innovation.com/ianus-perseus-cold-gas/ (accessed on 25 September 2023).
52. Skidmore, L.; Lightsey, E.G. Design of a Cold Gas Propulsion System for the SunRISE Mission. Master's Thesis, Georgia Institute of Technology, Atlanta, GA, USA, 2021.
53. Dailey, J. AFRL Celebrates Launch of Small-Sat Ascent to GEO Space. The Air Force Research Laboratory. 2021. Available online: https://www.afrl.af.mil/News/Article/2859902/afrl-celebrates-launch-of-small-sat-ascent-to-geo-space/ (accessed on 26 September 2023).
54. Lightsey, E.G.; Stevenson, T.; Sorgenfrei, M. Development and testing of a 3-d-printed cold gas thruster for an interplanetary cubesat. *Proc. IEEE* **2018**, *106*, 379–390. [CrossRef]
55. Hart, S.T.; Lightsey, E.G. Design of the VISORS and SWARM-EX Propulsion Systems. Master's Thesis, Georgia Tech, Atlanta, GA, USA, 2010.
56. NEA Scout Propulsion System. VACCO Industries. Available online: https://cubesat-propulsion.com/nea-scout-propulsion-system/ (accessed on 26 September 2023).
57. CuSP Propulsion System. VACCO Industries. Available online: https://cubesat-propulsion.com/cusp-propulsion-system/ (accessed on 26 September 2023).
58. Sweeting, M.N.; Lawrence, T.; Sellers, J.; Leduc, J. Low-cost orbit manoeuvres for minisatellites using novel water resisto-jet thrusters. In Proceedings of the IAF, International Astronautical Congress, 49th, Melbourne, Australia, 28 September–2 October 1998.
59. Darfilal; Gibbon, D. Ground and flight tests of AlSat-1B butane propulsion system. *Propuls. Power Res.* **2022**, *11*, 74–84. [CrossRef]
60. Amri, R.; Gibbon, D. In orbit performance of butane propulsion system. *Adv. Sp. Res.* **2012**, *49*, 648–654. [CrossRef]
61. Gibbon, D.; Coxhill, I.; Nicolini, D.; Correia, R.; Page, J. The design, development and in-flight operation of a water resistojet micropropulsion system. In Proceedings of the 40th AIAA/ASME/SAE/ASEE Joint Propulsion Conference and Exhibit, Fort Lauderdale, FL, USA, 12 July 2004; p. 3798.
62. Romei, F.; Grubisic, A.; Gibbon, D.; Lane, O.; Hertford, R.A.; Roberts, G.T. A thermo-fluidic model for a low power xenon resistojet. In Proceedings of the Joint Conference of 30th ISTS, 34th IEPC and 6th NSAT, Hyogo-Kobe, Japan, 4–10 July 2015; 15p.
63. Ketsdever, A.D.; Wadsworth, D.C.; Vargo, S.E.; Muntz, E.P.; Air Force Research Lab Edwards Afb Ca Propulsion Directorate West. Design, optimization and fabrication of a free molecule micro-resistojet for microspacecraft thrust generation. In Proceedings of the Small Satellite Conference, Logan, UT, USA, 20 November 1998.
64. Ketsdever, A.D.; Lee, R.H.; Lilly, T.C. Performance testing of a microfabricated propulsion system for nanosatellite applications. *J. Micromech. Microeng.* **2005**, *15*, 2254. [CrossRef]
65. Lee, R.; Bauer, A.; Killingsworth, M.; Lilly, T.; Duncan, J.; Ketsdever, A. Performance characterization of the free molecule micro-resistojet utilizing water propellant. In Proceedings of the 43rd AIAA/ASME/SAE/ASEE Joint Propulsion Conference & Exhibit, Cincinnati, OH, USA, 8–11 July 2007; p. 5185.
66. Pallichadath, V.; Turmaine, L.; Melaika, A.; Gelmi, S.; Ramisa, M.V.; Rijlaarsdam, D.; Silva, M.A.C.; Guerrieri, D.C.; Uludag, M.S.; Zandbergen, B. In-orbit micro-propulsion demonstrator for PICO-satellite applications. *Acta Astronaut.* **2019**, *165*, 414–423. [CrossRef]
67. Cervone, A.; Zandbergen, B.; Guerrieri, D.C.; De Athayde Costa e Silva, M.; Krusharev, I.; Van Zeijl, H. Green micro-resistojet research at Delft University of Technology: New options for Cubesat propulsion. *CEAS Sp. J.* **2017**, *9*, 111–125. [CrossRef]
68. Moore, G.; Holemans, W.; Huang, A.; Lee, J.; McMullen, M.; White, J.; Twiggs, R.; Malphrus, B.; Fite, N.; Klumpar, D. 3D Printing and MEMS Propulsion for the RAMPART 2U CUBESAT. In Proceedings of the Small Satellite Conference, Logan, UT, USA, 19 May 2010.
69. Underwood, C.; Pellegrino, S.; Lappas, V.J.; Bridges, C.P.; Baker, J. Using CubeSat/micro-satellite technology to demonstrate the Autonomous Assembly of a Reconfigurable Space Telescope (AAReST). *Acta Astronaut.* **2015**, *114*, 112–122. [CrossRef]
70. Passaro, A.; Bulit, A. Development and Test of XR-150, a New High-Thrust 100 W Resistojet. In Proceedings of the 33rd International Electric Propulsion Conference, Washington, DC, USA, 6–10 October 2013; pp. 2013–2219.
71. Cifali, G.; Gregucci, S.; Andreussi, T.; Andrenucci, M. Resistojet thrusters for auxiliary propulsion of full electric platforms. In Proceedings of the 35th International Electric Propulsion Conference, Atlanta, GA, USA, 8–12 October 2017.
72. XR Resistojet Product Family. SITAEL S.P.A. 2015. Available online: https://www.sitael.com/space/advanced-propulsion/electric-propulsion/ (accessed on 26 September 2023).
73. Hejmanowski, N.J.; Woodruff, C.A.; Burton, R.L.; Carroll, D.L.; Palla, A.D.; Cardin, J.M. CubeSat high impulse propulsion system (CHIPS) design and performance. In Proceedings of the 63rd JANNAF Propulsion Meeting (8th Spacecraft Propulsion), Phoenix, AZ, USA, 5–8 December 2016.

74. Performance Matrices for Cua Propulsion Systems. CU Aerospace. 2021. Available online: https://cuaerospace.com/Portals/0/SiteContent/assets/PDF/CUA%20Hardware%20Compiled%20210624.pdf?ver=OSNk_O8jswxha_HxRfRvcA== (accessed on 26 September 2023).
75. Comet Water-Based Propulsion for Small Satellites. Bradford Space. 2019. Available online: https://static1.squarespace.com/static/603ed12be884730013401d7a/t/6054f3b8d71b8a772c358b92/1616180155614/be_datasheet_comet_2019oct.pdf (accessed on 26 September 2023).
76. Sarda, K.; CaJacob, D.; Orr, N.; Zee, R. Making the invisible visible: Precision RF-emitter geolocation from space by the hawkeye 360 pathfinder mission. In Proceedings of the Small Satellite Conference, Logan, UT, USA, 4 August 2018.
77. Woodruff, C.; Carroll, D.; King, D.; Burton, R.; Hejmanowski, N. Monofilament Vaporization Propulsion (MVP)-CubeSat Propulsion System with Inert Polymer Propellant. In Proceedings of the Small Satellite Conference, Logan, UT, USA, 4 August 2018.
78. Woodruff, C.A.; Parta, M.; King, D.M.; Woodruff, A.L.; Burton, R.L.; Carroll, D.L. Monofilament Vaporization Propulsion (MVP) Flight-like System Performance. In Proceedings of the Small Satellite Conference, Logan, UT, USA, 6–11 August 2022.
79. Djamal, D.; Mohamed, K.; Aslan, A.R. RESISTOJET propulsion system for small satellite. In Proceedings of the 2019 9th International Conference on Recent Advances in Space Technologies (RAST), Istanbul, Turkey, 11–14 June 2019; pp. 159–166.
80. Romei, F.; Grubišić, A.N. Validation of an additively manufactured resistojet through experimental and computational analysis. *Acta Astronaut.* **2020**, *167*, 14–22. [CrossRef]
81. Asakawa, J.; Koizumi, H.; Nishii, K.; Takeda, N.; Murohara, M.; Funase, R.; Komurasaki, K. Fundamental ground experiment of a water resistojet propulsion system: AQUARIUS installed on a 6U CubeSat: EQUULEUS. *Trans. Jpn. Soc. Aeronaut. Sp. Sci. Aerosp. Technol.* **2018**, *16*, 427–431. [CrossRef]
82. Yaginuma, K.; Asakawa, J.; Nakagawa, Y.; Tsuruda, Y.; Koizumi, H.; Kakihara, K.; Yanagida, K.; Murata, Y.; Ikura, M.; Matsushita, S. AQT-D: CubeSat Demonstration of a Water Propulsion System Deployed from ISS. *Trans. Jpn. Soc. Aeronaut. Sp. Sci. Aerosp. Technol.* **2020**, *18*, 141–148. [CrossRef]
83. DATASHEET | ARM-A. Aurora Propulsion Technologies. Available online: https://aurorapt.fi/downloads/ARM-A.pdf (accessed on 26 September 2023).
84. AURORASAT-1. Aurora Propulsion Technologies. Available online: https://aurorapt.fi/aurorasat-1/ (accessed on 26 September 2023).
85. The Steam Thruster. Steamjet Space Systems. Available online: https://steamjet.space/#products (accessed on 26 September 2023).
86. Nosseir, A.E.S.; Pasini, A.; Cervone, A. Modular impulsive green-monopropellant propulsion system for micro/nano satellites high-thrust orbital maneuvers (MIMPS-G). In Proceedings of the International Astronautical Congress, CyberSpace Edition, Online, 12–14 October 2020; pp. 12–14.
87. Masse, R.; Overly, J.; Allen, M.; Spores, R. A new state-of-the-art in AF-M315E thruster technologies. In Proceedings of the 48th AIAA/ASME/SAE/ASEE Joint Propulsion Conference & Exhibit, Atlanta, GA, USA, 30 July–1 August 2012; p. 4335.
88. Tsay, M.; Lafko, D.; Zwahlen, J.; Costa, W. Development of Busek 0.5 N green monopropellant thruster. In Proceedings of the Small Satellite Conference, Logan, UT, USA, 13 November 2013.
89. Anflo, K.; Crowe, B. In-space demonstration of an ADN-based propulsion system. In Proceedings of the 47th AIAA/ASME/SAE/ASEE Joint Propulsion Conference & Exhibit, San Diego, CA, USA, 31 July–3 August 2011; p. 5832.
90. Anflo, K.; Moore, S. Expanding the ADN-based monopropellant thruster family. In Proceedings of the Small Satellite Conference, Logan, UT, USA, 10–13 August 2009.
91. King, D.; Woodruff, C.; Camp, J.; Carroll, D. Development and Testing of a Low Flame Temperature, Peroxide-Alcohol-Based Monopropellant Thruster. In Proceedings of the 35th Annual Small Satellite Conference, Virtual, 7–12 August 2021.
92. Overton, S.; Allen, M.; Masse, B.; Sparse, R.; Driscoll, L. *CubeSat Mission Benefits and Integration of High Thrust*; High ΔV Green Propulsion: Redmon, WA, USA, 2015.
93. 1N, 20N, 400N and Heritage Thruster | Cheimical Monopropellant Thruster Family. ArianeGroup. Available online: https://www.space-propulsion.com/brochures/hydrazine-thrusters/hydrazine-thrusters.pdf (accessed on 27 September 2023).
94. Monopropellant Thrusters. Moog, Inc. Available online: https://www.moog.com/content/dam/moog/literature/sdg/space/propulsion/moog-MonopropellantThrusters-Datasheet.pdf (accessed on 27 September 2023).
95. Propulsion Products and Services. Northrop Grumman. Available online: https://www.northropgrumman.com/space/propulsion-products-and-services (accessed on 27 September 2023).
96. Modular Propulsion Systems Innovative Propulsion Solutions for CubeSats and SmallSats. Aerojet Rocketdyne. 2018. Available online: https://www.rocket.com/sites/default/files/documents/CubeSat%20Mod%20Prop-2sided.pdf (accessed on 27 September 2023).
97. Masse, R.K.; Spores, R.; Allen, M. AF-M315E advanced green propulsion–GPIM and beyond. In Proceedings of the AIAA Propulsion and Energy 2020 Forum, Virtual, 24–28 August 2020; p. 3517. [CrossRef]
98. Tsay, M.; Feng, C.; Paritsky, L.; Zwahlen, J.; Lafko, D.; Robin, M. Complete EM system development for Busek's 1U CubeSat green propulsion module. In Proceedings of the 52nd AIAA/SAE/ASEE Joint Propulsion Conference, Salt Lake City, UT, USA, 25–27 July 2016; p. 4905.
99. Dinardi, A.; Persson, M. High performance green propulsion (HPGP): A flight-proven capability and cost game-changer for small and secondary satellites. In Proceedings of the Small Satellite Conference, Logan, UT, USA, 15 October 2012.

100. Dinardj, A.; Anflo, K.; Friedhoff, P. On-orbit commissioning of high performance green propulsion (HPGP) in the SkySat constellation. In Proceedings of the Small Satellite Conference, Logan, UT, USA, 5 August 2017.
101. Talaksi, A.; Lightsey, E.G. Manufacturing, Integration, and Testing of the Green Monopropellant Propulsion System for NASA's Lunar Flashlight Mission. *Masters Rep. Georg. Inst. Technol.* **2020**. Available online: https://www.ssdl.gatech.edu/sites/default/files/ssdl-files/papers/mastersProjects/AE%208900%20Paper_Talaksi.pdf (accessed on 26 March 2024).
102. Zaluki, M.; Hasanof, T.; Schetkovskiy, A.; McKechnie, T.; Cavender, D.; Burnside, C.; Dankanich, J. Green monopropellant 100 mn thruster. In Proceedings of the AIAA Propulsion and Energy 2021 Forum, Virtual, 9–11 August 2021. [CrossRef]
103. Andrews, D.; Lightsey, E.G. Design of a Green Monopropellant Propulsion System for the Lunar Flashlight Mission. *Am. Inst. Aeronaut. Astronaut. J.* **2019**. Available online: https://ssdl.gatech.edu/sites/default/files/ssdl-files/papers/conferencePapers/Design%20of%20a%20Green%20Monopropellant%20Propulsion%20System%20for%20the%20Lunar.pdf (accessed on 26 March 2024).
104. Cavender, D. Emerging Low Toxicity 'Green' Chemical Propulsion Technologies for Smallsats. NASA. Available online: https://plasmapros.com/wp-content/uploads/S3VI-Webinar-Presentation-Emerging-Green-Prop-Technology_UPDATED_02.10.21-1-1.pdf (accessed on 27 September 2023).
105. NASA Calls End to Lunar Flashlight After Some Tech Successes. Jet Propulsion Laboratory. 2023. Available online: https://www.jpl.nasa.gov/news/nasa-calls-end-to-lunar-flashlight-after-some-tech-successes (accessed on 27 September 2023).
106. Lunar Flashlight Propulsion System X16029000-01. VACCO Industries. Available online: https://www.cubesat-propulsion.com/wp-content/uploads/2017/08/X16029000-01-data-sheet-080217.pdf (accessed on 27 September 2023).
107. Cardin, J.; Hsu, J.; Sorathia, J. Proto-Flight Testing of a Green Monopropellant Integrated Propulsion System. In Proceedings of the 35th Annual Small Satellite Conference, Virtual, 7–12 August 2021.
108. Monopropellant Propulsion Unit for Cubesats (Mpuc) System. CU Aerospace. 2020. Available online: https://satcatalog.s3.amazonaws.com/components/911/SatCatalog_-_Champaign-Urbana_Aerospace_-_MPUC_2U_-_Datasheet.pdf (accessed on 27 September 2023).
109. Propulsion System EPSS C2. NanoAvionics. 2020. Available online: https://satcatalog.s3.amazonaws.com/components/901/SatCatalog_-_NanoAvionics_-_EPSS_C2_-_Datasheet.pdf?lastmod=20210723064738 (accessed on 27 September 2023).
110. Nosseir, A.E.S.; Cervone, A.; Pasini, A. Modular impulsive green monopropellant propulsion system (mimps-g): For cubesats in leo and to the moon. *Aerospace* **2021**, *8*, 169. [CrossRef]
111. Porter, A.; Freedman, M.; Grist, R.; Wesson, C.; Hanson, M. Flight qualification of a water electrolysis propulsion system. In Proceedings of the Small Satellite Conference, Virtual, 7–12 August 2021.
112. James, K.; Moser, T.; Conley, A.; Slostad, J.; Hoyt, R. Performance characterization of the HYDROS^{TM} water electrolysis thruster. In Proceedings of the Small Satellite Conference, Logan, UT, USA, 10 August 2015.
113. PM200. AAC Clyde Space. Available online: https://www.aac-clyde.space/what-we-do/space-products-components/pm200 (accessed on 3 October 2023).
114. D-Orbit's First ION Satellite Carrier Mission Has Launched on VV16! Dawn Aerospace. Available online: https://www.dawnaerospace.com/latest-news/ionscvlucas (accessed on 3 October 2023).
115. Kakami, A.; Kuranaga, A.; Yano, Y. Premixing-type liquefied gas bipropellant thruster using nitrous oxide/dimethyl ether. *Aerosp. Sci. Technol.* **2019**, *94*, 105351. [CrossRef]
116. Tummala, A.R.; Dutta, A. An overview of cube-satellite propulsion technologies and trends. *Aerospace* **2017**, *4*, 58. [CrossRef]
117. Nicholas, A.; Finne, T.; Galysh, I.; Mai, A.; Yen, J.; Sawka, W.; Ransdell, J.; Williams, S. SpinSat mission overview. In Proceedings of the Small Satellite Conference, Logan, UT, USA, 19 November 2013.
118. Sawka, W.N.; McPherson, M. Electrical solid propellants: A safe, micro to macro propulsion technology. In Proceedings of the 49th AIAA/ASME/SAE/ASEE Joint Propulsion Conference, San Jose, CA, USA, 14–17 July 2013; p. 4168.
119. Siegried, J. Attitude Control on the Pico Satellite Solar Cell Testbed-2. In Proceedings of the 26th Annual AIAA/USU Conference on Small Satellites, Logan, UT, USA, 13–16 August 2012.
120. Nakano, M.; Koizumi, H.; Watanabe, M.; Arakawa, Y. Laser ignition microthruster experiments on KKS-1. *Trans. Jpn. Soc. Aeronaut. Sp. Sci. Aerosp. Technol.* **2010**, *8*, Pb_7–Pb_11. [CrossRef] [PubMed]
121. Koizumi, H.; Asakawa, J.; Nakagawa, Y.; Kojima, S.; Kawahara, H.; Komurasaki, K.; Nakano, M.; Sahara, H.; Banno, M.; Matsushima, J. Micropropulsion Systems Enabling Full Active Debris Removal by a small satellite ADRAS-1. In Proceedings of the Small Satellite Conference 2016, Logan, UT, USA, 11 October 2016.
122. Nelson, S.D.; Current, P. Modular Architecture Propulsion System (MAPS^{TM}). In Proceedings of the 2018 Joint Propulsion Conference, Cincinnati, OH, USA, 9–11 July 2018; p. 4704.
123. Oh, H.-U.; Kim, T.-G.; Han, S.-H.; Lee, J. Verification of MEMS fabrication process for the application of MEMS solid propellant thruster arrays in space through launch and on-orbit environment tests. *Acta Astronaut.* **2017**, *131*, 28–35. [CrossRef]
124. Isakari, S.; Asakura, T.; Haraguchi, D.; Yano, Y.; Kakami, A. Performance evaluation and thermography of solid-propellant microthrusters with laser-based throttling. *Aerosp. Sci. Technol.* **2017**, *71*, 99–108. [CrossRef]
125. Lemmer, K. Propulsion for cubesats. *Acta Astronaut.* **2017**, *134*, 231–243. [CrossRef]
126. Jens, E.T.; Karp, A.C.; Nakazono, B.; Williams, K.T.; Rabinovitch, J.; Dyrda, D.; Mechentel, F.S. Low pressure ignition testing of a hybrid smallsat motor. In Proceedings of the AIAA Propulsion and Energy 2019 Forum, Indianapolis, IN, USA, 19–22 August 2019; p. 4009. [CrossRef]

127. Smith, T.K.; Lewis, Z.; Olsen, K.; Bulcher, A.M.; Whitmore, S.A. A Miniaturized Green End-Burning Hybrid Propulsion System for CubeSats. In Proceedings of the Small Satellite Conference, Logan, UT, USA, 10 March 2020.
128. O'Reilly, D.; Herdrich, G.; Kavanagh, D.F. Electric propulsion methods for small satellites: A review. *Aerospace* **2021**, *8*, 22. [CrossRef]
129. Wollenhaupt, B.; Hammer, A.; Herdrich, G.; Fasoulas, S.; Roser, H. A very low power arcjet (VELARC) for small satellite missions. In Proceedings of the 32nd International Electric Propulsion Conference, Wiesbaden, Germany, 11–15 September 2011; pp. 1988–2007.
130. Sankovic, J.; Jacobson, D. Performance of a miniaturized arcjet. In Proceedings of the 31st Joint Propulsion Conference and Exhibit, San Diego, CA, USA, 10–12 July 1995; p. 2822.
131. Burton, R.L.; Eden, J.G.; Park, S.J.; de Chadenedes, M.; Garrett, S.; Raja, L.L.; Sitaraman, H.; Laystrom-Woodard, J.; Benavides, G.; Carroll, D. Development of the MCD thruster for nanosat propulsion. In Proceedings of the JANNAF Propulsion Meeting, Colorado Springs, CO, USA, 3–7 May 2010; Volume 1387.
132. De Chadenedes, M.L. *Propulsion Performance of a Microcavity Discharge Device*; University of Illinois: Champaign, IL, USA, 2011.
133. Carroll, D.L.; Cardin, J.M.; Burton, R.L.; Benavides, G.F.; Hejmanowski, N.; Woodruff, C.; Bassett, K.; King, D.; Laystrom-Woodard, J.; Richardson, L. Propulsion unit for CUBESATS (PUC). In Proceedings of the 62nd JANNAF Propulsion Meeting (7th Spacecraft Propulsion), Nashville, TN, USA, 1–4 June 2015; pp. 1–5.
134. Burton, R.L.; Eden, J.G.; Park, S.-J.; Yoon, J.K.; De Chadenedes, M.; Garrett, S.; Raja, L.L.; Sitaraman, H.; Laystrom-Woodard, J.; Benavides, G. Initial development of the microcavity discharge thruster. In Proceedings of the 31st International Electric Propulsion Conference, Ann Arbor, MI, USA, 20–24 September 2009.
135. Abaimov, M.D.; Sinha, S.; Bilén, S.G.; Micci, M.M. CubeSat Microwave Electrothermal Thruster (CμMET). In Proceedings of the 33rd International Electric Propulsion Conference The George Washington University, Washington, DC, USA, 6 October 2013; pp. 6–10.
136. Gallucci, S.E.; Micci, M.M.; Bilén, S.G. Design of a Water-Propellant 17.8-GHz Microwave Electrothermal Thruster. In Proceedings of the 35th International Electric Propulsion Conference, Atlanta, GA, USA, 8–12 October 2017.
137. Abaimov, M.D.; Micci, M.M.; Bilén, S.G. A 17.8-GHz Microwave Electrothermal Thruster for CubeSats and Small Satellites. In Proceedings of the IEPC 2016, Cambridge, MA, USA, 17 August 2016.
138. Micci, M.M.; Bilén, S.G.; Clemens, D.E. History and current status of the microwave electrothermal thruster. *Prog. Propuls. Phys.* **2009**, *1*, 425–438.
139. Harper, J. *Pocket Rocket: A 1U+ Propulsion System Design to Enhance Cubesat Capabilities*; California Polytechnic State University: San Luis Obispo, CA, USA, 2020.
140. Van Ness, P.; Jr, G.R.; Gnagy, S.; Diamantopoulous, S.; Greig, A. Pressurized 1U CubeSat Propulsion System. In Proceedings of the Small Satellite Conference, Logan, UT, USA, 9 August 2019.
141. Greig, A.; Charles, C.; Boswell, R.W. Spatiotemporal study of gas heating mechanisms in a radio-frequency electrothermal plasma micro-thruster. *Front. Phys.* **2015**, *3*, 84. [CrossRef]
142. Rostello, M. Preliminar sizing of an electrospray thruster. In Proceedings of the Small Satellite Conference, Logan, UT, USA, 5 August 2017.
143. Goebel, D.M.; Katz, I. *Fundamentals of Electric Propulsion: Ion and Hall Thrusters*; John Wiley & Sons: Hoboken, NJ, USA, 2008.
144. Ziemer, J.; Marrese-Reading, C.M.; Arestie, S.M.; Conroy, D.G.; Leifer, S.D.; Demmons, N.R.; Gamero-Castaño, M.; Wirz, R.E. LISA colloid microthruster technology development plan and progress. In Proceedings of the 36th International Electric Propulsion Conference, Vienna, Austria, 15–20 September 2019.
145. Demmons, N.R.; Courtney, D.; Alvarez, N.; Wood, Z. Component-level development and testing of a colloid micro-thruster (CMT) system for the LISA mission. *AIAA Propuls. Energy 2019 Forum* **2019**, 3815. [CrossRef]
146. Magnusson, J.; Collins, A.L.; Wirz, R.E. Lifetime considerations for electrospray thrusters. *Aerospace* **2020**, *7*, 153. [CrossRef]
147. Fedkiw, T.; Wood, Z.D.; Demmons, N.R. Environmental and lifetime testing of the bet-300-p electrospray thruster. In Proceedings of the AIAA Propulsion and Energy 2020 Forum, Virtual, 24–28 August 2020; p. 3614. [CrossRef]
148. Electrospray Thrusters. Busek Co. Inc. Available online: https://www.busek.com/electrospray-thrusters (accessed on 4 October 2023).
149. Krejci, D.; Mier-Hicks, F.; Fucetola, C.; Lozano, P.; Schouten, A.H.; Martel, F. Design and Characterization of a Scalable ion Electrospray Propulsion System. In Proceedings of the Small Satellite Conference, Logan, UT, USA, 10 August 2015.
150. Krejci, D.; Mier-Hicks, F.; Thomas, R.; Haag, T.; Lozano, P. Emission characteristics of passively fed electrospray microthrusters with propellant reservoirs. *J. Spacecr. Rockets* **2017**, *54*, 447–458. [CrossRef]
151. Gates, D.H.K. *AeroCube-8—Orbital Debris Assessment Report (ODAR)*; Tech Report; RPRT: Buffalo, NY, USA, 2014.
152. Petro, E.; Bruno, A.; Lozano, P.; Perna, L.E.; Freeman, D. Characterization of the TILE electrospray emitters. In Proceedings of the AIAA Propulsion and Energy 2020 Forum, Virtual, 24–28 August 2020; p. 3612.
153. Schroeder, M.; Womack, C.; Gagnon, A. Maneuver Planning for Demonstration of a Low-Thrust Electric Propulsion System. In Proceedings of the Small Satellite Conference, Logan, UT, USA, 10 March 2020.
154. Hunter, R.C.; Agasid, E.F.; Baker, C.E.; Treptow, J.V.; Frost, C.R.; Mayer, D.J.; Luna, A.G.; De Rosee, R.; Nguyen, A.N.; Fishman, J.L. Nasa Small Spacecraft Technology (Sst) Program and Recent Technology Demonstrations. In Proceedings of the 4s Symposium, Vilamoura, Portugal, 16–20 May 2022.

155. Huang, C.; Jianling, L.I.; Mu, L.I. Performance measurement and evaluation of an ionic liquid electrospray thruster. *Chinese J. Aeronaut.* **2021**, *336*, 126822. [CrossRef]
156. Jia-Richards, O. *Design and Analysis of a Stage-Based Electrospray Propulsion System for CubeSats*; Massachusetts Institute of Technology: Cambridge, MA, USA, 2019.
157. Yost, B.; Weston, S.; Benavides, G.; Krage, F.; Hines, J.; Mauro, S.; Etchey, S.; O'Neill, K.; Braun, B. State-of-the-art small spacecraft technology. In Proceedings of the 35th Annual Small Satellite Conference, Virtual, 7–12 August 2021.
158. Krejci, D.; Lozano, P. Space propulsion technology for small spacecraft. *Proc. IEEE* **2018**, *106*, 362–378. [CrossRef]
159. Mühlich, N.S.; Gerger, J.; Seifert, B.; Aumayr, F. Performance improvements of IFM Nano Thruster with highly focused ion beam generated with a compact electrostatic lens module. *Acta Astronaut.* **2022**, *201*, 464–471. [CrossRef]
160. Marcuccio, S.; Genovese, A.; Andrenucci, M. Experimental performance of field emission microthrusters. *J. Propuls. Power* **1998**, *14*, 774–781. [CrossRef]
161. Mueller, J.; Hofer, R.; Ziemer, J. Survey of propulsion technologies applicable to cubesats. In Proceedings of the Joint Army-Navy-NASA-Air Force (JANNAF), Colorado Springs, CO, USA, 3 May 2010.
162. Paita, L.; Ceccanti, F.; Spurio, M.; Cesari, U.; Priami, L.; Nania, F.; Rossodivita, A.; Andrenucci, M. Alta's FT-150 FEEP microthruster: Development and qualification status. In Proceedings of the 31st International Electric Propulsion Conference, IEPC-09-186, Ann Arbor, MI, USA, 20–24 September 2009.
163. Mueller, J. Thruster options for microspacecraft: A review and evaluation of state-of-the-art and emerging technologies. *Micropropuls. Small Spacecr.* **2000**, *147*, 45.
164. Marcuccio, S.; Giusti, N.; Pergola, P. Slit FEEP thruster performance with ionic liquid propellant. In Proceedings of the 49th AIAA/ASME/SAE/ASEE Joint Propulsion Conference, San Jose, CA, USA, 15–17 July 2013; p. 4034.
165. Misuri, T. SITAEL Low Power Electric Propulsion Systems for Small Satellites. In Proceedings of the 34th International Electric Propulsion Conference, Kobe-Hyogo, Japan, 4–10 July 2015.
166. Scharlemann, C.; Tajmar, M. Development of propulsion means for microsatellites. In Proceedings of the 43rd AIAA/ASME/SAE/ASEE Joint Propulsion Conference & Exhibit, Cincinnati, OH, USA, 8–11 July 2007; p. 5184.
167. Scharlemann, C.; Tajmar, M.; Genovese, A.; Buldrini, N.; Schnitzer, R. In-FEEP qualification test program for LISA pathfinder. In Proceedings of the 44th AIAA/ASME/SAE/ASEE Joint Propulsion Conference & Exhibit, Hartford, CT, USA, 21–23 July 2008; p. 4825.
168. Mühlich, N.S.; Seifert, B.; Aumayr, F. IFM Nano Thruster performance studied by experiments and numerical simulations. *J. Phys. D Appl. Phys.* **2020**, *54*, 95203. [CrossRef]
169. Krejci, D.; Reissner, A. 138 Propulsion Units Launched in 4 Years: A Review and Lessons Learned. In Proceedings of the Small Satellite Conference, Logan, UT, USA, 6–11 August 2022.
170. Vasiljevich, I.; Tajmar, M.; Grienauer, W.; Plesescu, F.; Buldrini, N.; del Amo, J.G.; Domunguez, B.C.; Betto, M. Development of an indium mN-FEEP thruster. In Proceedings of the 44th AIAA/ASME/SAE/ASEE Joint Propulsion Conference & Exhibit, Hartford, CT, USA, 21–23 July 2008; p. 4534.
171. Krejci, D.; Reissner, A.; Schönherr, T.; Seifert, B.; Saleem, Z.; Alejos, R. Recent flight data from IFM nano thrusters in a low earth orbit. In Proceedings of the 36th International Electric Propulsion Conference, Vienna, Austria, 15–20 September 2019; pp. 15–20.
172. Krejci, D.; Reissner, A.; Seifert, B.; Jelem, D.; Hörbe, T.; Plesescu, F.; Friedhoff, P.; Lai, S. Demonstration of the ifm nano feep thruster in low earth orbit. In Proceedings of the 4s Symposium, Sorrento, Italy, 28 May–1 June 2018.
173. Kramer, A.; Bangert, P.; Schilling, K. UWE-4: First Electric Propulsion on a 1U CubeSat—In-Orbit Experiments and Characterization. *Aerospace* **2020**, *7*, 98. [CrossRef]
174. Bock, D.; Tajmar, M. Highly miniaturized FEEP propulsion system (NanoFEEP) for attitude and orbit control of CubeSats. *Acta Astronaut.* **2018**, *144*, 422–428. [CrossRef]
175. Tsay, M.; Model, J.; Barcroft, C.; Frongillo, J.; Zwahlen, J.; Feng, C. Integrated testing of iodine bit-3 rf ion propulsion system for 6u cubesat applications. In Proceedings of the 35th International Electric Propulsion Conference Georgia Institute of Technology, Atlanta, GA, USA, 8–12 October 2017; pp. 8–12.
176. Tsay, M.; Frongillo, J.; Hohman, K.; Malphrus, B.K. LunarCube: A deep space 6U CubeSat with mission enabling ion propulsion technology. In Proceedings of the Small Satellite Conference, Logan, UT, USA, 10 August 2015.
177. Sohl, G.; Fosnight, V.V.; Goldner, S.J.; Speiser, R.C. Cesium electron-bombardment ion microthrusters. *J. Spacecr. Rocket.* **1967**, *4*, 1180–1183. [CrossRef]
178. Wirz, R.; Polk, J.; Marrese, C.; Mueller, J.; Escobedo, J.; Sheehan, P. Development and testing of a 3cm electron bombardment micro-ion thruster. In Proceedings of the International Electric Propulsion Conference, Pasadena, CA, USA, 15–19 October 2001.
179. Wirz, R.E. Miniature ion thrusters: A review of modern technologies and mission capabilities. In Proceedings of the 34th International Electric Propulsion Conference, Pasadena, CA, USA, 15–19 October 2015.
180. Wirz, R.; Polk, J.; Marrese, C.; Mueller, J. Experimental and computational investigation of the performance of a micro-ion thruster. In Proceedings of the 38th AIAA/ASME/SAE/ASEE Joint Propulsion Conference & Exhibit, Indianapolis, IN, USA, 7–10 July 2002; p. 3835.
181. Koizumi, H.; Kuninaka, H. Performance evaluation of a miniature ion thruster μ1 with a unipolar and bipolar operation. In Proceedings of the 32nd Int. Elect. Propuls. Conf, Wiesbaden, Germany, 11 September 2011; pp. 1–10.

182. Koizumi, H.; Komurasaki, K.; Aoyama, J.; Yamaguchi, K. Engineering model of the miniature ion propulsion system for the nano-satellite: HODOYOSHI-4. *Trans. Jpn. Soc. Aeronaut. Sp. Sci. Aerosp. Technol.* **2014**, *12*, Tb_19–Tb_24. [CrossRef] [PubMed]
183. Koizumi, H.; Satogata, R. Miniature Ion Thruster Propulsion System, In-Flight Operation First Operation of an Ion Thruster on a Small Satellite (Less than 100 kg). University of Tokyo. 2014. Available online: https://www.t.u-tokyo.ac.jp/en/press/foee/press/setnws_e8c60028f0bb_141212-01_eng.html (accessed on 5 October 2023).
184. Ataka, Y.; Nakagawa, Y.; Koizumi, H.; Komurasaki, K. Improving the performance of a water ion thruster using biased electrodes. *Acta Astronaut.* **2021**, *187*, 133–140. [CrossRef]
185. Propulsion System Options. Pale Blue. Available online: https://pale-blue.co.jp/product/ (accessed on 5 October 2023).
186. Asakawa, J.; Koizumi, H.; Yaginuma, K.; Nakagawa, Y. Pre-Flight Testing Results of Multiple Water Propulsion Systems-Resistojet and Ion Thruster for SmallSats. In Proceedings of the Small Satellite Conference, Logan, UT, USA, 6–11 August 2022.
187. Komatsu, Y.; Tsutsui, Y.; Katsumata, H.; Wada, A.; Kakehashi, Y.; Fujimoto, K.; Nakamura, K.; Kaneko, Y.; Iwata, T. RAISE-3 for Agile On-Orbit Demonstration of Innovative Satellite Technologies: Mission Definition and Conceptual Design. In Proceedings of the 35th Annual Small Satellite Conference, Virtual, 7–12 August 2021.
188. Navin, J. JAXA Epsilon Fails on Sixth Flight Carrying RAISE-3 and Others. NASA Spaceflight. 2022. Available online: https://www.nasaspaceflight.com/2022/10/epsilon-raise-3/ (accessed on 5 October 2023).
189. Tomaswick, A. Pale Blue Successfully Operates Its Water-Based Propulsion System in Orbit. Universe Today. 2023. Available online: https://pale-blue.co.jp/news/314/ (accessed on 26 March 2024).
190. Leiter, H.J.; Lauer, D.; Bauer, P.; Berger, M.; Rath, M. The Ariane group electric propulsion program 2019–2020. In Proceedings of the 36th International Electric Propulsion Conference, Vienna, Austria, 15–20 September 2019; p. 81.
191. ArianeGroup Electric Ion Space Propulsion Systems and Thrusters. Available online: https://www.space-propulsion.com/spacecraft-propulsion/propulsion-systems/electric-propulsion/index.html (accessed on 5 October 2023).
192. Feili, D.; Lotz, B.; Bonnet, S.; Meyer, B.K.; Loeb, H.W.; Puetmann, N. µNRIT-2.5-A new optimized microthruster of Giessen University. In Proceedings of the 31st International Electric Propulsion Conference, Ann Arbor, MI, USA, 20–24 September 2009.
193. Trudel, T.A.; Bilén, S.G.; Micci, M.M. Design and performance testing of a 1-cm miniature radio-frequency ion thruster. In Proceedings of the 31st Internationational Electric Propulsion Conference, Ann Arbor, MI, USA, 20–24 September 2009; Volume 167, pp. 20–24.
194. Lubey, D.; Bilén, S.G.; Micci, M.M.; Taunay, P.-Y. Design of the miniature microwave-frequency ion thruster. In Proceedings of the 32nd International Electric Propulsion Conference, Wiesbaden, Germany, 11–15 September 2011.
195. Collingwood, C.M.; Gabriel, S.B.; Corbett, M.H.; Jameson, P. The MiDGIT thruster: Development of a multi-mode thruster. In Proceedings of the 31st International Electric Propulsion Conference, Ann Arbor, MI, USA, 20–24 September 2009.
196. Collingwood, C. *Investigation of a Miniature Differential Ion Thruster*; University of Southampton: Southampton, UK, 2011.
197. Rafalskyi, D.; Aanesland, A. A neutralizer-free gridded ion thruster embedded into a 1U cubesat module. In Proceedings of the 35th International Electric Propulsion Conference, Atlanta, GA, USA, 8–12 October 2017; pp. 8–12.
198. Rafalskyi, D.; Martínez, J.M.; Habl, L.; Rossi, E.Z.; Proynov, P.; Boré, A.; Baret, T.; Poyet, A.; Lafleur, T.; Dudin, S. In-orbit demonstration of an iodine electric propulsion system. *Nature* **2021**, *599*, 411–415. [CrossRef] [PubMed]
199. NPT30-I2-1U. ThrustMe. 2021. Available online: https://www.thrustme.fr/base/stock/ProductBannerFiles/2_thrustme-npt30-i2.pdf (accessed on 5 October 2023).
200. Jones, A. French Startup Demonstrates Iodine Propulsion in Potential Boost for Space Debris Mitigation Efforts. 2021. Available online: https://spacenews.com/french-startup-demonstrates-iodine-propulsion-in-potential-boost-for-space-debris-mitigation-efforts/ (accessed on 6 October 2023).
201. ThrustMe. NPT30-I2 Iodine Electric Propulsion System Launched on Board the NorSat-TD Satellite. ThrustMe. 2023. Available online: https://www.thrustme.fr/post/89-thrustme-npt30-i2-iodine-electric-propulsion-system-launched-on-board-the-norsat-td-satellite (accessed on 6 October 2023).
202. Yanhui, J.; Tianping, Z.; Chenchen, W.; Yujun, K. The Latest Development of Low Power Electric Propulsion for Small Spacecraft. In Proceedings of the 35th International Electric Propulsion Conference Georgia Institute of Technology, Atlanta, GA, USA, 8–12 October 2017.
203. Pu, Y.; Li, X.; Wu, C.; Sun, X.; Jia, L.; Zhang, T.; Lv, F.; Chen, X. Numerical simulation and experimental research of LRIT-30 radio frequency ion thruster. *AIP Adv.* **2021**, *11*, 055313. [CrossRef]
204. Lascombes, P.; Montès, M.; Fiorentino, A.; Gelu, T.; Fillastre, M.; Gurciullo, A. Lessons learnt from operating the first cubesat mission equipped with a hall thruster. In Proceedings of the 35th Annual Small Satellite Conference, Virtual, 7–12 August 2021.
205. Werner, D. Exotrail Demonstrates Miniature Hall-Effect Thruster in Orbit. SpaceNews. 2021. Available online: https://spacenews.com/exotrail-demonstrates-miniature-hall-effect-thruster-in-orbit/ (accessed on 6 October 2023).
206. Gurciullo, A.; Jarrige, J.; Lascombes, P.; Packan, D. Experimental performance and plume characterisation of a miniaturised 50W Hall thruster. In Proceedings of the IEPC 2019, Vienna, Austria, 16–20 September 2019.
207. BHT-100. Busek Co. Inc. Available online: https://www.busek.com/bht100-hall-thruster (accessed on 6 October 2023).
208. Hruby, P.; Demmons, N.; Courtney, D.; Tsay, M.; Szabo, J.; Hruby, V. Overview of Busek electric propulsion. In Proceedings of the 36th International Electric Propulsion Conference, Vienna, Austria, 15–19 September 2019; pp. 15–20.

209. Misuri, T.; Ducci, C.; Gregucci, S.; Pedrini, D.; Cannelli, F.; Cesari, U.; Nania, F.; Vicini, A.; Pace, G.; Magistro, F. SITAEL HT100 Thruster Unit, Full Ground Qualification. In Proceedings of the 36th International Electric Propulsion Conference University of Vienna, Vienna, Austria, 15–20 September 2019; pp. 15–20.
210. HT 100. SITAEL S.P.A. Available online: http://www.sitael-hellas.com/wp-content/uploads/2015/10/HT-100.pdf (accessed on 6 October 2023).
211. Petrenko, O.; Tolok, S.; Maslov, V.; Kulagin, S.; Serbin, V.; Alekseenko, O.; Shcherbak, D. Electric propulsion system SPS-25 with Hall Thruster. In Proceedings of the International Astronautical Congress, IAC, Washington, DC, USA, 21–25 October 2019; p. IAC-19_C4_4_4_x50659.
212. SPS-25. SETS Space Electric Thruster Systems. Available online: https://sets.space/sps25/ (accessed on 6 October 2023).
213. Khoo, K.S.; Laterza, M.; Potrivitu, G.-C.; Lim, J.W.M. Novel cathodeless and very low-power Hall thruster: Qualification and integration on a 3U platform for an in-orbit demonstration mission. In Proceedings of the 37th International Electric Propulsion Conference, Cambridge, MA, USA, 23 June 2022.
214. MUSIC Electric Propulsion System. Aliena. Available online: https://www.aliena.sg/music (accessed on 6 October 2023).
215. Laterza, M.; Potrivitu, G.-C.; Agarwal, D.; Khoo, K.S.; Pontianus, N.; Lim, J.W.M.; Eunseo, E.H.; Supriyadi, S.D.; Li, C.; Liau, L. MUlti-Stage Ignition Compact thruster concept and testing. In Proceedings of the 37th International Electric Propulsion Conference, EPC-2022–294, Cambridge, MA, USA, 26 June 2022.
216. Halo Thrusters. ExoTerra. Available online: https://www.exoterra.com/thrusters (accessed on 6 October 2023).
217. Werner, D. ExoTerra Gains Flight Heritage for Halo Thrusters. SpaceNews. 2023. Available online: https://spacenews.com/exoterra-gains-flight-heritage-for-halo-thrusters/ (accessed on 6 October 2023).
218. Aurora. Orbion Space Technology, Inc. Available online: https://orbionspace.com/wp-content/uploads/2021/08/Orbion_Aurora_Datasheet_2021.pdf (accessed on 6 October 2023).
219. Sommerville, J.D.; Fruncek, C.E.; King, L.B.; Makela, J.M.; Terhune, K.J.; Washeleski, R.L.; Myers, R.M. Performance of the Aurora low-power Hall-effect thruster. In Proceedings of the 36th International Electric Propulsion Conference, Vienna, Austria, 15–20 September 2019; pp. 15–20.
220. Pigeon, C.E.; Orr, N.G.; Larouche, B.P.; Tarantini, V.; Bonin, G.; Zee, R.E. A Low Power Cylindrical Hall Thruster for Next Generation Microsatellites. In Proceedings of the Small Satellite Conference, Logan, UT, USA, 10 August 2015.
221. Pigeon, C. *Development of a Miniature Low Power Cylindrical Hall Thruster for Microsatellites*; University of Toronto: Toronto, ON, Canada, 2017.
222. Smith, A.W.; Cappelli, M.A. On the role of fluctuations, cathode placement, and collisions on the transport of electrons in the near-field of Hall thrusters. *Phys. Plasmas* **2010**, *17*, 9. [CrossRef]
223. Burton, R.L.; Turchi, P.J. Pulsed plasma thruster. *J. Propuls. Power* **1998**, *14*, 716–735. [CrossRef]
224. Pulsed Plasma Thruster (PPT) Projects. Mars Space Ltd. 2018. Available online: http://mars-space.co.uk/ppt (accessed on 6 October 2023).
225. Ciaralli, S.; Coletti, M.; Gabriel, S.B. Results of the qualification test campaign of a Pulsed Plasma Thruster for Cubesat Propulsion (PPTCUP). *Acta Astronaut.* **2016**, *121*, 314–322. [CrossRef]
226. Li, J.; Greenland, S.; Post, M.; Coletti, M. A highly miniaturized uPPT thruster for attitude-orbit control. In Proceedings of the 6th European CubeSat Symposium, Estavayer-le-Lac, Switzerland, 14–16 October 2014.
227. Fiber-Fed Pulsed Plasma Thruster (Fppt) System. Cu Aerospace. 2022. Available online: https://cuaerospace.com/Portals/0/SiteContent/assets/PDF/FPPT-Datasheet-v20.pdf (accessed on 6 October 2023).
228. Woodruff, C.A.; Parta, M.; King, D.M.; Burton, R.L.; Carroll, D.L. Fiber-fed Pulsed Plasma Thruster (FPPT) with Multi-axis Thrust Vectoring. In Proceedings of the Small Satellite Conference, Logan, UT, USA, 6–11 August 2022.
229. Keidar, M.; Haque, S.; Zhuang, T.; Shashurin, A.; Chiu, D.; Teel, G.; Agasid, E.; Tintore, O.; Uribe, E. Micro-cathode arc thruster for phonesat propulsion. In Proceedings of the Small Satellite Conference, Logan, UT, USA, 13 November 2013.
230. King, J.T.; Kolbeck, J.; Kang, J.S.; Sanders, M.; Keidar, M. Performance analysis of nano-sat scale μCAT electric propulsion for 3U CubeSat attitude control. *Acta Astronaut.* **2021**, *178*, 722–732. [CrossRef]
231. Krishnan, M.; Velas, K.; Leemans, S. Metal Plasma Thruster for Small Satellites. *J. Propuls. Power* **2020**, *36*, 535–539. [CrossRef]
232. Krishnan, M.; Frankovich, J. AASC's MPT* Propulsion for CubeSats. In Proceedings of the 35th Annual Small Satellite Conference, Virtual, 7–12 August 2021.
233. Kronhaus, I.; Pietzka, M.; Schilling, K.; Schein, J. Pico-Satellite Orbit Control by Vacuum Arc Thrusters as enabling Technology for Formations of small Satellites. In Proceedings of the 5th International Conference on Spacecraft Formation Flying Missions and Technologies, Munich, Germany, 19–31 May 2013; pp. 29–31.
234. Kronhaus, I.; Schilling, K.; Jayakumar, S.; Kramer, A.; Pietzka, M.; Schein, J. Design of the UWE-4 picosatellite orbit control system using vacuum-arc-thrusters. In Proceedings of the 33rd International Electric Propulsion Conference, IEPC-2013, Washington, DC, USA, 6–10 October 2013; Volume 195, pp. 6–10.
235. Bmp-200 Micro-Pulsed Plasma Thruster. Busek Co. Inc. 2019. Available online: https://satsearch.co/products/busek-bmp-220 (accessed on 6 October 2023).
236. Bayley, D.; Shoptaugh, B.; Percoski, W.; Lawrence, T. The FalonOPS Program: Space Operations at the United States Air Force Academy. In Proceedings of the SpaceOps 2010 Conference, Huntsville, AL, USA, 25–30 April 2010.

237. Blanchet, A.; Herrero, L.; Voisin, L.; Pilloy, P.; Courteville, D. Plasma jet pack technology for Nano-Microsatellites. In Proceedings of the International Electric Propulsion Conference, IEPC-2019-271, Vienna, Austria, 15–20 September 2019.
238. Schein, J.; Gerhan, A.; Rysanek, F.; Krishnan, M. Vacuum arc thruster for cubesat propulsion. In Proceedings of the IEPC-0276, 28th IEPC, Toulouse, France, 21 March 2003; Volume 100.
239. Kenyon, S.; Bridges, C.P.; Liddle, D.; Dyer, R.; Parsons, J.; Feltham, D.; Taylor, R.; Mellor, D.; Schofield, A.; Linehan, R. STRaND-1: Use of a $500 Smartphone as the Central Avionics of a Nanosatellite. In Proceedings of the 2nd International Astronautical Congress 2011, (IAC'11), Cape Town, South Africa, 5 October 2011.
240. Tran, Q.V.; Lim, W.S.; Bui, T.D.V.; Low, K.S.; Kang, B. Development of a dual-axis pulsed plasma thruster for nanosatellite applications. In Proceedings of the 4S Symposium, Sorrento, Italy, 28 May–1 June 2018.
241. Bui, T.; Tran, Q.; Lew, J.; Selvadurai, S.; Tan, B.; Ling, A.; Yang, L.; Seng, L. Design and Development of AOBA VELOX-IV nanosatellite for future Lunar Horizon Glow mission. In Proceedings of the Small Satellite Conference, Logan, UT, USA, 4 August 2018.
242. Northway, P. *Innovations in Pulsed Plasma Thrusters to Enable Cubesat Science Missions*; University of Washington: Washington, DC, USA, 2020.
243. Scharlemann, C.; Seifert, B.; Schnitzer, R.; Kralofsky, R.; Obertscheider, C.; Taraba, M. PEGASUS—A review of in-orbit operation and obtained results. *IAC-18 B* **2018**, *4*, 3.
244. Bellomo, N.; Magarotto, M.; Manente, M.; Trezzolani, F.; Mantellato, R.; Cappellini, L.; Paulon, D.; Selmo, A.; Scalzi, D.; Minute, M. Design and In-orbit Demonstration of REGULUS, an Iodine electric propulsion system. *CEAS Sp. J.* **2022**, *14*, 79–90. [CrossRef]
245. Sheehan, J.P.; Collard, T.A.; Ebersohn, F.H.; Longmier, B.W. Initial Operation of the CubeSat Ambipolar Thruster. In Proceedings of the 2015 IEEE International Conference on Plasma Sciences (ICOPS), Antalya, Turkey, 24–28 May 2015.
246. Sheehan, J.P.; Longmier, B.W.; Cutler, J. The Plasma Ambipolar Thruster for Responsive In-Orbit Transfers (PATRIOT) Mission. In Proceedings of the 11th Anuual Summer CubeSat Developers' Workshop, Logan, UT, USA, 3 August 2014.
247. Siddiqui, U.; Cretel, C. Updated performance measurements and analysis of the phase four RF thruster. In Proceedings of the 2018 Joint Propulsion Conference, Cincinnati, OH, USA, 9–11 July 2018; p. 4817.
248. Foust, J. Phase Four Launches First Plasma Propulsion Systems. SpaceNews. 2021. Available online: https://spacenews.com/phase-four-launches-first-plasma-propulsion-systems/ (accessed on 6 October 2023).
249. Tsuda, Y.; Mori, O.; Funase, R.; Sawada, H.; Yamamoto, T.; Saiki, T.; Endo, T.; Yonekura, K.; Hoshino, H.; Kawaguchi, J. Achievement of IKAROS—Japanese deep space solar sail demonstration mission. *Acta Astronaut.* **2013**, *82*, 183–188. [CrossRef]
250. Katan, C. Nasa's next solar sail: Lessons learned from nanosail-d2. In Proceedings of the 26th Annual AIAA/USU Conference on Small Satellites: Enhancing Global Awareness through Small Satellites, Logan, UT, USA, 13–16 August 2012. no. M12-1762.
251. Johnson, L.; Whorton, M.; Heaton, A.; Pinson, R.; Laue, G.; Adams, C. NanoSail-D: A solar sail demonstration mission. *Acta Astronaut.* **2011**, *68*, 571–575. [CrossRef]
252. Alhorn, D.; Casas, J.; Agasid, E.; Adams, C.; Laue, G.; Kitts, C.; O'Brien, S. Nanosail-d: The small satellite that could! In Proceedings of the 25th Annual AIAA/USU Conference on Small Satellites, Logan, UT, USA, 8–11 August 2011.
253. Sobey, A.R.; Lockett, T.R. Design and development of NEA Scout solar sail deployer mechanism. In Proceedings of the 43rd Aerospace Mechanisms Symposium, Santa Clara, CA, USA, 4 May 2016.
254. Spencer, D.A.; Betts, B.; Bellardo, J.M.; Diaz, A.; Plante, B.; Mansell, J.R. The LightSail 2 solar sailing technology demonstration. *Adv. Sp. Res.* **2021**, *67*, 2878–2889. [CrossRef]
255. LightSail, a Planetary Society Solar Sail Spacecraft. The Planetary Society. Available online: https://www.planetary.org/sci-tech/lightsail (accessed on 6 October 2023).
256. Stohlman, O.R.; Lappas, V. Development of the Deorbitsail flight model. In Proceedings of the Spacecraft Structures Conference, National Harbor, MD, USA, 13–17 January 2014; p. 1509.
257. Bridges, C. DeorbitSail Update and Initial Camera Image. AMSAT-UK. 2015. Available online: https://amsat-uk.org/2015/11/13/deorbitsail-update-and-initial-camera-image/ (accessed on 6 October 2023).
258. Song, S.-A.; Yoo, Y.; Han, C.-G.; Koo, S.; Suk, J.; Kim, S. System Design of Solar Sail Deployment and its Effect on Attitude Dynamics for Cube Satellite CNUSAIL-1. In Proceedings of the The Asia-Pacific International Symposium on Aerospace Technology (APISAT-2014), Shanghai, China, 24–26 September 2014; pp. 24–26.
259. Wang, Z. Design of a scalable nano university satellite bus (IlliniSat-2 bus) command and data handling system and power system. In Proceedings of the Small Satellite Conference, Logan, UT, USA, 4 August 2018.
260. CubeSail, Designed by CU Aerospace and the University of Illinois, Is a Low-Cost Flight Experiment Based on the UltraSail Concept. CU Aerospace. Available online: https://www.cubesail.us/ (accessed on 6 October 2023).
261. Stankey, H.C.; Hoyt, R.P. In-Flight Performance of the Terminator Tape End-of-Life Deorbit Module. In Proceedings of the 35th Annual Small Satellite Conference, Virtual, 7–12 August 2021.
262. Henry, C. Tethers Unlimited Says Early Results of Deorbit Hardware Test Promising. SpaceNews. 2020. Available online: https://spacenews.com/tethers-unlimited-says-early-results-of-deorbit-hardware-test-promising/ (accessed on 6 October 2023).
263. Le, C. *TEPCE: A Tethered Electrodynamic Propulsion CubeSat Experiment*; Technical report; US Naval Research Laboratory: Washington, DC, USA, 2022.

264. Li, G.; Spence, L.; Miller, M.; Pandya, M.; Stankey, N.; Hancock, A.; Lu, R.; Park, C.; Rajesh, A.; Beloiu, A. Lessons Learned from the Development and Flight of the First Miniature Tethered Electrodynamics Experiment (MiTEE-1). In Proceedings of the 35th Annual Small Satellite Conference, Virtual, 7–12 August 2021.
265. Nohmi, M. Initial experimental result of pico-satellite KUKAI on orbit. In Proceedings of the 2009 International Conference on Mechatronics and Automation, Changchun, China, 9–12 August 2009; pp. 2946–2951.
266. Masahiro, N. Past results and future missions of STARS series satellite. In Proceedings of the AIAC18: 18th Australian International Aerospace Congress (2019): HUMS-11th Defence Science and Technology (DST) International Conference on Health and Usage Monitoring (HUMS 2019): ISSFD-27th International Symposium on Space Flight Dynamics (ISSFD), Engineers Australia, Canberra, Australia, 8 January 2024; pp. 935–940.
267. Bae, Y.K. Photonic laser propulsion: Proof-of-concept demonstration. *J. Spacecr. Rockets* **2008**, *45*, 153–155. [CrossRef]
268. Bae, Y.K. Demonstration of Amplified Radiation Pressure Propulsion with an Active Optical Cavity. *Preprint* **2020**. [CrossRef]
269. Bae, Y.K. Photonic laser thruster: 100 times scaling-up and propulsion demonstration. *J. Propuls. Power* **2021**, *37*, 400–407. [CrossRef]
270. Pomager, J. Photonic Railway: Will Laser Propulsion Enable Interstellar Travel? Available online: https://www.photonicsonline.com/doc/photonic-railway-will-laser-propulsion-enable-interstellar-travel-0001 (accessed on 6 October 2023).
271. Zubrin, R.M.; Andrews, D.G. Magnetic sails and interplanetary travel. *J. Spacecr. Rocket.* **1991**, *28*, 197–203. [CrossRef]
272. Bassetto, M.; Perakis, N.; Quarta, A.A.; Mengali, G. Refined MagSail thrust model for preliminary mission design and trajectory optimization. *Aerosp. Sci. Technol.* **2023**, *133*, 108113. [CrossRef]
273. Funaki, I.; Yamakawa, H. Solar wind sails. In *Exploring the Solar Wind*; IntechOpen: London, UK, 2012.
274. Johnson, L.; Polzin, K. Electric Sail Propulsion for Deep Space Missions. In Proceedings of the International Astronautical Congress (IAC), Washington, DC, USA, 21 October 2019. no. MSFC-E-DAA-TN74139.
275. Koizumi, H.; Kawahara, H.; Yaginuma, K.; Asakawa, J.; Nakagawa, Y.; Nakamura, Y.; Kojima, S.; Matsuguma, T.; Funase, R.; Nakatsuka, J. Initial flight operations of the miniature propulsion system installed on small space probe: PROCYON. *Trans. Jpn. Soc. Aeronaut. Sp. Sci. Aerosp. Technol.* **2016**, *14*, Pb_13–Pb_22. [CrossRef] [PubMed]
276. Colón, B.J.; Glaser, M.J.; Lightsey, E.G.; Bruno, A.R.; Cavender, D.P.; Lozano, P. Spectre: Design of a Dual–Mode Green Monopropellant Propulsion System. AAS-094. In Proceedings of the 44th Annual American Astronautical Society Guidance, Navigation, and Control Conference, Breckenridge, CO, USA, 9 February 2022.
277. ArgoMoon Propulsion System. VACCO Industries. Available online: https://cubesat-propulsion.com/wp-content/uploads/2017/08/X17025000-data-sheet-080217.pdf (accessed on 6 October 2023).
278. Clark, S. US Space Command Says It Needs More Maneuverable Satellites. Ars Technica. 2023. Available online: https://arstechnica-com.cdn.ampproject.org/c/s/arstechnica.com/space/2023/07/us-space-command-says-it-needs-more-maneuverable-satellites/amp/ (accessed on 6 October 2023).
279. Bultitude, J.; Suresh, S.; Deuitch, A.; Cho, J.; Fettes, L.; Burkhardt, Z.; O'Leary, A.; Harris, M.; Jelderda, M.; Faber, D. First Flight of RAFTI Orbital Refueling Interface. In Proceedings of the International Astronautical Congress, Dubai, United Arab Emirates, 25–29 October 2021.
280. Steigerwald, W. NASA's Robotic OSAM-1 Mission Completes its Critical Design Review. NASA. 2022. Available online: https://www.nasa.gov/centers-and-facilities/goddard/nasas-robotic-osam-1-mission-completes-its-critical-design-review/ (accessed on 6 October 2023).
281. Krejci, D.; Jenkins, M.G.; Lozano, P. Staging of electric propulsion systems: Enabling an interplanetary Cubesat. *Acta Astronaut.* **2019**, *160*, 175–182. [CrossRef]
282. Gerrish, H.P., Jr. *Solar Thermal Propulsion at NASA Marshall Space Flight Center Huntsville, AL*; NTRS-NASA Technical Reports Server: Huntsville, AL, USA, 2016.
283. Kennedy, F.G.; Palmer, P.L. Design and Proto-flight Test Strategy for a Microscale Solar Thermal Engine. *Sp. Technol.* **2003**, *23*, 11–26.
284. Zhumaev, Z.S.; Shcheglov, G.A. Operations dynamics analysis of solar thermal propulsion for CubeSats. *Adv. Sp. Res.* **2019**, *64*, 815–823. [CrossRef]
285. Zhang, H.; Huang, M.; Hu, X. Integrated design of solar thermal propulsion system for microsatellite with liquid ammonia as propellant. *Adv. Sp. Res.* **2023**, *71*, 456–476. [CrossRef]
286. Song, F.; Zheng, H.; Zhang, Y.; Xu, Q.; Gao, K.; Tian, Y.; Song, C.; Luo, Q.; Yao, H.; Liu, X. Feasibility analysis of solar thermal propulsion system with thermal energy storage. *Adv. Sp. Res.* **2023**, *71*, 2493–2508. [CrossRef]